2023

The Investigation of Novel Bovine Oocyte-Specific Long Non-coding RNAs and Their Roles in Oocyte Maturation and Early Embryonic Development

Jaelyn Zoe Current
West Virginia University, jzc0001@mix.wvu.edu

THE INVESTIGATION OF NOVEL BOVINE OOCYTE-SPECIFIC LONG NON-CODING RNAS AND THEIR ROLES IN OOCYTE MATURATION AND EARLY EMBRYONIC DEVELOPMENT

Jaelyn Z. Current

Dissertation submitted to the Davis College of Agriculture, Natural Resources & Design at West Virginia University

in partial fulfillment of the requirements for the degree of

Doctor of Philosophy

in

Reproductive Physiology

Jianbo Yao, Ph.D., Chair

Robert Dailey, Ph.D.

Ida Holásková, Ph.D.

Melanie Clemmer, Ph.D.

I-Chung Chen, Ph.D.

Division of Animal and Nutritional Sciences

Morgantown, WV

2023

KEYWORDS: Non-coding RNA, lncRNA, oocyte quality, oocyte maturation, early embryonic development, siRNA-mediated knockdown, follicle size, heat stress

ABSTRACT

THE INVESTIGATION OF NOVEL BOVINE OOCYTE-SPECIFIC LONG NON-CODING RNAS AND THEIR ROLES IN OOCYTE MATURATION AND EARLY EMBRYONIC DEVELOPMENT

Jaelyn Z. Current

Early embryonic loss is a significant factor in livestock species' infertility, resulting in an economic deficit. In cattle, the *in vivo* fertilization rate is ~90%, with an average calving rate of about 55%, indicating an embryonic-fetal mortality rate of roughly 35%. Further, 70-80% of total embryonic loss in cattle occurs during the first three weeks after insemination, particularly between days 7-16. Growing evidence indicates that the oocyte plays an active role in regulating critical aspects of the reproductive process required for successful fertilization, embryo development, and pregnancy. However, defining oocyte quality remains enigmatic. Recently, many have abandoned the notion that one transcript or gene network modulates oocyte competence. Instead, it is speculated that a vast network of transcripts regulates gene expression.

With the advent of deep sequencing technology, it was discovered that roughly 1.2% of the human genome represents protein-coding exons, whereas the remaining classifies as non-coding RNA. What once was thought of as “genetic noise” from leaky transcriptional machinery has more recently come to the foreground of modern research in molecular biology due to its broad versatility in regulating gene expression. Specifically, long non-coding RNAs (lncRNAs) have been reported to play critical roles in various biological processes. Despite their gaining popularity, most lncRNA studies focus on identifying differentially expressed lncRNAs throughout bodily systems and are left to predict their functional roles using bioinformatic and comparative analyses. Recently, lncRNAs have been identified as critical regulators of embryonic genome activation in humans, mice, pigs, goats, and rabbits. Further investigations of lncRNAs in mouse oocytes and early embryos have revealed essential roles in regulating oocyte maturation and early embryonic development. However, the functional role of lncRNAs in bovine oocytes remains to be elucidated.

Previously, using RNA sequencing, our laboratory identified 1,535 lncRNAs present in bovine oocytes. The top three candidate genes, *OOSNCR1*, *OOSNCR2*, and *OOSNCR3*, were characterized in bovine somatic tissues, the cells within the ovarian follicle, and throughout early embryonic development. Our data revealed that *OOSNCR1* and *OOSNCR2* are oocyte-specific, with *OOSNCR3* being highly abundant in the fetal ovary and detected at low levels in the spleen. Follicular cell expression revealed that all three lncRNAs were detected throughout the follicle. Further, all three lncRNAs were expressed highest in the oocyte, decreasing expression as the distance from the oocyte increased. Moreover, expression throughout oocyte maturation and early embryonic development revealed that *OOSNCR1*, *OOSNCR2*, and *OOSNCR3* were highest during oocyte maturation, decreased at fertilization, and ceased altogether by the 16-cell stag Collectively, the expression data suggested all three transcripts were maternal effect gene. Maternal origin was confirmed using an RNA polymerase II inhibitor, α-amanitin.

The functional role of *OOSNCR1, OOSNCR2,* and *OOSNCR3* during oocyte maturation and early embryonic development was evaluated using siRNA-mediated knockdown. Injection of the cumulus-enclosed germinal vesicle (GV) oocyte did not affect cumulus expansion; however, oocyte survival at 12 hours post-insemination was significantly reduced following the microinjection procedure. Additionally, lncRNA knockdown decreased the relative abundance of maternal effect genes *NPM2, GDF9, BMP15,* and *JY-1* and resulted in blastocyst rates close to zero. Using siRNA-mediated knockdown in the presumptive zygote, the percentage of embryos reaching the blastocysts stage was decreased by roughly half for all three lncRNAs.

The potential relationship between lncRNA expression and oocyte quality was investigated. In addition to *OOSNCR1, OOSNCR2,* and *OOSNCR3, OOSNCR4* and *OOSNCR5* were selected from the RNA sequencing dataset as highly abundant lncRNAs in bovine oocytes. All lncRNAs were quantified in oocytes of various qualities. Specifically, lncRNA expression was examined in oocytes (1) collected from small and large follicles before and after maturation, (2) differentially stained using brilliant cresyl blue (BCB), and (3) exposed to heat stress (41^0C) during oocyte maturation. Data revealed that *OOSNCR1* and *OOSNCR3* were accumulated during maturation, whereas *OOSNCR2* and *OOSNCR4* were degraded. Further, *OOSNCR1, OOSNCR2,* and *OOSNCR4* were more abundant in oocytes collected from small follicles. Specifically, *OOSNCR2* and *OOSNCR4* were expressed highest in immature oocytes. Conversely, *OOSNCR3* was more abundant in mature oocytes collected from large follicles. Following BCB staining, *OOSNCR3* was expressed lower in BCB+ oocytes. Finally, maturation in a heat-stressed environment decreased cumulus cell expansion. Heat stress during maturation also caused *OOSNCR1* to decrease expression, whereas *OOSNCR3, OOSNCR4,* and *OOSNCR5* expression increased.

Overall, the data herein revealed dynamic expression profiles of novel lncRNAs and suggests a functional requirement of *OOSNCR1, OOSNCR2,* and *OOSNCR3* during bovine oocyte maturation and early embryogenesis.

DEDICATION

To my nieces and nephew, Sawyer, Josie, Lainey, Juniper, and Rhett, you guys always reminded me that every failed science experiment was still a chance to do science, and a chance to do science means an opportunity to learn something new…and most likely make a massive mess in the process. So ask questions, never stop learning, and make a huge mess.

To my family for constantly reminding me to take a day off and go outside. It didn't feel like it then, but those breaks got me through the long exhausting days.

To my fiancé, Roger, your never-ending support, terrible pep talks, and unconditional love kept me grounded when science proved over and over again to be impossible.

Thank you to each of you for loving me through the stress of graduate school.

ACKNOWLEDGEMENTS

Foremost, I would like to thank my advisor Dr. Jianbo Yao. During my time as his student, he has continually supported, encouraged, and mentored me. He has taught me to relax, embrace the process and take one day at a time. His constant positive encouragement gave me confidence in myself and my ability to learn new challenging things. He has shown me what a real mentor is, provided me with endless "chit-chat," and made every hard day in graduate school end a positive one. Most importantly, he taught me how to decide when "…it's not critical."

Next, I would like to thank my committee members: Dr. Robert Dailey, Dr. Ida Holásková, Dr. Melanie Clemmer, and Dr. I-Chung Chen, for serving on my graduate committee. Dr. Dailey, you have taught me so much beyond what I thought my brain could hold. I cannot express enough gratitude that you stayed late every night and were often in your office on weekends. You never turned me away and always answered every one of my questions. Ida, I would have no idea how to do statistics if not for you. Thank you for taking the extra time to slow down and explain every step. Each of you pushed me incessantly during journal club, and I am forever grateful for that. Dr. Clemmer and Dr. Chen, you openly welcomed me to the clinic to explore the clinical applications of our work and pushed me during my prelims. Your perspectives and backgrounds were valued every step of the way.

Next, a thank you to my labmates: Dr. Mingxiang Zhang and Dr. Heather Chaney. To say grad school was interesting with you two would be an understatement. Our friendship, support, journal clubs, failures, shenanigans, and laughs made grad school the best years of my life. We became a family, and the Yaozzers will always hold a special place in my heart. Thank you to both of you for the memories.

Next, thank you to the undergraduate students who patiently stuck with us through the long nights, failures, and pandemic. Kaleb Royer, Megan Morral, Maighan Bailey, Heather Rubilla, Brady Nicewarner, Emery Kronemery, Victoria Nist, Emily Dugan, and Gianna Chimino. I appreciate all the laughs and hard work. Each of you made me a better mentor.

Next, my family, each of you, provided unconditional love and support from home that constantly reminded me to chase my passion and [one day] finish school. But most importantly, thank you for the constant reminder to "finish that Ph.D.!" *A special shout out to my best friend Shelby for always providing a couch to crash on during my ovary runs.

Next, Corey, Kindra, The Hyde Family, the lovely employees at Hyde's Meat Packing, and Jake, Nate, Lori, James, and all my fellow gut table friends at JBS for their generous donation and assistance in procuring ovaries (and miscellaneous parts). The ovary girl is forever indebted to each of you, as I would never have gotten this degree without each and every one of you.

And finally, I would like to thank the WVU Reproductive Physiology program. To every professor, mentor, researcher, and student who came through this program before me for making the amazing people I trained under. I've met the most incredible minds through this program and am truly honored to be a part of it. Thank you, Mountaineer family.

TABLE OF CONTENTS

LIST OF ABBREVIATIONS

BMP	Bone Morphogenic Protein
CCs	Cumulus Cells
CL	Corpus Luteum
DMRs	Differentially Methylated Regions
dpc	Days *post coitum*
ECM	Extracellular Matrix
EVs	Extracellular Vesicles
FSH	Follicle Stimulating Hormone
GCs	Granulosa Cells
GV	Germinal Vesicle
GVBD	Germinal Vesicle Breakdown
LH	Luteinizing Hormone
LncRNAs	Long Non-Coding RNAs
mGCs	Mural Granulosa Cells
MII	Metaphase II
miRNAs	MicroRNAs
MPF	Maturation Promoting Factors
MZT	Maternal to Zygote Transition
ncRNAs	Non-Coding RNAs
ORF	Open Reading Frame
OOSNCR1	Oocyte-specific non-coding RNA 1
OSFs	Oocyte-secreted Factors
PGCs	Primordial Germ Cells
PKA	Protein Kinase A
PMF	Primordial Follicle
siRNAs	Small Interfering RNAs
TCs	Theca Cells
TFs	Transcription Factors
TZPs	Transzonal Projections
ZGA	Zygotic Genome Activation

Review of Literature

Introduction

Cattle production systems build on the foundational principle of maximizing the number of cows that produce a marketable calf yearly. However, calf crop percentages often fail to meet expectations due to reproductive failures. Early embryonic loss is a significant factor in livestock species' infertility, resulting in an economic deficit. It is estimated that annually there is a $1.2 billion industry loss due to embryonic mortality (Spencer, 2013). The original definition of embryonic mortality, strictly interpreted, referred to fertility losses during the embryonic period (i.e., conception to completion of differentiation, which in the cow occurs at approximately 45 days) (Ayalon, 1978). More recently, early embryonic loss periods have been categorized with physiological development during pregnancy (Reese et al., 2020). The early embryonic period (conception to d28) is divided into two loss periods: fertilization & pre-blastocyst and premature embryonic mortality. The late embryonic and fetal periods are grouped and represent the late embryonic mortality/early fetal loss periods.

In cattle, the *in vivo* fertilization rate is ~90%, with an average calving rate of about 55%, indicating an embryonic-fetal mortality rate of roughly 35% (Diskin et al., 2006). Further, 70-80% of total embryonic loss in cattle occurs during the first three weeks after insemination, particularly between days 7-16 (Spencer, 2013). Bilodeau-Goeseels and Kastelic reviewed the literature and compiled a list of endogenous and exogenous causes of embryonic mortality; chromosome abnormalities, inadequate corpus luteum (CL) function, short duration of the luteal phase, deviations in follicular development, aberrations in hormone concentrations, heat stress, nutrition, energy status, and protein and fatty acid intake (Bilodeau-Goeseels and Kastelic, 2003). This

review will focus on deviations in ovarian function and examine the functional roles of oocyte quality on embryonic survival.

Growing evidence indicates that the oocyte plays an active role in regulating critical aspects of the reproductive process required for successful fertilization, embryo development, and pregnancy. The influence of oocyte quality on the embryo's developmental potential has been recognized in cattle (Lonergan et al., 2001; Merton et al., 2003; Lonergan, 2011). Sirard et al. reviewed the vast literature and clarified the roles of oocyte maturation and follicular differentiation in oocyte competence (Sirard et al., 2006). In summary, the oocyte must display developmental competence to achieve reproductive success. Meaning the oocyte must resume meiosis, cleave upon fertilization, develop to the blastocyst stage (namely activate the embryonic genome), establish a pregnancy, and sustain fetal growth and development until birth. Oocyte maturation consists of three levels: (1) meiotic maturation – the spontaneous cascade of nuclear events induced by the luteinizing hormone (LH) surge or by the removal of the oocyte from its follicular environment (2) cytoplasmic maturation – a series of spontaneous changes marked by modifying the transcription and translation machinery in addition to a re-distribution of organelles and (3) molecular maturation – maternal mRNAs and proteins are produced intrinsically and "stockpiled" until after ovulation and are hypothesized to determine the fate of the early embryo. Due to the oocyte placement within the follicle, the influence of the follicular environment on the oocyte's successful acquisition of developmental competence directly corresponds to the follicular phase.

Setting the Stage: The Indifferent Gonad

More than a century ago, August Weissman theorized the early germplasm, a substance independent from all other cells of the body (somatoplasm), is the essential element of germ cells

and acts as the hereditary material passed from one generation to the following (Weissmann, 1893). Although modified, the premise of Weissman's theory rings true as germ cells remain the only known vehicles of hereditary transmission. The first germline cells are called primordial germ cells (PGCs) among metazoan embryos. The differentiation and development of PGCs is an early event in mammalian embryogenesis vital to establishing normal fertility of the offspring and the correct dissemination of the genetic and epigenetic information to the next generation.

Research in the 1890s laid the foundation for inheritance studies when human PGCs were first visualized (Felix, 1911; Fuss, 1911; Fuss, 1912). Despite its origin in humans, intricate studies using mice models and stem cell technologies have been crucial in revealing the complex molecular events underlying the process. The formation of PGCs occurs in animals by one of two mechanisms: inheritance of germ plasma or inductive signaling (De Felici, 2013). Many organisms, including invertebrate and nonmammalian vertebrate species such as *Drosophila, Caenorhabditis*, and species within *Anura* (frogs), have germ cells that arise through the inheritance of germ plasma. Germ plasma is a collection of maternally derived cytoplasmic RNAs, RNA-binding proteins, and various organelles accumulated in the mature oocyte that segregates during the first divisions of the early embryo to form the cells that will ultimately become PGCs (De Felici, 2013). Deviating from the majority, most mammalian species are hypothesized to undergo inductive signaling shortly before or during gastrulation to give rise to their PGCs. During inductive signaling, specific signals secreted by neighboring cells induce PGC precursors within the epiblast cells to commit and differentiate to the PGC lineage (De Felici, 2013). Shortly after, the precursors are identified as PGCs localized to the extraembryonic region. PGCs are regarded as a heterogeneous cell population that constantly changing at each development stage. PGC

development begins with PGC specification, then enters three simultaneous processes: migration, proliferation, and epigenesis dynamics, and concludes when the gametes enter meiosis.

PGC Specification: The literature agrees that PGC specification is driven by bone morphogenetic protein (BMP) released by extraembryonic tissues that target the pluripotent proximal epiblast cells and prime them to become mesoderm cells during 5-6 days *post coitum* (dpc) in the mouse embryo (Felici, 2009). Approximately twelve hours later, six clustered E-cadherin/fragilis expressing cells located within the proximal epiblast on the posterior side receiving the highest doses of BMP4, MAPK (Aubin et al., 2004) and expressing *SMAD*1-5 are committed to the germ cell lineage following *PRDM1* (*BLIMP1*) and *PDM14* expression (Felici, 2009). Finally, PGC precursors are specified as PGCs as they move along extraembryonic mesoderm cells at the base of the allantois marked by STELLA, TNAP, KIT, and SSEA-1 expression.

At the genomic level, there are at least three key events to achieve PGC specification: (1) repression of the somatic mesodermal program, (2) reacquisition of potential pluripotency, and (3) genome-wide epigenetic reprogramming (Yamaji et al., 2008). Repression of the somatic mesodermal program is achieved through the association of PRDM1 and the methyltransferase PRMT5 most likely through symmetrical methylation of arginine 3 on histones H4 and H2A. Reacquisition of potential pluripotency requires PRDM14 indicated by *Sox2* and *Nanog* expression in cooperation with OCT4. Finally, genome-wide epigenetic reprogramming commences following modifications of several histones associated with an active or repressed chromatin state.

Migration: It is undisputed that the indifferent gonad is established by the colonization of PGCs migrating to the gonadal ridge. However, the mechanisms of PGC migration remain as diverse as the species that play host to them. Active and passive movements, single and grouping

movements, attractive and repulsive forces exerted by the surrounding tissues, and interactions with the extracellular matrix (ECM); have all been shown to be involved and likely play a role in the process. For example, human PGCs preferentially migrate along autonomic nerve fibers close to the Schwann cells to ascend the mesentery of the hindgut to the gonadal ridge (Møllgård et al., 2010). It is hypothesized that the nerve fibers and/or the Schwann cells may release chemoattractants that support PGC migration.

Moreover, several studies have demonstrated that mouse PGCs may use a variety of integrins for dynamic adhesive interactions with ECM molecules, such as fibronectin, laminin, and collagen IV, enforced explicitly by the notion that PGCs lacking β1 integrins fail to migrate correctly to the gonadal ridge (De Felici, 2013). Many studies have revealed that both human and mouse PGCs show several features of motile cells, including distinctive appearance and pseudopodia with the ability to move actively on cellular and extracellular matrix substrates (De Felici, 2013). Thus, it is likely that the underlying mechanisms of migration among and within multiple species are complex and likely involve a variety of modes of migration.

Regardless of the mechanism, PGC migration in the mouse is systematically divided into three stages (Felici, 2009): (1) 8-9 dpc: PGCs travel into the developing hindgut epithelium from the base of the allantois. This migration is likely governed by E-Cadherin (E-cad) downregulation, LFITM1 repulsive, and LFITM3 attractive homing of the PGCs to the hindgut epithelium. (2) 9.5-10.5 dpc: PGCs exit the hindgut and move directly into the gonadal ridges. The second migration phase is likely controlled by the acquisition/reacquisition of a motile phenotype, E-cad upregulation, intercellular contact among PGCs, interactions with the ECM through β1 integrin, SF-1/CXR4 and/or KL/kit chemoattractive action. (3) 11.5-12.5 dpc: The final migration stage occurs through the dorsal mesentery into the developing gonads and most likely utilizes many of

the same factors involved in the second migratory stage. However, the destiny of these late migrating PGCs remains undefined. Specifically, it is unknown if these PGCs contribute to the germ cell population within the gonads, if they are dispersed to other tissues to die via apoptosis, or if they have some different unknown developmental fate, such as giving rise to germ cell tumors (Cook et al., 2009).

Proliferation and Epigenesis Dynamics: While migrating to the gonadal ridge, PGCs undergo rapid proliferation and extensive nuclear reprogramming from 8.5 to 13.5 dpc. At this stage, PGCs undergo mitotic proliferation, increasing their number roughly 400 times from about 50 to 20,000 cells per embryo in 7-8 mitotic cycles (Tam and Snow, 1981). During this time frame, it is hypothesized that PGCs are also undergoing a transition in their energy metabolism from anaerobic to aerobic, supported by the observations of migratory PGCs containing less than ten mitochondria. In contrast, ovarian PGCs have 100 and oogonia 200 (Motta et al., 2000). With energy demands changing, various soluble and membrane-bound growth factors sustain PGC growth, prevent apoptosis, and/or stimulate their proliferation (De Felici et al., 2004). Simultaneously, PGCs undergo extensive genome-wide epigenetic reprogramming involving modifications of histones associated with open or inaccessible chromatin state.

During mouse PGC specification (starting at 6.25 dpc) and migration, immunofluorescence staining studies have revealed repressive histone modification H3K9me2 becomes globally depleted by 8 dpc while remaining high at pericentric heterochromatin (Ramakrishna et al., 2021). Alternatively, during this same period, H3K27me3 levels become progressively enriched globally. As PRMT5 translocates from the cytoplasm to the nucleus to associate with BLIMP1, repressive modifications of histones H2A and H4 also increase (Ancelin et al., 2006). Starting around 8.5 dpc, a decline in DNA methylation is associated with the downregulation of *de novo*

methyltransferases DNMT3A and 3b and DNMT1 co-factor UHRF1 (Ramakrishna et al., 2021). Despite the decline during this period, some DNA methyltransferases remain active as many loci retain high DNA methylation levels. Altogether, the mechanisms dictating DNA methylation levels at different genomic regions remain poorly understood.

Collectively, these data suggest that following specification and during migration to the gonadal ridge, these pre-gonadal PGCs establish a distinctive epigenome characterized by low levels of DNA methylation and H3K9me2 paired with elevated H3K27me3 and H2A/H4R3me2s (Ramakrishna et al., 2021). Once colonized at the gonad, a more complex and complete epigenomic reprogramming event occurs, characterized by DNA methylation at its lowest and changes in the chromatin landscape. In the mouse, this epigenomic reprogramming begins around 11 dpc and is completed by 13.5 dpc. During this period specific to mammals, genomic imprints are erased from the differentially methylated regions (DMRs), allowing for the subsequent re-establishment of sex-specific genomic patterns (Ramakrishna et al., 2021). As research expands and utilizes new technologies, the exact significance of the changes mentioned herein and the mechanisms involved will be revealed.

Entering Meiosis: Once they arrive at the gonadal ridge, PGCs are rapidly surrounded by cords of somatic cells and begin differentiating into oogonia. Farini and De Felici compiled the literature to propose a model of the molecular signals required to initiate meiosis and, ultimately, the differentiation of oogonia (Farini and De Felici, 2022). According to their hypothesis, intrinsic factors such as unique epigenetic status and the RNA-binding protein DAZL expression act upon germ cells, making them responsive to extrinsic factors secreted by cells within the ovary-mesonephros region such as retinoic acid (RA) and members of the TGFβ family, specifically BMP2 to initiate meiosis. These factors first cause the downregulation of pluripotency genes.

Second, RA and BMP-dependent transcription factors cause an amplification of a broad transcription program necessary to activate the meiotic cell cycle.

Simultaneous with the molecular signaling cascade occurring within, gonadal PGCs undergo morphological and metabolic changes to support differentiation and entry into meiosis. In humans, by the ninth week of gestation, oogonia become apparent by their regular and smooth cellular profile, reduced lipid inclusion and glycogen granules in the cytoplasm, and increased number of mitochondria, all accompanied by high mitotic activity (De Felici, 2013). Additionally, oogonia tend to form clusters (or nests) of dividing cells connected by cytoplasm, termed intercellular bridges, originating from an incomplete division of the cell bodies during cytokinesis (Ruby et al., 1970). Proliferation lasts five days in the mouse, at which point the oogonia enter meiosis. In contrast, the mitotic proliferation of oogonia in humans occurs until the fifth month of fetal life, demonstrating a significant overlap with the period of entry into meiosis (10-11 weeks), where mitotic oogonia and primary oocytes in different stages of meiosis coexist (Baker, 1963). By the end of the proliferation stage in humans (around the fifth month of gestation), the number of oogonia is estimated to be around 10,000,000 (Baker, 1963).

Due to the asynchronous meiotic entry, some oogonia initiate meiosis and differentiate into oocytes, while others continue to multiply until weeks 17-18 of gestation. Those that continue to proliferate are mainly localized to the periphery of the ovaries, expressing pluripotency markers, whereas the more differentiated oocytes are deeper within the medulla (Farini and De Felici, 2022). By gestational week 18, most oogonia have initiated meiosis, with the oocytes arrested at the diplotene stage of the first meiotic division surrounded by pre-granulosa cells forming a single-layered primordial follicle (PMF) (Farini and De Felici, 2022).

The Simultaneous Processes of Folliculogenesis and Oogenesis

The processes of folliculogenesis and oogenesis work concurrently to result in the ovulation of a developmentally competent oocyte capable of achieving fertilization, establishing pregnancy, and producing viable offspring. Although coinciding, each process relies on distinct molecular and morphological changes that converge to create an optimal environment that houses the fully matured oocyte. This section will discuss the development of the follicle and the crucial roles of the follicular nurse and interstitial cells in nurturing the developing germ cells in the adult gonad to form preovulatory follicles.

Folliculogenesis: The Development of the Follicle

The mammalian follicle consists of an ovum surrounded by layers of follicular nurse cells communicating with the germ cell through a bidirectional system using transzonal projections (TZPs). In addition, the entire follicle encapsulated by a basement membrane is surrounded by androgen-producing cells, also known as theca cells (TCs).

Origins of the follicular nurse cells: Recent lineage tracing studies suggest granulosa cells (GCs) have at least two sources (Piprek, 2016). Using *FOXL2*-dependent Cre activity and the R26R reporter, Mork et al. found that follicles located in the ovarian medullary region activated immediately after birth contained *FOXL2*-positive cells (Mork et al., 2012). In contrast, GCs associated with primordial follicles found in the ovarian cortex and activated post-pubertally and throughout adult life derived from a second perinatal wave of cells from the ovarian surface epithelium expressing the adult stem cell marker, *LGR5* (Rastetter et al., 2014). Based on their distinct developmental dynamics, the existence of the two classes of PMFs was independently verified using inducible mouse models (Zheng et al., 2014).

Origins of the androgen-producing cells: Female androgen-producing cells are assumed to arise from similar progenitors as their male counterparts. The homolog to TCs within the interstitial compartment of the male gonad is the Leydig cells adjacent to the Sertoli cells outside the blood-testis barrier. In male mice, fetal Leydig cells (FLCs) arise 24 h after Sertoli cell specification at approximately 12.5 dpc (Barsoum and Yao, 2010). Following birth, FLCs are gradually replaced by the male androgen-producing cells, adult Leydig cells (ALCs). Despite many years of research, the origins of FLCs remain widely debated. Potential sources speculated to be the origin of FLCs include neural crest cells, coelomic epithelium, mesonephros, adrenogonadal primordium, and perivascular cells (Piprek, 2016). Although many questions remain regarding the embryonic origins of TCs, recent work has shown that similar to Leydig cells, TCs likely have multiple cellular origins, most likely mesenchymal stromal precursor cells or steroidogenic cells with an abundance of smooth endoplasmic reticulum (Piprek, 2016) or more specifically a subset of indigenous embryonic ovarian cells expressing *WT1* and migrating mesonephric mesenchymal cells expressing *GLI1* (Liu et al., 2015).

With many parallels drawn between TCs and ALCs, it is essential to note the differences. In contrast to ALCs commencing steroidogenesis soon after initial testis formation, TCs do not begin producing androgens until after birth with the induction of folliculogenesis following the luteinizing hormone (LH) surge (Fortune and Armstrong, 1977; Mannan and O'Shaughnessy, 1991). It is only upon the development of the primary follicle that TCs migrate and proliferate in the regions adjacent to the follicle (Kotsuji et al., 1990; Tajima et al., 2007).

Building the follicle: In mice between 17.5 dpc to postnatal day 5, there is the breakdown of germ cell cysts to form PMFs accompanied by a massive loss of germ cells (Pepling and Spradling, 2001; Menke et al., 2003). The remaining germ cells arrested at prophase become

encapsulated by a flattened epithelium (pre-granulosa cells) that differentiate to form GCs. This pool of PMFs constitutes the ovarian follicle reserve. It is agreed upon that during the postnatal life in females, there is a finite set of germ cells within this quiescent reserve (S.H. Green and S. Zuckerman, 1951). However, despite its wide acceptance, controversial debates remain arguing the regeneration of female germline stem cells (White et al., 2012; Park et al., 2013; Park and Tilly, 2015; de Souza et al., 2017; M.H. Dong et al., 2022). Recently, new evidence in naked mole rats has challenged the dogma. Specifically, highly desynchronized germ cell development in conjunction with maintenance of a small population of PGCs allows naked mole-rats to undergo oogenesis entirely postnatally throughout their 30-year reproductive lifespan, never achieving ovarian senescence (Brieño-Enríquez et al., 2023).

PMFs will be recruited from the ovarian reserve to enter the growing pool. This transition from PMF to the primary follicle is characterized by the morphological changes observed when flattened squamous GCs become cuboidal. As the oocyte continues to grow, primary follicles transition to secondary follicles following GC proliferation and additional layers of TCs forming along the basement membrane surrounding the follicle. At these stages, follicular growth is independent of gonadotropins and driven by a complex bidirectional communication between the oocyte and the somatic cells (Eppig, 2001).

Communication within the follicle: The current orthodoxy in mammalian follicles is that the GCs located at the furthest reaches of the follicle communicate with the oocyte via paracrine signaling, while the innermost layer of follicular cells, the cumulus cells (CCs) of the *corona radiata*, communicate with the oocyte through gap junctions within cellular projections that extend through the zona pellucida and terminate at the oocyte's plasma membrane (Gilbert et al., 2015). These cellular projections, more commonly known as TZPs, appear during the secondary follicle

stage (Robert, 2021) and have been investigated as a potential means of transporting large cargo. Specifically, researchers have attempted to characterize TZPs and visualize the transfer of genomic material to supply the quiescent oocyte with outside information that contributes to the maternal reserves that are pivotal to oocyte competence and early embryogenesis.

TZPs were first detected fortuitously in early microscopy studies investigating the structure and function of the Golgi apparatus and mitochondria (Loyez, 1905; Brambell, 1926; Zlotnik, 1948; Zamboni, 1974). Over 105 years, TZPs were documented as being present, with very few studies characterizing them. Only in the discovery of tunneling nanotubules (TNTs) Field (Hurtig et al., 2010) did TZPs come into the foreground of cell-to-cell communication research. In 2014, Macaulay et al. published a characterization study on TZP structure via a combination approach utilizing scanning electron microscopy, confocal microscopy, immunofluorescence, *in situ* hybridization, transmission electron microscopy, and autoradiography (Macaulay et al., 2014). According to their results, TZPs have an actin filament backbone and are much larger than the previously documented fine intercellular structures (20-500 nm), with a diameter of 2 μm. Transmission electron microscopy revealed TZPs invaginated inside the oocyte without membrane fusion and are held in place by adherent-like structures on the oocyte membrane in combination with extending microvilli that envelop the projection bulb. Furthermore, an electron-dense material was visualized in the antrum of the TZPs, possibly indicating the presence and transfer of protein aggregates.

In 2019, Baena and Teraskai performed the most extensive TZP characterization study to date (Baena and Terasaki, 2019). They combined scanning electron and transmission electron microscopy with imaging software and custom scripts. Through their investigation, they were able to generate computer models for the complex communication network utilized within the

mammalian follicle. Their computer models concluded that most TZPs protruding from GCs do not reach the oocyte and branch off and form gap junctions with each other. Those that reach the oocyte are usually contacted on their shaft by the oocyte microvilli corroborating previous findings (Macaulay et al., 2014). Surprisingly, their model discovered that GCs possess randomly oriented cytoplasmic projections strikingly similar to TZPs. Therefore, they propose that GCs use cytoplasmic projections to search for the oocyte, and the CCs differentiation directly results from the contact-mediated paracrine interaction with the oocyte.

Hormone dependence of the antral follicle: Throughout development, ovarian follicles are regulated by endocrine, paracrine, and autocrine factors (Edson et al., 2009). Before antral formation, follicular growth is independent of gonadotropins. However, antral follicles require gonadotropin support to reach preovulatory status and ovulation once formed. Following an increase in GnRH secretion from the surge center of the hypothalamus, heterodimeric glycoprotein hormones follicle-stimulating hormone (FSH) and LH are secreted by the anterior lobe of the pituitary gland. FSH and LH are glycoproteins comprised of distinct β-subunits and a common α-subunit and are required for stage-dependent regulation of follicular development (Matzuk and Li, 2013).

In antral follicles, FSH is required for GC proliferation, LH receptor expression, and estradiol production (Piprek, 2016). FSH initiates the classical adenylyl cyclase (AC)/cAMP/protein kinase A (PKA) pathway when it binds to its receptor, causing phosphorylation and activation of the transcription factor cAMP-response element binding protein (CREB). Numerous target genes are upregulated upon phosphorylation, including aromatase and LH receptor (Piprek, 2016). Following genetic ablation of FSHβ or FSH receptors, follicles cannot develop to the antral stage without affecting preantral folliculogenesis (Kumar et al., 1997; Dierich

et al., 1998). In contrast, LH plays essential roles in antral follicle development, ovulation, and luteinization (Matzuk and Li, 2013). Specifically, critical enzymes within the steroidogenesis pathway are under LH control, namely; steroidogenic acute regulatory protein (STAR) (responsible for transporting cholesterol to the inner mitochondrial membrane), CYP11A1 (converts cholesterol to pregnenolone), CYP17A1 (converts pregnenolone to dehydroepiandrosterone [DHEA]), and 3β-hydroxysteroid dehydrogenase (3β-HSD, converts DHEA into androstenedione) (Piprek, 2016).

Oogenesis: Maturation of the Female Germ Cell

What was once referred to as the passenger now takes the front seat as the driver. Within the follicle, the oocyte communicates with adjacent cumulus cells via gap junctions and paracrine signaling to dictate CC phenotype and lineage while maintaining their appropriate differentiation status (Matzuk and Li, 2013). This bidirectional signaling network is essential for folliculogenesis, oocyte growth, and the acquisition of oocyte developmental competence. Oocytes regulate various follicular functions through oocyte-secreted factors (OSFs), including growth and proliferation, apoptosis, differentiation and steroidogenesis, metabolism, and oocyte maturation.

Follicular cell growth and proliferation are vital features of follicular development. In 2006, Gilchrist et al. concluded that GDF9 and GDF9-related molecules using the TGFβ/activin/GDF9 type-I receptors, ALK4 and 5, and activation of the SMAD2/3 pathway are the indispensable oocyte paracrine signals required for oocyte-stimulation of GC proliferation (Gilchrist et al., 2006). Further, in mice, phosphorylation of the SMAD2/3 linker region by extracellular signal-regulated kinases 1 and 2 (ERK1/2) mediates GDF9 activation of the SMAD2/3 pathway (Sasseville et al., 2010). With the literature complied, it is widely agreed upon that an intrinsic developmental program dictated by the oocyte controls GC proliferation.

Apoptosis, or programmed cell death, is a genetically controlled cellular death occurring naturally throughout ovarian folliculogenesis. As follicles leave the PMF pool and continue toward ovulation, most undergo atresia, a process mediated by apoptosis (Matzuk and Li, 2013). Current research dictates that extensive apoptosis among CCs contributes to an unfavorable microenvironment resulting in follicular atresia. A study conducted in the early 2000s reported evidence supporting the oocytes' roles in preventing cumulus cell apoptosis. This group found that oocyte removal from the cumulus-oocyte complex (COC) increased apoptosis among CCs (Hussein et al., 2005). Further, they found that the low incidence of apoptosis within CCs was due to establishing a paracrine network of BMP growth factors and their binding proteins, specifically oocyte-secreted factors BMP6 and BMP15 (Hussein et al., 2005). Collectively, these data further support the dogma that oocytes secrete paracrine factors to establish and maintain an immediate microenvironment distinct from the rest of the follicle (Eppig, 2001).

Before antral formation, the GC population is relatively homogeneous. However, with the establishment of an antrum, the GC population is separated into two functional cell types, the mural GC (mGCs), which are responsible for steroidogenesis, and the CCs, which are adjacent to the oocyte (Piprek, 2016). From a molecular standpoint, mGCs express higher levels of luteinizing hormone/choriogonadotropin receptor (*LHCGR*), steroidogenic enzyme P450 side-chain cleavage enzyme (*CYP11A1*), and immune marker CD34 antigen (*CD34*). In contrast, CCs express more abundant anti-Mullerian hormone (*AMH*) and androgen receptor (*AR*) (Matzuk and Li, 2013). Again, the oocyte is believed to be the main driving force establishing the differentiation of the two GC populations (Diaz et al., 2007).

Antral follicles rely on gonadotropins FSH and LH secreted from the anterior pituitary for their development and ovulation. It has long been hypothesized that the oocyte regulates

steroidogenesis and luteinization of GCs based on observations from a study that removed follicular oocytes from estrous rabbits, resulting in the luteinization of GCs (El-Fouly et al., 1970). Three days after the ovariectomy, the lutein tissue produced progesterone at the same level as a corpora lutea three days after natural ovulation. Further supporting this notion, OSFs prevent *LHCGR* expression in CCs, restricting its expression to mural GCs. Following oocytectomy, *LHCGR* expression in the CCs and progesterone production increased (Eppig et al., 1997).

In 1998, a study demonstrated that during follicular development, the oocyte secrets a factor with steroid-regulating activity in increasing amounts; however, the CCs' responsiveness to this factor declines during luteinization (Vanderhyden and Macdonald, 1998). Later studies would characterize the long-sought-after oocyte-derived luteinization inhibitors as BMP family members, specifically GDF9 and BMP15 (Otsuka et al., 2011). In the mouse, recombinant GDF9 promotes progesterone production in the GCs (Elvin et al., 1999). In the rat GCs, GDF9 stimulates basal progesterone and estradiol production while suppressing FSH-stimulated steroidogenesis (Vitt et al., 2000). In cattle, GDF9 induced by insulin-like growth factor 1 (IGF1) inhibited GC production of progesterone and estradiol (Spicer et al., 2006). Like GDF9, BMP15 inhibits FSH-induced progesterone synthesis and other steroidogenesis enzymes such as STAR and CYP11A1; however, BMP15 does not affect FSH-stimulated estradiol production (Matzuk and Li, 2013). More recently, serum concentrations of GDF9 and BMP15 have been associated with the number of oocytes retrieved during IVF and are being considered for their potential clinical use as biomarkers (Shamsa et al., 2022).

Commonly called *nurse cells*, GCs, specifically CCs, are known to nurture the oocyte. For example, murine and bovine oocytes prefer to utilize pyruvate as an energy source the CCs produce. In contrast, porcine oocytes use glucose as their primary substrate for energy production

(Shi and Sirard, 2022). For years, evidence suggested oocytes and CCs worked together to utilize glucose; however, the molecular mechanisms remained unknown until evidence of OSFS, BMP15, and fibroblast growth factor 8B (FGF8B) cooperating in promoting glycolysis in CCs was reported (Sugiura et al., 2007). Another synergistic activity between oocytes and CCs is cholesterol biosynthesis, with the mRNA abundance of multiple genes involved in the cholesterol biosynthesis pathway upregulated in CCs compared to oocytes (Su et al., 2008). In addition, in *vitro* studies using mice have demonstrated that BMP15 and GDF9 can increase cholesterol biosynthesis in CC (Su et al., 2008). These data taken together suggest that mice oocytes are deficient in cholesterol and, under their direct influence, rely on supplementation from nearby CCs during development.

A decrease in triglyceride, phospholipids, cholesterol, and total lipids during oocyte maturation suggests an essential role for lipids during oocyte maturation (Shi and Sirard, 2022). Studies investigating genes involved in lipid metabolism were conducted on porcine and bovine ovaries (Uzbekova et al., 2015; Bertevello et al., 2018) and revealed diverse transcription patterns of genes related to fatty acid metabolism in the different follicular compartments. These data suggest that the various follicular compartments may play a role in lipid homeostasis. More recently, a study examined the ability of two model OSFs, cumulin, and BMP15, to regulate oocyte maturation and cumulus-oocyte cooperativity (Richani et al., 2022). They revealed that exposure to the OSFs during maturation altered the proteomic and multispectral autofluorescence profiles of both the oocyte and CCs. In the oocytes, cumulin significantly upregulated proteins involved in the nuclear function. In the CCs, both OSFs caused marked upregulation of various metabolic processes, including lipid, nucleotide, and carbohydrate metabolism, with downregulation of mitochondrial metabolic processes.

In addition to glycolysis and cholesterol biosynthesis, the oocyte is also deficient in certain amino acids, such as L-alanine and L-histidine (Matzuk and Li, 2013). The CC provides metabolic support to the oocyte through well-established communication lines. The most cited transferred molecules are cyclic nucleotides cAMP and cGMP, amino acids, and energy substrates, specifically lactate, pyruvate, and phosphocreatine (Marchais et al., 2022). The CCs play essential roles in the uptake of these amino acids and their subsequent delivery to the oocyte via TZPs, highlighting another critical role in the intricate relationship between the two cell types.

A signaling cascade surrounding a universal cytoplasmic maturation-promoting factor (MPF) that plays a vital role in maturational events in the oocyte, specifically germinal vesicle breakdown (GVBD) is the long-standing hypothesis for oocyte meiotic arrest regulation (Jones, 2004). MPF is a heterodimer composed of cyclin-dependent kinase 1 (CDK1) and Cyclin B (Pan and Li, 2019). In the quiescent oocyte, continued production and transfer of cAMP from the surrounding somatic cells maintain MPF inactivation through the following signaling cascade (Pan and Li, 2019). High levels of cAMP continuously activate PKA, resulting in the phosphorylation and activation of nuclear kinase Weel/MytI. This activation inactivates cell division cycle 25B (CDC25B), the activator of cyclin-dependent kinases. Lack of CDK1 activation in MPF by CDC25B, MPF remains inactive. The continuous inactivation of MPF via delivery of somatic cell-derived cAMP results in a fully-grown oocyte arrested with its chromosomes at the diplotene stage. The oocyte remains in this intricate balance of inactivation, beginning in the PMF, and remains arrested until the surge of pituitary-derived LH is released (Dekel et al., 1981; Mehlmann, 2005). In addition to LH secretion, FSH stimulation increases permeability in gap junctions by increasing trafficking and assembly of connexin43 (CX43) to plasma membrane gap junctional plaques

disrupting the delivery of cAMP inhibitory signals from the somatic cells to the oocyte (Burghardt et al., 1995).

Since the turn of the century, research has continued to investigate the regulation of oocyte meiotic arrest. The current perspective is as follows (Pan and Li, 2019). It is still widely accepted that elevated levels of cAMP are required to maintain meiotic arrest at dictyate prophase I. Further, the oocyte utilizes a unique PGR-Gs-NDCY system to produce adequate endogenous cAMP and inhibit phosphodiesterase (PDE3) activity. While oocyte-derived cAMP remains essential to maintain meiotic arrest, cGMP produced by the surrounding CCs is required for maintaining elevated cAMP levels through the suppression of PD43 activity in the oocyte. The mGC and CCs express NPPC (a cognate ligand of the natriuretic peptide receptor) and its receptor NPR2. The selective activation of the NPPC/NPR2 system aids in producing cGMP within GCs. To further elevate intraoocyte cGMP, inosine-5'-monophosphate (IMP) dehydrogenase (IMPDH) converts IMP to guanosine monophosphate (GMP) to create more substrate for NPR2 activity. The oocyte regulates the entire system by monitoring the NPPC/NPR2 system activity and IMPDH actions by secreting GDF9 and BMP15. Thus, the oocyte drives the surrounding CCs to synthesize cGMP while producing its cAMP via its GPR-Gs-ADCY cascade, precisely maintaining meiotic arrest at prophase I of meiosis in preparation for the LH surge.

Simultaneously with the follicular functions regulated by oocytes through the OSFs mentioned above, oocyte maturation occurs. Oocyte maturation can be broken into three stages further to dissect the association of follicular and intraoocyte events: (1) meiotic maturation, (2) cytoplasmic maturation, and (3) molecular maturation (Sirard et al., 2006). Meiotic maturation is the cascade of nuclear events previously induced by the LH surge or the oocyte removal from the follicle. Cytoplasmic maturation begins when the oocyte ceases RNA and protein synthesis by

modifying the transcription and translation machinery depicted by nucleolus condensation, RNA stabilization, and ribosome depletion (Hyttel et al., 1986; Hyttel et al., 1989; Fair et al., 1995). For perspective, the half-life of mRNA in different somatic cells is variable but is generally short (a few hours) (Kidder and Pedersen, 1982). Following modifications during cytoplasmic maturation, the oocyte becomes rich in highly stable mRNA with a half-life of ~2.5 weeks (Piko and Clegg, 1982). The second phase of cytoplasmic maturation occurs close to the LH surge when there is a re-distribution of organelles, specifically the mitochondria and cortical granules (Sirard et al., 2006). The third and final stage of oocyte maturation is known as molecular maturation and is the least defined. The current model dictates that specific mRNAs, proteins, and other regulatory molecules are produced and stored in the oocyte's cytoplasm as a reservoir in preparation for post-fertilization events (Sirard et al., 2006).

Ovulation: Release of the Mature Oocyte

For a follicle to ovulate, progesterone concentrations must be low < 1 ng/mL; (Ireland and Roche, 1982) to allow for an increase in LH pulse frequency to continue supporting follicle growth. In response to the increase in LH pulse frequencies, follicles secrete rising levels of estradiol that trigger a surge release of GnRH followed by LH, resulting in the ovulation of a dominant follicle (Fortune et al., 1988). Immediately following the LH surge, induced dephosphorylation and inactivation of the NPR2 guanylyl cyclase results in a rapid decrease of cGMP first in CCs, followed by the oocyte as the signal traverses the TZPs (Pan and Li, 2019). The rapid decline of intraoocyte cGMP causes the release of oocyte-derived factors, suppressing critical genes in the CCs, including *NPR2* and *LHR*, further enhancing the effects of LH stimulation. Collectively, these signals collaborate to propagate the results of the LH surge throughout the follicle, ensuring the continuation of meiosis.

The CCs respond to the LH surge by synthesizing a cumulus matrix enriched in hyaluronan (HA). This expansion surrounding an embedded oocyte is required to initiate successful ovulation. The LH surge induces essential genes such as pentraxin 3 (*PTX3*), hyaluronan synthase 2 (*HAS2*), tumor necrosis factor α-induced protein 6 (*TNFAIP6*), and prostaglandin-endoperoxide synthase 2 (*PTGS2*) to aid in producing the cumulus matrix (Richards, 2005; Hernandez-Gonzalez et al., 2006). Additionally, PTGS2 is a critical enzyme for the biosynthesis of prostaglandins, which are required for follicular rupture and ovulation. As seen previously, the OSFs GDF9 and BMP15 regulate gene expression, promoting CC expansion and ovulation through the induction of the aforementioned vital genes (Matzuk and Li, 2013). Therefore, through paracrine signaling, the oocyte modulates CC expansion as an integral regulator of all aspects of ovarian folliculogenesis.

Early Embryonic Development: Fusion of the Gametes for the Next Generation

At the end of oocyte maturation, transcriptionally quiescent oocytes at the metaphase II (MII) stage are released from their follicle and journey to the uterus. Successful fertilization occurs in the ampulla of the oviduct when motile sperm penetrate the cumulus oophorus, bind to the zona pellucida, and enter the ovum. With the fusion of the gametes, the zygote enters the next phase of its development, undergoing critical early embryonic development events that ultimately decide its fate.

Remarkably, the zygote begins transcriptionally silent, with all initial developmental events controlled by stored maternal RNAs and proteins collectively referred to as maternal-effect genes (Li et al., 2010). The maternal transcripts stored in the cytoplasm allow for progression through the first embryonic division in mice (Braude and Pelham, 1979) and humans (Vassena et al., 2011) and the third embryonic division in rabbits (Manes, 1973), sheep (Crosby et al., 1988), and cattle (Barnes and First, 1991). Due to their origins, the initial pool of zygotic transcripts before

zygotic genome activation (ZGA) is collectively called the maternal transcriptome (Tora and Vincent, 2021).

The maternal transcriptome consists of maternal-effect genes transcribed during oogenesis and enables the activation of the embryonic genome. To differentiate between maternal and embryonic transcripts, embryos are co-cultured with α-amanitin. This RNA polymerase inhibitor results in a developmental block during the maternal to-zygotic transition (Barnes and First, 1991). Although some maternal effect genes are expressed solely in female gametes, others can be detected following the activation of the embryonic genome, complicating the differentiation between maternal and embryonic origins (Li et al., 2010).

Maternal-effect genes were first described in *Drosophila* in the 1980s, branching into other model organisms in the 1990s (Li et al., 2010). However, it was not until 2000 that maternal-effect genes were first described in mammals (Christians et al., 2000; Tong et al., 2000). Following fertilization, maternal factors function to (1) process the male genome, (2) remove the maternal transcriptome, and (3) activate the embryonic genome. Failure to complete these three tasks in mice results in arrested progression during cleavage-stage embryogenesis (Li et al., 2010). Well-characterized maternal-effect genes include *HSF1* (Christians et al., 2000), *MATER* (Tong et al., 2000), *FIGLA* (Huntriss et al., 2002), *JY-1* (Bettegowda et al., 2007), *KPNA7* (Tejomurtula et al., 2009), *NOBOX* (Tripurani et al., 2011), and *ZNFO* (Hand et al., 2017). Early cleavage events post-fertilization requires these maternal-effect genes. They have similar mRNA and protein expression profiles: abundant presence in the oocyte and early-stage embryos before embryonic genome activation, followed by a sharp decrease in expression after ZGA.

With the fusion of the gametes, the embryo begins its first critical transition in development as it switches from dependence on maternal proteins stored in the oocyte to proteins produced by

the activation of the embryonic genome. To accomplish this transition, different machinery and mechanisms are implemented to overhaul the maternal transcriptome. Following oocyte growth, the steps mediating the initiation of oocyte maturation to the activation of the zygotic genome rely upon the post-transcriptional regulation of the stored maternal transcripts via two main mechanisms: (1) activation of translation by cytoplasmic re-adenylation and (2) degradation of maternal mRNA initiated by deadenylation (Tora and Vincent, 2021). The degradation of maternal RNAs completed by the 8-16 cell stage (Barnes and First, 1991) in cattle paired with its ZGA constitutes the maternal to zygote transition (MZT). To successfully transition from maternal to zygotic and erasure the oocyte's identity, waves of degradation of specific RNAs associated with translation activation of other RNAs are essential (Tora and Vincent, 2021). These waves are crucial for removing transcripts that are no longer useful and/or could become detrimental to downstream developmental events and pave the wave for newly transcribed regulators (Svoboda et al., 2017).

In mice, ZGA and patterns of maternal RNA degradation are accompanied by two major transient waves of *de novo* transcription (Hamatani et al., 2004). The first wave corresponds to ZGA appearing in the 2-cell stage mouse embryo. The second wave, named mid-preimplantation gene activation (MGA), proceeds with dynamic morphological and functional changes within the embryo during the morula to blastocysts stage. In contrast to mice, cattle exhibit ZGA at the 8- to 16-cell stage, indicated by significant changes in the ultrastructure of blastomere nucleoli and its pattern of protein synthesis (Kaňka et al., 2009). With observations corroborating previous findings in the mouse, it is accepted that there is a low transcriptional activity (minor genome activation) between the 1- and 4-cell bovine embryo followed by the major genome activation at the 8-cell stage (Kaňka et al., 2009).

As noted above, ZGA relies heavily on the degradation of maternal RNAs. Although the exact mechanisms controlling RNA degradation remain a popular topic among researchers, various pathways exist. One mechanism utilizes small non-coding RNAs, specifically microRNAs (miRNAs) and small interfering RNAS (siRNAs). These small non-coding RNAs are loaded into the RNA-inducing silencing complex (RISC) and then used by the RISC complex to target specific mRNAs. Once found, targeted mRNAs are cleaved or translationally repressed. Other means of degradation occur through the ubiquitin-proteasome pathways (Suzumori et al., 2003) or by macroautophagy which causes proteins and organelles to become captured by double-membrane vesicles (autophagosome) that fuse with the cell's lysosomes causing degradation (Li et al., 2010).

In addition to massive shifts in the embryo's transcriptional program, widespread changes in chromatin structure and epigenetic information restructure the embryonic epigenome (Halstead et al., 2020). The process of reprogramming erases the maternal and paternal epigenetic code leaving an open chromatin landscape providing a clean slate for the embryonic epigenome. Moreover, the chromatin structure defines the cell's identity and function through cell-specific gene expression patterns dictated by the transcriptional machinery's ability to operate within the given landscape (Eckersley-Maslin et al., 2018). Overall, the zygote is enriched in epigenetic factors linked to relaxed chromatin. In contrast, factors associated with chromatin compaction become more widespread during ZGA, insinuating a more permissive chromatin landscape in pre-ZGA embryos (Halstead et al., 2020).

With ZGA and chromatin remodeling working interdependently as development progresses, enrichment of chromatin-accessible sites demonstrates different motif enrichment patterns implicating distinct sets of transcription factors (TFs) in either human (OTX2, GSC, POU5F1) (Wu et al., 2018) or mice ZGA (RARG, NR5A2, ESRRB) (Wu et al., 2016). Although

some TFs appear to regulate ZGA across multiple species, such as Kruppel-like factors (KLFs), double homeobox (DUX), ZSCAN4, and CTCF, the level of conservation among mammalians remains undefined (Halstead et al., 2020). With variation among species, significant implications arise when drawing conclusions across model systems.

With a growing interest in the global chromatin landscape, the development of low input or single-cell assays profiling chromatin remodeling provides a genome-wide map of accessible chromatin in gametes and early embryos in humans and mice (Lu et al., 2016; Wu et al., 2016; Guo et al., 2017; Inoue et al., 2017: 27; Jachowicz et al., 2017; Jung et al., 2017; Wu et al., 2018; Liu et al., 2019). Unsurprisingly, these studies have revealed that gametes and embryos have highly dynamic chromatin landscapes. Currently, studies are integrating chromatin accessibility with the transcriptome to construct regulatory networks that map chromatin architecture and identify TFs associated with early embryonic development and lineage specification (Wu et al., 2016).

In 2021 one of the first groups to study the landscape of accessible chromatin in bovine oocytes and early embryos published a genome-wide map of accessible chromatin revealing four distinct profiles: (1) low accessibility in oocytes (GV and MII) and during minor ZGA at the 2- to 4-cell stage, (2) high accessibility during major ZGA at the 8- to 16-cell and morula stage, (3) less accessibility at the blastocysts stage, and (4) the highest accessibility in elongating embryos (Ming et al., 2021). Additionally, most ATAC-seq peaks were detected in the intergenic and intron regions. Although regarded as “junk DNA,” studies have demonstrated that mutations in such loci can alter chromatin state and DNA conformation (Freedman et al., 2011; Cowper-Sal·lari et al., 2012; Schierding et al., 2014). Furthermore, “junk DNA” has been documented to comprise long-

range regulatory elements that interact with distal genes to influence their expression (Dryden et al., 2014).

Lastly, this group examined chromatin signatures associated with bovine *in vivo* and *in vitro*-derived blastocysts to understand better the epigenetic mechanisms leading to embryonic loss and pregnancy failure observed among *in vitro*-produced embryos. Although the global accessibility of chromatin did not vary much between *in vivo* and *in vitro*-derived embryos, the chromatin accessibilities of specific genes were dramatically different (Ming et al., 2021). Specifically, differential expression was seen among genes involved in protein metabolism, macromolecule assembly and localization, organelle organization, and mitochondrion function (Ming et al., 2021). Interestingly, their results suggest a dysregulation of chromatin dynamics due to the *in vitro* manipulation during bovine early embryo development.

The Non-Coding Genome: Junk or the Missing Piece?

Non-coding RNAs (ncRNAs) are RNA molecules that do not code for a protein. What once was thought of as "genetic noise" from leaky transcriptional machinery has more recently come to the foreground of modern research in molecular biology due to its broad versatility in regulating gene expression. With estimates for protein-coding genes as high as 100,000 in the mid-1980s, it was not until after the human genome project that researchers realized that, in general, only 1.2% of the human genome represents protein-coding exons, whereas 24% and 75% attributed to intronic and intergenic non-coding DNA (Rao, 2017). NcRNAs are characterized by specific expressions during certain developmental stages in certain tissues or disease states and play multiple roles in gene expression regulation (Rao, 2017). With the advent of deep sequencing technology, the field of ncRNAs continues to rapidly and exponentially expand. As a result, the classification system is constantly evolving to include discoveries, and thus there are multiple

methodologies to classify non-coding RNAs. According to a study in 2019, there are two broad categories assigned to ncRNAs based on their functionalities; (1) housekeeping ncRNAs – RNAs that are abundantly and ubiquitously expressed in cells, primarily regulating generic cellular functions (i.e., ribosomal RNA [rRNA] and transfer RNA [tRNA]) and (2) regulatory ncRNAs – RNAs that are usually considered as key regulatory RNA molecules that function as regulators of gene expression at epigenetic, transcriptional, and post-transcriptional levels (i.e., microRNA [miRNA], piwi-interacting RNA [piRNA], long non-coding RNA [lncRNA]) (P. Zhang et al., 2019). This review will focus on lncRNAs' roles in reproduction and early embryonic development.

According to a review published in 2015, there are currently multiple classes and categories of lncRNAs. Classification is based on several criteria and features, including transcript length, association with annotated protein-coding genes, other DNA elements of known functions; repeats, mRNA resemblance, biochemical pathway or stability, sequence or structure conservation, biological states, subcellular localization, and function (St. Laurent et al., 2015). As research pushes forward, the accepted lncRNA properties and criteria for their identification and naming continue to evolve. Still, it is generally accepted that lncRNAs exhibit the following features (Taylor et al., 2015): (1) transcript lengths are > 200 nucleotides with a median size of ~500 nucleotides; 98% are spliced, with 80% having 2-4 exons and a majority of them exist as a single isoform. (2) Most are polyadenylated. (3) Many show nuclear enrichment and chromatin association, although cytoplasmic forms exist; coding potentials are low as the open reading frame (ORF) is absent. (4) Cumulative abundance is lower when compared to mRNAs, and expression is more tissue-specific. (5) Some lncRNAs have a circular structure.

The biogenesis of lncRNAs is like that of mRNAs. RNA polymerase II (RNA pol II) transcribes them from genomic loci with similar chromatin states; they are often 5' capped, spliced, and polyadenylated at the 3' end. In most cases, lncRNAs lack any biochemical distinction from mRNAs besides the absence of a translated ORF (Quinn and Chang, 2016). Some general trends that discriminate lncRNAs from mRNAs include lncRNAs tend to be shorter than mRNAs, have fewer but longer exons, are expressed at relatively low levels, and exhibit poorer primary sequence conservation (Quinn and Chang, 2016). More specifically, lncRNAs can be transcribed from intergenic, exonic, or distal protein-coding regions of the genome by RNA pol II (Dhanoa et al., 2018). Following transcription, the premature lncRNA undergoes processing to be 3' polyadenylated and receives a methyl-guanosine cap on its 5' end. After processing, the lncRNA will often undergo alternative splicing.

LncRNAs diverge from mRNA in their ability to exhibit more specific expression profiles expressed in a cell type-, tissue-, developmental stage-, or disease state-specific manner (Quinn and Chang, 2016). Furthermore, lncRNA expression patterns often correlate with mRNA expression patterns both in *cis* and *trans* suggesting that lncRNAs may be co-regulated in different expression networks (Quinn and Chang, 2016). Regarding chromatin state, lncRNAs appear to follow the same rules as protein-coding genes. Expressed lncRNA promoters are enriched for active histone modifications similar to their protein-coding counterparts (Quinn and Chang, 2016). However, when comparing promoters, mRNA promoters are bidirectional in that their RNA pol II can generate a transcript in either direction. In contrast, most lncRNAs display a bias for productive splicing and elongation of sense transcripts (Quinn and Chang, 2016).

Things become more complicated during the post-transcriptional processing phase of lncRNA biogenesis. To reach their mature forms, RNA transcripts (mRNA and lncRNA) undergo

extensive co-transcriptional and post-transcriptional processing events such as 5' capping, splicing, polyadenylation, and base modifications (Quinn and Chang, 2016). In addition, some lncRNAs will experience alternative forms of processing that thus distinguish them from other RNA transcripts. Examples include (A) RNase P cleavage of tRNA precursors during maturation, (B) the formation of secondary structures that dictate future functions, (C) the generation of circular RNA through nonsequential exon-exon back-splicing, (D) ciRNAs formed through the circularization from stabilized introns after canonical splicing that formed branched intronic RNA, (E) formation of exon-intron circRNAs that retain unspliced introns, and the (F) generation of sno-lncRNAs (Quinn and Chang, 2016).

As research continues, taxonomies will inevitably be redefined to construct a more organized classification system for lncRNAs. Until then, many researchers have discussed lncRNAs in the context of their functional roles in regulating gene expression. The following sections provide examples of molecular processes controlled by lncRNAs at the transcriptional and post-transcriptional levels.

Regulation at the Transcriptional Level: Many lncRNAs have been characterized to regulate expression by recruiting epigenetic factors, functioning as protein complex scaffolds, sequestering signals, and acting as decoys. The most prominent example of gene silencing using a protein scaffold is exhibited by the ncRNA *XIST* strictly *cis*-acting ability to inactive the second X chromosome in females. To do so, *XIST* recruits the Polycomb group proteins (PcG) to trimethylated histone H3 on lysine 27 (H3K27me3) to render the chromosome transcriptionally silent (Plath et al., 2003). Once recruited, the Polycomb Repressive Complex 2 (PRC2), comprised of H3K27 histone methyl transferase (HMTase) EZH2 and core components of Suz12 and EED, initiates the histone modification allowing Polycomb Repressive Complex 1 (PRC1) to maintain

the modification and promote chromosome compaction (Sparmann and van Lohuizen, 2006). Once initiated, lncRNA *FIRRE* must sustain previously established H3K27me3 on the inactive X chromosome to maintain compaction (Yang et al., 2015). In contrast, *trans*-acting *HOTAIR* binds PRC2 to deposit H3K27me3 40 kilobases downstream at the *HOXD* chromosomal loci rendering it silent (Rinn et al., 2007). In addition to modifying histone states, lncRNAs provide signals for DNA methylation deposition. For example, GADD45A, a stress response protein that promotes active DNA demethylation, directly interacts with the R-loop formed by lncRNA *TARID* at the *TCF21* promoter to recruit the demethylation machinery to promoter containing CpG islands (Arab et al., 2019). Alternatively, lncRNAs prevent DNA methylation deposition by sequestering DNA methyltransferase 3B (DNMT1) (Taylor et al., 2015). A study in 2016 demonstrated that *lncPRESS1* acts as a "decoy" to sequester SIRT6, a chromatin-bound deacetylase, to maintain H3K56ac/K9ac enrichment at promoters of ESC-specific genes and protect pluripotency (Jain et al., 2016). Lastly, lncRNAs directly interact with TFs to regulate gene expression. LncRNAs *GAS5* (Kino et al., 2010) and *PANDA* (Hung et al., 2011) directly bind TFs limiting their access to their DNA targets. Contrary to lncRNA *BCAR4,* which enables TF recruitment to DNA (Xing et al., 2014).

Regulation at the Post-Transcriptional Level: LncRNAs can regulate gene expression not only at the transcriptional level but also at the post-transcriptional level. For example, *PNCTR* is upregulated in cancer cells and antagonizes the splicing regulation function of PTBP1, a natural repressor of differentiation-specific alternative splicing events, to increase cell survival (Yap et al., 2018). Additionally, *PNCTR* contains hundreds of PTBP1-specific motifs allowing it to sequester a substantial faction of cellular PTBP1, further inhibiting splicing within the cell. Another form of regulation at the post-transcriptional level is through microRNA sponges. Under normal

conditions, ZEB1 and ZEB2, known TFs associated with the epithelial-mesenchymal transition (EMT), are regulated by *mir-205*. However, in cancerous conditions, lncRNA *PNUTS* levels increase, competitively binding *mir-205* and making it unavailable to its targets ZEB1 and ZEB2. When ZEB1 and ZEB2 cannot be degraded, EMT proceeds, and cancer progresses (Grelet et al., 2017). *MALAT1* interacts with pre-messenger RNAs at active gene loci, suggesting it may influence RNA processing by recruiting or modifying other localized proteins (Engreitz et al., 2014). Additionally, *MALAT1* binds serine-arginine splicing factors (SRSFs), inducing their localization within nuclear speckles, and following its depletion, changes in alternative splicing of endogenous mRNAs are observed (Tripathi et al., 2010).

The Functional Roles of lncRNAs in Reproduction and Early Embryonic Development

Given the diverse roles of lncRNAs essential throughout all bodily systems, there is no surprise by their presence in reproductive tissues. Although experiments are ongoing, studies investigating lncRNAs in reproduction outside of murine and human studies remain underrepresented. Therefore, this review will focus on the functional and mechanistic roles of various lncRNAs throughout reproductive tissues, cells, and early developmental processes, focusing on multiple species.

PGC Specification: As mentioned previously, PGCs are the pluripotent cells that migrate along the gonadal ridge, where they will ultimately contribute to the developing gonad. Two proteins, *BLIMP1/PRDM1*, and *PRDM14*, are required for PGC specification in mice (Felici, 2009). In mice, *BLIMP1/PRDM1* acts as a transcriptional repressor to block genes involved in somatic development while binding near other genes necessary for PGC specification. Mouse PGCs have 5,046 *BLIMP1/PRDM1* binding sites; 313 are associated with non-coding genes and remain uncharacterized (Magnúsdóttir et al., 2013). Due to lncRNAs association with repressing

transcription, it is speculated that *BLIMP1/PRDM1* binds lncRNAs to activate targets (Taylor et al., 2015) indirectly. In 2020, a study in chickens using a combined approach of single-cell sequencing paired with molecular validation studies identified *lncPGCAT-1* as a regulator of PGC formation (Zuo et al., 2020). Furthermore, they found that *lncPGCAT-1* regulated PGC formation by modulating *MAPK1* and interacting with *ILF3* to activate the MAPK signaling pathway.

Once they arrive at the gonadal ridge, PGCs begin differentiating into oogonia. RNA-binding protein, DAZL, acts upon germ cells, making them responsive to extrinsic factors secreted by cells within the ovary-mesonephros regions to initiate meiosis. DAZL binds RNA in the cytoplasm (Collier et al., 2005) and translocates into and out of the nucleus during germ cell development (Reijo et al., 2000). Due to interactions with RNA in the cytoplasm and nuclear compartment, DAZL may regulate coding and non-coding RNAs essential to PGC formation and/or differentiation.

Folliculogenesis: With the development of the follicle, three different cell types emerge, working in unison. A basement membrane lined with TCs encapsulates the ovum surrounded by mGCs and CCs. Recently, studies have characterized lncRNAs within the follicles and mGCs of pigs, mice, humans, sheep, and chickens. A study using pigs in 2019 reported that following Zearalenone exposure, there was a dramatic increase in apoptosis within mGCs induced by lncRNAs activating the JAK2-STAT3 signaling pathway (F.-L. Zhang et al., 2019). Later that year, a different group reported that lncRNA *Gm2044* promotes 17β-estradiol synthesis in mouse pre-antral follicular mGCs and acts as a *miR-138-5p* sponge to inhibit its direct target, *Nr5a1*, to promote 17β-estradiol synthesis through the activation of *CYP19A1* (Hu et al., 2019). Ongoing studies investigating patients with endometriosis discovered that mGCs with a down-regulation of

MALAT1 expression might decrease oocyte quality by inhibiting GC proliferation via enhancing *P21* expression through activation of the MAPK pathway (Y. Li et al., 2019).

Following a genome-wide analysis of lncRNAs and mRNAs in chicken ovarian follicles, 16,354 mRNAs and 8,691 lncRNAs were obtained, with 160 mRNAs and 550 lncRNAs differentially expressed (Peng et al., 2019). Gene ontology (GO) and Kyoto Encyclopedia of Genes and Genomes (KEGG) enrichment analysis revealed differentially expressed genes involved in ovarian follicular development, including oocyte meiosis, oocyte maturation, and cell cycle regulation. In 2021 researchers reported that lncRNA *FDNCR* directly binds *miR-543-3p*, causing an increase in *DCN* expression and promoting GC apoptosis through inhibition of the TGF-β pathway of Hu sheep (Yao et al., 2021). Moreover, researchers reported that *lnc13814* promoted cell apoptosis in duck GCs by acting as a sponge directly binding *apla-mir-145-4*, causing an increase in DNA damage-inducible transcript 3 (*DDIT3)* expression (Wu et al., 2021). Despite their roles in regulating androgen receptor signaling in prostate and breast cancer (Kumar et al., 2021), lncRNA presence and functional roles within theca cells remain elusive.

Oogenesis: A bidirectional communication system is established between the ovum and surrounding CCs within the mammalian follicle, transmitting messages via gap junctions. A study in 2014 using microscopy revealed an electron-dense material in the antrum of the TZP, suggesting the presence of protein aggregates passing between cell types (Macaulay et al., 2016). Transcriptomic comparisons between GV and MII oocytes reported no significant difference in the overall RNA context between the stages of maturation. However, specific analyses revealed increases in the abundance of 1.8% transcripts in MII oocytes. When three candidate genes were measured in mature intact COCs and denuded MII oocytes, transcripts only accumulated during oocyte maturation when CCs were present, suggesting CCs can act as an exogenous source of

RNA for the oocyte. Furthermore, confocal microscopy validated the presence of RNA-containing particles distributed within the TZPs.

Within the healthy female follicle, the follicular cells interact with the follicular microenvironment and relay signals to the developing oocyte. These signals induce changes within the oocyte to increase its survivability in the dynamic environment. Under stress conditions, intercellular homeostasis is maintained by shuttling stress signals packaged in extracellular vesicles (EVs) to the oocyte to adjust the metabolism to the new environment (De Maio, 2011). Recently, lncRNAs detected in EVs have exposed a dynamic crosstalk among cells in a tumor microenvironment modulating cancer progression and its chemotherapeutic response (Zhang et al., 2020). Knowing that RNA can transfer via EVs between CCs to the oocyte during maturation, regulatory lncRNAs produced by the CCs may have functional roles in oocyte developmental competence and warrant further investigation.

Current studies investigating lncRNA involvement in oocyte maturation focus on bioinformatic analysis to identify candidate genes. In 2020, Wang et al. reported the identification of 1,535 oocyte lncRNAs, and following comparisons to lncRNAs present in bovine tissues, 970 appear to be unique to bovine oocytes (J. Wang et al., 2020). LncRNA *MSTRG.17927* has been identified in ovine oocytes to mediate the regulation of phosphatidylinositol 3-kinase signaling (PI3K) during oocyte maturation (J.-J. Wang et al., 2020). In porcine oocytes following recombinant porcine FSH treatment, a comprehensive analysis of mRNAs and lncRNAs revealed 43,499 mRNAs and 21,703 lncRNAs identified, including 21,300 novel lncRNAs and 403 known lncRNAs with 585 mRNAs and 398 lncRNAs being differentially expressed (Mao et al., 2022). Moreover, lncRNA *MSTRG.3902.1* was identified as the target gene for *NR5A2* and involved in regulating follicular development, ovulation, and estrogen production. A human study collected

CCs from aged women and reported a down-regulation of 28 lncRNAs (Caponnetto et al., 2022). Integrated analysis revealed 11 differentially expressed lncRNAs and mRNAs bound by miRNAs regulating the PI3K-Akt, FOXO, and p53 signaling pathways.

Early Embryonic Development: Following the fusion of gametes, the zygote enters the next phase of its development. The maternal transcriptome drives key early embryonic development events regulated by stored maternal reserves. Recently, lncRNAs have been functionally characterized as critical regulators of ZGA in humans (Bouckenheimer et al., 2016), mice (Hamazaki et al., 2015a), pigs (Zhong et al., 2018), and rabbits (Shi et al., 2021). Karlic et al. reported 1,600 lncRNAs expressed in mice during the oocyte-to-embryo transition, with lncRNAs expressed less than mRNAs and having fewer exons with shorter 5' terminal exons (Karlic et al., 2017). Additionally, they reported that maternal lncRNAs appeared to undergo cytoplasmic polyadenylation, giving rise to trans-acting siRNAs. RNA sequencing identified 800 mRNAs and 250 lncRNAs as differentially expressed from 4-cell and 8-cell goat embryos enriched in terms of the retinoic acid receptor signaling pathway and regulation of pluripotency of stem cells (Deng et al., 2018). Moreover, microinjection of siRNA against *lnc_137* resulted in a developmental arrest. Single-cell RNA sequencing using human pre-implantation embryos and human embryonic stem cells reported 22,687 maternally expressed genes, including 8,701 lncRNAs, of which 2,733 were novel (Yan et al., 2013).

Across the various species presented, the data suggest different lncRNAs have active roles in gene expression during the pre-implantation period; however, many still need to be characterized. As ZGA begins, it is essential for the embryo to not only turn off the maternal transcriptome but also to ensure maternal clearance during MZT. Shi et al. reported stable lncRNA expression in oocytes, 2-cell, 4-cell, and 8-cell stage embryos, significantly decreasing at the

morula stage (Shi et al., 2021). Using comparative analysis tools, GO predicted high enrichment of terms related to translation, RNA processing, peptide metabolic/biosynthesis process, organonitrogen compound biosynthesis process, and amide biosynthetic process. KEGG analysis projected involvement in pathways for the spliceosome, RNA transport, ribosome, pyrimidine metabolism, protein processing in the endoplasmic reticulum, and mRNA surveillance (Shi et al., 2021).

More recently, genome-wide DNA methylation profiles of genes during human pre-implantation embryonic development using reduced representation bisulfite sequencing (RRBS) revealed a majority of both lncRNA and protein-coding genes were demethylated at the 2-cell stage with lncRNA promoters exhibiting a higher degree of methylation than protein-coding genes (Li et al., 2017). Comprehensive analysis suggests that involved lncRNAs regulate gene expression through various molecular mechanisms, including mRNA splicing, translation regulation, and mRNA catabolism.

By examining the literature, there is no doubt that lncRNAs exist in reproductive systems. However, the current focus of livestock model systems remains on lncRNA detection using bioinformatic analysis and comparative analysis tools to predict functional roles. To date, few papers exist exploring the active role of lncRNAs in bovine embryos. In 2014, Caballero et al. reported the expression and intracellular location of three lncRNAs found in bovine oocytes and early embryos. Further, they investigated the functional roles of one lncRNA using siRNA-mediated knockdown in the zygote (Caballero et al., 2014). Expression data revealed that all three lncRNAs were cytoplasmic and highly abundant in the GV and MII oocyte, with one lncRNA exhibiting fluctuations from the zygote to the 16-cell stage. At this point, it disappeared, and the other two lncRNAs showed a steady decrease until their absence at the blastocyst stage. All three

candidate lncRNAs were detected in polyribosomes of both immature and mature oocytes. Following the knockdown of candidate 1, embryos exhibited accelerated developmental kinetics and were considerably larger than the controls (Caballero et al., 2014). These data suggest a functional role in regulating translation in early bovine embryos.

Statement of Problem

In cattle, the fertilization rate is ~90%, with an average calving rate of about 55%, indicating an embryonic-fetal mortality rate of roughly 35% (Diskin et al., 2006). Further, 70-80% of total embryonic loss in cattle occurs during the first three weeks after insemination, particularly between days 7-16 (Spencer, 2013). Thus, early embryonic loss is a significant factor in livestock species' infertility. Growing evidence indicates that the oocyte plays an active role in regulating critical aspects of the reproductive process required for successful fertilization, embryo development, and pregnancy. During early embryogenesis, maternal mRNAs that accumulate in the oocyte during oogenesis play essential roles during the initial stages of embryonic development before the activation of the embryonic genome (Hamatani et al., 2004).

Over the past decade, advancements in technology and the advent of deep sequencing have discovered that a substantial portion of the genome is transcribed; much more than the 1-3% that encodes proteins (Djebali et al., 2012). As a result, lncRNAs, a subclass of ncRNAs, have been identified to play critical roles in various biological processes, including chromatin modification (Plath et al., 2003), regulation of transcription (Kino et al., 2010), alternative splicing (Yap et al., 2018), and regulation of gene expression at post-transcriptional (Engreitz et al., 2014). Additionally, lncRNAs have been functionally characterized as critical regulators of embryonic genome activation in humans and mice (Hamazaki et al., 2015b; Bouckenheimer et al., 2016; Karlic et al., 2017).

To date, bovine oocyte-specific lncRNAs and their corresponding mechanisms required for and utilized by the oocyte and early embryo are poorly understood, and our understanding of the contribution of such factors to oocyte maturation and the maternal-to-embryonic transition during early embryogenesis in cattle is limited. Therefore, the present studies were conducted to identify novel oocyte-specific lncRNAs and elucidate their roles in oocyte maturation and early embryonic development.

REFERENCES

Ancelin, K., U. C. Lange, P. Hajkova, R. Schneider, A. J. Bannister, T. Kouzarides, and M. A. Surani. 2006. Blimp1 associates with Prmt5 and directs histone arginine methylation in mouse germ cells. Nat. Cell Biol. 8:623–630. doi:10.1038/ncb1413.

Arab, K., E. Karaulanov, M. Musheev, P. Trnka, A. Schäfer, I. Grummt, and C. Niehrs. 2019. GADD45A binds R-loops and recruits TET1 to CpG island promoters. Nat. Genet. 51:217–223. doi:10.1038/s41588-018-0306-6.

Aubin, J., A. Davy, and P. Soriano. 2004. In vivo convergence of BMP and MAPK signaling pathways: impact of differential Smad1 phosphorylation on development and homeostasis. Genes Dev. 18:1482–1494. doi:10.1101/gad.1202604.

Ayalon, N. 1978. A Review of Embryonic Mortality in Cattle. J. Reprod. Fertil. 54:483–493.

Baena, V., and M. Terasaki. 2019. Three-dimensional organization of transzonal projections and other cytoplasmic extensions in the mouse ovarian follicle. Sci. Rep. 9:1262. doi:10.1038/s41598-018-37766-2.

Baker, T. G. 1963. A Quantitative and Cytological Study of Germ Cells in Human Ovaries. Proc. R. Soc. Lond. B Biol. Sci. 158:417–433.

Barnes, F. L., and N. L. First. 1991. Embryonic transcription in in vitro cultured bovine embryos. Mol. Reprod. Dev. 29:117–123. doi:10.1002/mrd.1080290205.

Barsoum, I. B., and H. H.-C. Yao. 2010. Fetal Leydig cells: progenitor cell maintenance and differentiation. J. Androl. 31:11–15. doi:10.2164/jandrol.109.008318.

Bertevello, P. S., A.-P. Teixeira-Gomes, A. Seyer, A. Vitorino Carvalho, V. Labas, M.-C. Blache, C. Banliat, L. A. V. Cordeiro, V. Duranthon, P. Papillier, V. Maillard, S. Elis, and S. Uzbekova. 2018. Lipid Identification and Transcriptional Analysis of Controlling Enzymes in Bovine Ovarian Follicle. Int. J. Mol. Sci. 19:3261. doi:10.3390/ijms19103261.

Bettegowda, A., J. Yao, A. Sen, Q. Li, K.-B. Lee, Y. Kobayashi, O. V. Patel, P. M. Coussens, J. J. Ireland, and G. W. Smith. 2007. JY-1, an oocyte-specific gene, regulates granulosa cell function and early embryonic development in cattle. Proc. Natl. Acad. Sci. 104:17602–17607. doi:10.1073/pnas.0706383104.

Bilodeau-Goeseels, S., and J. P. Kastelic. 2003. Factors affecting embryo survival and strategies to reduce embryonic mortality in cattle. Can. J. Anim. Sci. 83:659–671. doi:10.4141/A03-029.

Bouckenheimer, J., S. Assou, S. Riquier, C. Hou, N. Philippe, C. Sansac, T. Lavabre-Bertrand, T. Commes, J.-M. Lemaître, A. Boureux, and J. De Vos. 2016. Long non-coding RNAs in human early embryonic development and their potential in ART. Hum. Reprod. Update. 23:19–40. doi:10.1093/humupd/dmw035.

Brambell, F. W. R. 1926. The Oogenesis of the Fowl (Gallus bankiva). Philos. Trans. R. Soc. Lond. Ser. B Contain. Pap. Biol. Character. 214:113–151.

Braude, P. R., and H. R. Pelham. 1979. A microsystem for the extraction and in-vitro translation of mouse embryo mRNA. J. Reprod. Fertil. 56:153–158. doi:10.1530/jrf.0.0560153.

Brieño-Enríquez, M. A., M. Faykoo-Martinez, M. Goben, J. K. Grenier, A. McGrath, A. M. Prado, J. Sinopoli, K. Wagner, P. T. Walsh, S. H. Lopa, D. J. Laird, P. E. Cohen, M. D. Wilson, M. M. Holmes, and N. J. Place. 2023. Postnatal oogenesis leads to an exceptionally large ovarian reserve in naked mole-rats. Nat. Commun. 14:670. doi:10.1038/s41467-023-36284-8.

Burghardt, R. C., R. Barhoumi, T. C. Sewall, and J. A. Bowen. 1995. Cyclic AMP induces rapid increases in gap junction permeability and changes in the cellular distribution of connexin43. J. Membr. Biol. 148:243–253. doi:10.1007/BF00235042.

Caballero, J., I. Gilbert, E. Fournier, D. Gagné, S. Scantland, A. Macaulay, and C. Robert. 2014. Exploring the function of long non-coding RNA in the development of bovine early embryos. Reprod. Fertil. Dev. 27:40–52. doi:10.1071/RD14338.

Caponnetto, A., R. Battaglia, C. Ferrara, M. E. Vento, P. Borzì, M. Paradiso, P. Scollo, M. Purrello, S. Longobardi, T. D'Hooghe, D. Valerio, C. Di Pietro, and Italian Society of Embryology, Reproduction, Research (SIERR). 2022. Down-regulation of long non-coding RNAs in reproductive aging and analysis of the lncRNA-miRNA-mRNA networks in human cumulus cells. J. Assist. Reprod. Genet. 39:919–931. doi:10.1007/s10815-022-02446-8.

Christians, E., A. A. Davis, S. D. Thomas, and I. J. Benjamin. 2000. Maternal effect of Hsf1 on reproductive success. Nature. 407:693–694. doi:10.1038/35037669.

Collier, B., B. Gorgoni, C. Loveridge, H. J. Cooke, and N. K. Gray. 2005. The DAZL family proteins are PABP-binding proteins that regulate translation in germ cells. EMBO J. 24:2656–2666. doi:10.1038/sj.emboj.7600738.

Cook, M. S., D. Coveney, I. Batchvarov, J. H. Nadeau, and B. Capel. 2009. BAX-mediated cell death affects early germ cell loss and incidence of testicular teratomas in Dnd1Ter/Ter mice. Dev. Biol. 328:377–383. doi:10.1016/j.ydbio.2009.01.041.

Cowper-Sal·lari, R., X. Zhang, J. B. Wright, S. D. Bailey, M. D. Cole, J. Eeckhoute, J. H. Moore, and M. Lupien. 2012. Breast cancer risk–associated SNPs modulate the affinity of chromatin for FOXA1 and alter gene expression. Nat. Genet. 44:1191–1198. doi:10.1038/ng.2416.

Crosby, I. M., F. Gandolfi, and R. M. Moor. 1988. Control of protein synthesis during early cleavage of sheep embryos. J. Reprod. Fertil. 82:769–775. doi:10.1530/jrf.0.0820769.

De Felici, M. 2013. Origin, Migration, and Proliferation of Human Primordial Germ Cells. In: Oogenesis. 1st ed. Springer, London. p. 30–48.

De Felici, M., M. L. Scaldaferri, M. Lobascio, S. Iona, V. Nazzicone, F. G. Klinger, and D. Farini. 2004. Experimental approaches to the study of primordial germ cell lineage and proliferation. Hum. Reprod. Update. 10:197–206. doi:10.1093/humupd/dmh020.

De Maio, A. 2011. Extracellular heat shock proteins, cellular export vesicles, and the Stress Observation System: a form of communication during injury, infection, and cell damage. It is never known how far a controversial finding will go! Dedicated to Ferruccio Ritossa. Cell Stress Chaperones. 16:235–249. doi:10.1007/s12192-010-0236-4.

Dekel, N., T. S. Lawrence, N. B. Gilula, and W. H. Beers. 1981. Modulation of cell-to-cell communication in the cumulus-oocyte complex and the regulation of oocyte maturation by LH. Dev. Biol. 86:356–362. doi:10.1016/0012-1606(81)90193-7.

Deng, M., Z. Liu, C. Ren, G. Zhang, J. Pang, Y. Zhang, F. Wang, and Y. Wan. 2018. Long noncoding RNAs exchange during zygotic genome activation in goat. Biol. Reprod. 99:707–717. doi:10.1093/biolre/ioy118.

Dhanoa, J. K., R. S. Sethi, R. Verma, J. S. Arora, and C. S. Mukhopadhyay. 2018. Long non-coding RNA: its evolutionary relics and biological implications in mammals: a review. J. Anim. Sci. Technol. 60:25. doi:10.1186/s40781-018-0183-7.

Diaz, F. J., K. Wigglesworth, and J. J. Eppig. 2007. Oocytes determine cumulus cell lineage in mouse ovarian follicles. J. Cell Sci. 120:1330–1340. doi:10.1242/jcs.000968.

Dierich, A., M. R. Sairam, L. Monaco, G. M. Fimia, A. Gansmuller, M. LeMeur, and P. Sassone-Corsi. 1998. Impairing follicle-stimulating hormone (FSH) signaling in vivo: Targeted disruption of the FSH receptor leads to aberrant gametogenesis and hormonal imbalance. Proc. Natl. Acad. Sci. 95:13612–13617. doi:10.1073/pnas.95.23.13612.

Diskin, M. G., J. J. Murphy, and J. M. Sreenan. 2006. Embryo survival in dairy cows managed under pastoral conditions. Anim. Reprod. Sci. 96:297–311. doi:10.1016/j.anireprosci.2006.08.008.

Djebali, S., C. A. Davis, A. Merkel, A. Dobin, T. Lassmann, A. Mortazavi, A. Tanzer, J. Lagarde, W. Lin, F. Schlesinger, C. Xue, G. K. Marinov, J. Khatun, B. A. Williams, C. Zaleski, J. Rozowsky, M. Röder, F. Kokocinski, R. F. Abdelhamid, T. Alioto, I. Antoshechkin, M. T. Baer, N. S. Bar, P. Batut, K. Bell, I. Bell, S. Chakrabortty, X. Chen, J. Chrast, J. Curado, T. Derrien, J. Drenkow, E. Dumais, J. Dumais, R. Duttagupta, E. Falconnet, M. Fastuca, K. Fejes-Toth, P. Ferreira, S. Foissac, M. J. Fullwood, H. Gao, D. Gonzalez, A. Gordon, H. Gunawardena, C. Howald, S. Jha, R. Johnson, P. Kapranov, B. King, C. Kingswood, O. J. Luo, E. Park, K. Persaud, J. B. Preall, P. Ribeca, B. Risk, D. Robyr, M. Sammeth, L. Schaffer, L.-H. See, A. Shahab, J. Skancke, A. M. Suzuki, H. Takahashi, H. Tilgner, D. Trout, N. Walters, H. Wang, J. Wrobel, Y. Yu, X. Ruan, Y. Hayashizaki, J. Harrow, M. Gerstein, T. Hubbard, A. Reymond, S. E. Antonarakis, G. Hannon, M. C. Giddings, Y. Ruan, B. Wold, P. Carninci, R. Guigó, and T. R. Gingeras. 2012. Landscape of transcription in human cells. Nature. 489:101–108. doi:10.1038/nature11233.

Dong, L., X. Xin, H.-M. Chang, P. C. K. Leung, C. Yu, F. Lian, and H. Wu. 2022. Expression of long noncoding RNAs in the ovarian granulosa cells of women with diminished ovarian reserve using high-throughput sequencing. J. Ovarian Res. 15:119. doi:10.1186/s13048-022-01053-6.

Dong, M. H., Y. Y. Kim, and S.-Y. Ku. 2022. Identification of Stem Cell-Like Cells in the Ovary. Tissue Eng. Regen. Med. 19:675–685. doi:10.1007/s13770-021-00424-2.

Dryden, N. H., L. R. Broome, F. Dudbridge, N. Johnson, N. Orr, S. Schoenfelder, T. Nagano, S. Andrews, S. Wingett, I. Kozarewa, I. Assiotis, K. Fenwick, S. L. Maguire, J. Campbell, R. Natrajan, M. Lambros, E. Perrakis, A. Ashworth, P. Fraser, and O. Fletcher. 2014. Unbiased analysis of potential targets of breast cancer susceptibility loci by Capture Hi-C. Genome Res. 24:1854–1868. doi:10.1101/gr.175034.114.

Eckersley-Maslin, M. A., C. Alda-Catalinas, and W. Reik. 2018. Dynamics of the epigenetic landscape during the maternal-to-zygotic transition. Nat. Rev. Mol. Cell Biol. 19:436–450. doi:10.1038/s41580-018-0008-z.

Edson, M. A., A. K. Nagaraja, and M. M. Matzuk. 2009. The Mammalian Ovary from Genesis to Revelation. Endocr. Rev. 30:624–712. doi:10.1210/er.2009-0012.

El-Fouly, M. A., B. Cook, M. Nekola, and A. V. Nalbandov. 1970. Role of the Ovum in Follicular Luteinization. 87.

Elvin, J. A., A. T. Clark, P. Wang, N. M. Wolfman, and M. M. Matzuk. 1999. Paracrine Actions Of Growth Differentiation Factor-9 in the Mammalian Ovary. Mol. Endocrinol. 13:1035–1048. doi:10.1210/mend.13.6.0310.

Engreitz, J. M., K. Sirokman, P. McDonel, A. Shishkin, C. Surka, P. Russell, S. R. Grossman, A. Y. Chow, M. Guttman, and E. S. Lander. 2014. RNA-RNA Interactions Enable Specific Targeting of Noncoding RNAs to Nascent Pre-mRNAs and Chromatin Sites. Cell. 159:188–199. doi:10.1016/j.cell.2014.08.018.

Eppig, J. J. 2001. Oocyte control of ovarian follicular development and function in mammals. Reprod. Camb. Engl. 122:829–838.

Eppig, J. J., K. Wigglesworth, F. Pendola, and Y. Hirao. 1997. Murine oocytes suppress expression of luteinizing hormone receptor messenger ribonucleic acid by granulosa cells. Biol. Reprod. 56:976–984. doi:10.1095/biolreprod56.4.976.

Fair, T., P. Hyttel, and T. Greve. 1995. Bovine oocyte diameter in relation to maturational competence and transcriptional activity. Mol. Reprod. Dev. 42:437–442. doi:10.1002/mrd.1080420410.

Farini, D., and M. De Felici. 2022. The Beginning of Meiosis in Mammalian Female Germ Cells: A Never-Ending Story of Intrinsic and Extrinsic Factors. Int. J. Mol. Sci. 23:12571. doi:10.3390/ijms232012571.

Felici, M. D. 2009. Primordial germ cell biology at the beginning of the XXI Century. Int. J. Dev. Biol. 53:891–894. doi:10.1387/ijdb.082815mf.

Felix, W. 1911. Die Entwicklung der Harn- und Geschlechtsorgane. Leipzig: Hirzel.

Fortune, J. E., and D. T. Armstrong. 1977. Androgen production by theca and granulosa isolated from proestrous rat follicles. Endocrinology. 100:1341–1347. doi:10.1210/endo-100-5-1341.

Fortune, J. E., J. Sirois, and S. M. Quirk. 1988. The growth and differentiation of ovarian follicles during the bovine estrous cycle. Theriogenology. 29:95–109. doi:10.1016/0093-691X(88)90034-9.

Freedman, M. L., A. N. A. Monteiro, S. A. Gayther, G. A. Coetzee, A. Risch, C. Plass, G. Casey, M. De Biasi, C. Carlson, D. Duggan, M. James, P. Liu, J. W. Tichelaar, H. G. Vikis, M. You, and I. G. Mills. 2011. Principles for the post-GWAS functional characterization of cancer risk loci. Nat. Genet. 43:513–518. doi:10.1038/ng.840.

Fuss, A. 1911. Uber extraregionare Geschlechtszellen bei einem menschlichen Embryo von 4 Wochen. Anat Am. 39:407–409.

Fuss, A. 1912. Uber die Geschlechtszellen des Menschen und der Saugetiere. Arch Mikrosk Anat Entw Mech. 81:1–23.

Gilbert, I., A. Macaulay, and C. Robert. 2015. Oocyte developmental competence and embryo quality: distinction and new perspectives. Anim. Reprod. 12:397-407.

Gilchrist, R. B., L. J. Ritter, S. Myllymaa, N. Kaivo-Oja, R. A. Dragovic, T. E. Hickey, O. Ritvos, and D. G. Mottershead. 2006. Molecular basis of oocyte-paracrine signalling that promotes granulosa cell proliferation. J. Cell Sci. 119:3811–3821. doi:10.1242/jcs.03105.

Grelet, S., L. A. Link, B. Howley, C. Obellianne, V. Palanisamy, V. K. Gangaraju, J. A. Diehl, and P. H. Howe. 2017. A regulated PNUTS mRNA to lncRNA splice switch mediates EMT and tumour progression. Nat. Cell Biol. 19:1105–1115. doi:10.1038/ncb3595.

Guo, F., L. Li, J. Li, X. Wu, B. Hu, P. Zhu, L. Wen, and F. Tang. 2017. Single-cell multi-omics sequencing of mouse early embryos and embryonic stem cells. Cell Res. 27:967–988. doi:10.1038/cr.2017.82.

Halstead, M. M., X. Ma, C. Zhou, R. M. Schultz, and P. J. Ross. 2020. Chromatin remodeling in bovine embryos indicates species-specific regulation of genome activation. Nat. Commun. 11:4654. doi:10.1038/s41467-020-18508-3.

Hamatani, T., M. G. Carter, A. A. Sharov, and M. S. H. Ko. 2004. Dynamics of Global Gene Expression Changes during Mouse Preimplantation Development. Dev. Cell. 6:117–131. doi:10.1016/S1534-5807(03)00373-3.

Hamazaki, N., M. Uesaka, K. Nakashima, K. Agata, and T. Imamura. 2015a. Gene activation-associated long noncoding RNAs function in mouse preimplantation development. Development. 142:910–920. doi:10.1242/dev.116996.

Hamazaki, N., M. Uesaka, K. Nakashima, K. Agata, and T. Imamura. 2015b. Gene activation-associated long noncoding RNAs function in mouse preimplantation development. Development. 142:910–920. doi:10.1242/dev.116996.

Hand, J. M., K. Zhang, L. Wang, P. P. Koganti, K. Mastrantoni, S. K. Rajput, M. Ashry, G. W. Smith, and J. Yao. 2017. Discovery of a novel oocyte-specific Krüppel-associated box domain-containing zinc finger protein required for early embryogenesis in cattle. Mech. Dev. 144:103–112. doi:10.1016/j.mod.2017.02.003.

Hernandez-Gonzalez, I., I. Gonzalez-Robayna, M. Shimada, C. M. Wayne, S. A. Ochsner, L. White, and J. S. Richards. 2006. Gene expression profiles of cumulus cell oocyte complexes during ovulation reveal cumulus cells express neuronal and immune-related genes: does this expand their role in the ovulation process? Mol. Endocrinol. Baltim. Md. 20:1300–1321. doi:10.1210/me.2005-0420.

Hu, K., C. He, H. Ren, H. Wang, K. Liu, L. Li, Y. Liao, and M. Liang. 2019. LncRNA Gm2044 promotes 17β-estradiol synthesis in mpGCs by acting as miR-138-5p sponge. Mol. Reprod. Dev. 86:1023–1032. doi:10.1002/mrd.23179.

Hung, T., Yulei Wang, M. F. Lin, A. K. Koegel, Y. Kotake, G. D. Grant, H. M. Horlings, N. Shah, C. Umbricht, P. Wang, Yu Wang, B. Kong, A. Langerød, A.-L. Børresen-Dale, S. K. Kim, M. van de Vijver, S. Sukumar, M. L. Whitfield, M. Kellis, Y. Xiong, D. J. Wong, and H. Y. Chang. 2011. Extensive and coordinated transcription of noncoding RNAs within cell-cycle promoters. Nat. Genet. 43:621–629. doi:10.1038/ng.848.

Huntriss, J., R. Gosden, M. Hinkins, B. Oliver, D. Miller, A. J. Rutherford, and H. M. Picton. 2002. Isolation, characterization and expression of the human Factor In the Germline alpha (FIGLA) gene in ovarian follicles and oocytes. Mol. Hum. Reprod. 8:1087–1095. doi:10.1093/molehr/8.12.1087.

Hurtig, J., D. T. Chiu, and B. Önfelt. 2010. Intercellular nanotubes: insights from imaging studies and beyond. Wiley Interdiscip. Rev. Nanomed. Nanobiotechnol. 2:260–276. doi:10.1002/wnan.80.

Hussein, T. S., D. A. Froiland, F. Amato, J. G. Thompson, and R. B. Gilchrist. 2005. Oocytes prevent cumulus cell apoptosis by maintaining a morphogenic paracrine gradient of bone morphogenetic proteins. J. Cell Sci. 118:5257–5268. doi:10.1242/jcs.02644.

Hyttel, P., H. Callesen, and T. Greve. 1986. Ultrastructural features of preovulatory oocyte maturation in superovulated cattle. J. Reprod. Fertil. 76:645–656. doi:10.1530/jrf.0.0760645.

Hyttel, P., T. Greve, and H. Callesen. 1989. Ultrastructural aspects of oocyte maturation and fertilization in cattle. J. Reprod. Fertil. Suppl. 38:35–47.

Inoue, A., L. Jiang, F. Lu, T. Suzuki, and Y. Zhang. 2017. Maternal H3K27me3 controls DNA methylation-independent imprinting. Nature. 547:419–424. doi:10.1038/nature23262.

Ireland, J. J., and J. F. Roche. 1982. Effect of progesterone on basal LH and episodic LH and FSH secretion in heifers. J. Reprod. Fertil. 64:295–302. doi:10.1530/jrf.0.0640295.

Jachowicz, J. W., X. Bing, J. Pontabry, A. Bošković, O. J. Rando, and M.-E. Torres-Padilla. 2017. LINE-1 activation after fertilization regulates global chromatin accessibility in the early mouse embryo. Nat. Genet. 49:1502–1510. doi:10.1038/ng.3945.

Jain, A. K., Y. Xi, R. McCarthy, K. Allton, K. C. Akdemir, L. R. Patel, B. Aronow, C. Lin, W. Li, L. Yang, and M. C. Barton. 2016. LncPRESS1 Is a p53-Regulated LncRNA that Safeguards Pluripotency by Disrupting SIRT6-Mediated De-acetylation of Histone H3K56. Mol. Cell. 64:967–981. doi:10.1016/j.molcel.2016.10.039.

Jones, K. T. 2004. Turning it on and off: M-phase promoting factor during meiotic maturation and fertilization. Mol. Hum. Reprod. 10:1–5. doi:10.1093/molehr/gah009.

Jung, Y. H., M. E. G. Sauria, X. Lyu, M. S. Cheema, J. Ausio, J. Taylor, and V. G. Corces. 2017. Chromatin States in Mouse Sperm Correlate with Embryonic and Adult Regulatory Landscapes. Cell Rep. 18:1366–1382. doi:10.1016/j.celrep.2017.01.034.

Kaňka, J., K. Kepková, and L. Němcová. 2009. Gene expression during minor genome activation in preimplantation bovine development. Theriogenology. 72:572–583. doi:10.1016/j.theriogenology.2009.04.014.

Karlic, R., S. Ganesh, V. Franke, E. Svobodova, J. Urbanova, Y. Suzuki, F. Aoki, K. Vlahovicek, and P. Svoboda. 2017. Long non-coding RNA exchange during the oocyte-to-embryo transition in mice. DNA Res. 24:129–141. doi:10.1093/dnares/dsw058.

Khodayi, M., M. Khalaj-Kondori, M. A. Hoseinpour Feizi, M. Jabarpour Bonyadi, and M. Talebi. 2022. Plasma lncRNA profiling identified BC200 and NEAT1 lncRNAs as potential blood-based biomarkers for late-onset Alzheimer's disease. EXCLI J. 21:772–785. doi:10.17179/excli2022-4764.

Kidder, G. M., and R. A. Pedersen. 1982. Turnover of embryonic messenger RNA in preimplantation mouse embryos. J. Embryol. Exp. Morphol. 67:37–49.

Kino, T., D. E. Hurt, T. Ichijo, N. Nader, and G. P. Chrousos. 2010. Noncoding RNA gas5 is a growth arrest- and starvation-associated repressor of the glucocorticoid receptor. Sci. Signal. 3:ra8. doi:10.1126/scisignal.2000568.

Kotsuji, F., N. Kamitani, K. Goto, and T. Tominaga. 1990. Bovine theca and granulosa cell interactions modulate their growth, morphology, and function. Biol. Reprod. 43:726–732. doi:10.1095/biolreprod43.5.726.

Kumar, S., K. S. Prajapati, A. K. Singh, P. P. Kushwaha, M. Shuaib, and S. Gupta. 2021. Long non-coding RNA regulating androgen receptor signaling in breast and prostate cancer. Cancer Lett. 504:15–22. doi:10.1016/j.canlet.2020.11.039.

Kumar, T. R., Y. Wang, N. Lu, and M. M. Matzuk. 1997. Follicle stimulating hormone is required for ovarian follicle maturation but not male fertility. Nat. Genet. 15:201–204. doi:10.1038/ng0297-201.

Li, J., W. Han, X. Shen, S. Han, H. Ye, and G. Huang. 2017. DNA methylation signature of long noncoding RNA genes during human pre-implantation embryonic development. Oncotarget. 8:56829–56838. doi:10.18632/oncotarget.18072.

Li, L., L. Wang, H. Li, X. Han, S. Chen, B. Yang, Z. Hu, H. Zhu, C. Cai, J. Chen, X. Li, J. Huang, and D. Gu. 2018. Characterization of LncRNA expression profile and identification of novel LncRNA biomarkers to diagnose coronary artery disease. Atherosclerosis. 275:359–367. doi:10.1016/j.atherosclerosis.2018.06.866.

Li, L., P. Zheng, and J. Dean. 2010. Maternal control of early mouse development. Development. 137:859–870. doi:10.1242/dev.039487.

Li, R., Y.-E. Yang, J. Jin, M.-Y. Zhang, X. Liu, X.-X. Liu, Y.-H. Yin, and Y.-Q. Qu. 2019. Identification of lncRNA biomarkers in lung squamous cell carcinoma using comprehensive analysis of lncRNA mediated ceRNA network. Artif. Cells Nanomedicine Biotechnol. 47:3246–3258. doi:10.1080/21691401.2019.1647225.

Li, Y., Y. Liu, S. Chen, X. Chen, D. Ye, X. Zhou, J. Zhe, and J. Zhang. 2019. Down-regulation of long non-coding RNA MALAT1 inhibits granulosa cell proliferation in endometriosis by up-regulating P21 via activation of the ERK/MAPK pathway. Mol. Hum. Reprod. 25:17–29. doi:10.1093/molehr/gay045.

Liu, C., J. Peng, M. M. Matzuk, and H. H.-C. Yao. 2015. Lineage specification of ovarian theca cells requires multicellular interactions via oocyte and granulosa cells. Nat. Commun. 6:6934. doi:10.1038/ncomms7934.

Liu, L., L. Leng, C. Liu, C. Lu, Y. Yuan, L. Wu, F. Gong, S. Zhang, X. Wei, M. Wang, L. Zhao, L. Hu, J. Wang, H. Yang, S. Zhu, F. Chen, G. Lu, Z. Shang, and G. Lin. 2019. An integrated chromatin accessibility and transcriptome landscape of human pre-implantation embryos. Nat. Commun. 10:364. doi:10.1038/s41467-018-08244-0.

Lonergan, P. 2011. Influence of progesterone on oocyte quality and embryo development in cows. Theriogenology. 76:1594–1601. doi:10.1016/j.theriogenology.2011.06.012.

Lonergan, P., D. Rizos, F. Ward, and M. P. Boland. 2001. Factors influencing oocyte and embryo quality in cattle. Reprod. Nutr. Dev. 41:427–437. doi:10.1051/rnd:2001142.

Loyez, M. 1905. Developpement Ovarien des Oeufs Meroblastiques: A Vitellus Nutritif Abondant. Arch. Anat. Microsc. 8.

Lu, F., Y. Liu, A. Inoue, T. Suzuki, K. Zhao, and Y. Zhang. 2016. Establishing Chromatin Regulatory Landscape during Mouse Preimplantation Development. Cell. 165:1375–1388. doi:10.1016/j.cell.2016.05.050.

Macaulay, A. D., I. Gilbert, J. Caballero, R. Barreto, E. Fournier, P. Tossou, M.-A. Sirard, H. J. Clarke, É. W. Khandjian, F. J. Richard, P. Hyttel, and C. Robert. 2014. The gametic synapse: RNA transfer to the bovine oocyte. Biol. Reprod. 91:90. doi:10.1095/biolreprod.114.119867.

Macaulay, A. D., I. Gilbert, S. Scantland, E. Fournier, F. Ashkar, A. Bastien, H. A. S. Saadi, D. Gagné, M.-A. Sirard, É. W. Khandjian, F. J. Richard, P. Hyttel, and C. Robert. 2016. Cumulus Cell Transcripts Transit to the Bovine Oocyte in Preparation for Maturation. Biol. Reprod. 94:16. doi:10.1095/biolreprod.114.127571.

Magnúsdóttir, E., S. Dietmann, K. Murakami, U. Günesdogan, F. Tang, S. Bao, E. Diamanti, K. Lao, B. Gottgens, and M. Azim Surani. 2013. A tripartite transcription factor network regulates primordial germ cell specification in mice. Nat. Cell Biol. 15:905–915. doi:10.1038/ncb2798.

Manes, C. 1973. The participation of the embryonic genome during early cleavage in the rabbit. Dev. Biol. 32:453–459. doi:10.1016/0012-1606(73)90254-6.

Mannan, M. A., and P. J. O'Shaughnessy. 1991. Steroidogenesis during postnatal development in the mouse ovary. J. Endocrinol. 130:101–106. doi:10.1677/joe.0.1300101.

Mao, H., L. Chen, R. Bao, S. Weng, M. Wang, N. Xu, L. Qi, and J. Wang. 2022. Mechanisms of Oogenesis-Related Long Non-coding RNAs in Porcine Ovaries Treated With Recombinant Pig Follicle-Stimulating Hormone. Front. Vet. Sci. 8:838703. doi:10.3389/fvets.2021.838703.

Marchais, M., I. Gilbert, A. Bastien, A. Macaulay, and C. Robert. 2022. Mammalian cumulus-oocyte complex communication: a dialog through long and short distance messaging. J. Assist. Reprod. Genet. 39:1011–1025. doi:10.1007/s10815-022-02438-8.

Matzuk, M. M., and Q. Li. 2013. How the oocyte influences follicular cell function and why. In: Oogenesis. 1st ed. Springer, London. p. 75–100.

Mehlmann, L. M. 2005. Stops and starts in mammalian oocytes: recent advances in understanding the regulation of meiotic arrest and oocyte maturation. Reprod. Camb. Engl. 130:791–799. doi:10.1530/rep.1.00793.

Menke, D. B., J. Koubova, and D. C. Page. 2003. Sexual differentiation of germ cells in XX mouse gonads occurs in an anterior-to-posterior wave. Dev. Biol. 262:303–312. doi:10.1016/s0012-1606(03)00391-9.

Merton, J. S., A. P. W. de Roos, E. Mullaart, L. de Ruigh, L. Kaal, P. L. A. M. Vos, and S. J. Dieleman. 2003. Factors affecting oocyte quality and quantity in commercial application of embryo technologies in the cattle breeding industry. Theriogenology. 59:651–674. doi:10.1016/S0093-691X(02)01246-3.

Ming, H., J. Sun, R. Pasquariello, L. Gatenby, J. R. Herrick, Y. Yuan, C. R. Pinto, K. R. Bondioli, R. L. Krisher, and Z. Jiang. 2021. The landscape of accessible chromatin in bovine oocytes and early embryos. Epigenetics. 16:300–312. doi:10.1080/15592294.2020.1795602.

Møllgård, K., A. Jespersen, M. C. Lutterodt, C. Yding Andersen, P. E. Høyer, and A. G. Byskov. 2010. Human primordial germ cells migrate along nerve fibers and Schwann cells from the dorsal hind gut mesentery to the gonadal ridge. Mol. Hum. Reprod. 16:621–631. doi:10.1093/molehr/gaq052.

Mork, L., D. M. Maatouk, J. A. McMahon, J. J. Guo, P. Zhang, A. P. McMahon, and B. Capel. 2012. Temporal differences in granulosa cell specification in the ovary reflect distinct follicle fates in mice. Biol. Reprod. 86:37. doi:10.1095/biolreprod.111.095208.

Motta, P. M., S. A. Nottola, S. Makabe, and R. Heyn. 2000. Mitochondrial morphology in human fetal and adult female germ cells. Hum. Reprod. Oxf. Engl. 15 Suppl 2:129–147. doi:10.1093/humrep/15.suppl_2.129.

Ntostis, P., G. Swanson, G. Kokkali, D. Iles, J. Huntriss, A. Pantou, M. Tzetis, K. Pantos, H. M. Picton, S. A. Krawetz, and D. Miller. 2022. Trophectoderm non-coding RNAs reflect the higher metabolic and more invasive properties of young maternal age blastocysts. Syst. Biol. Reprod. Med. 0:1–17. doi:10.1080/19396368.2022.2153636.

Otsuka, F., K. McTavish, and S. Shimasaki. 2011. Integral Role of GDF-9 and BMP-15 in Ovarian Function. Mol. Reprod. Dev. 78:9–21. doi:10.1002/mrd.21265.

Pan, B., and J. Li. 2019. The art of oocyte meiotic arrest regulation. Reprod. Biol. Endocrinol. 17:8. doi:10.1186/s12958-018-0445-8.

Park, E.-S., and J. L. Tilly. 2015. Use of DEAD-box polypeptide-4 (Ddx4) gene promoter-driven fluorescent reporter mice to identify mitotically active germ cells in post-natal mouse ovaries. Mol. Hum. Reprod. 21:58–65. doi:10.1093/molehr/gau071.

Park, E.-S., D. C. Woods, and J. L. Tilly. 2013. Bone morphogenetic protein 4 promotes mammalian oogonial stem cell differentiation via Smad1/5/8 signaling. Fertil. Steril. 100:1468–1475. doi:10.1016/j.fertnstert.2013.07.1978.

Peng, Y., L. Chang, Y. Wang, R. Wang, L. Hu, Z. Zhao, L. Geng, Z. Liu, Y. Gong, J. Li, X. Li, and C. Zhang. 2019. Genome-wide differential expression of long noncoding RNAs and mRNAs in ovarian follicles of two different chicken breeds. Genomics. 111:1395–1403. doi:10.1016/j.ygeno.2018.09.012.

Pepling, M. E., and A. C. Spradling. 2001. Mouse ovarian germ cell cysts undergo programmed breakdown to form primordial follicles. Dev. Biol. 234:339–351. doi:10.1006/dbio.2001.0269.

Piko, L., and K. B. Clegg. 1982. Quantitative changes in total RNA, total poly(A), and ribosomes in early mouse embryos. Dev. Biol. 89:362–378. doi:10.1016/0012-1606(82)90325-6.

Piprek, R. P., ed. 2016. Molecular Mechanisms of Cell Differentiation in Gonad Development. Springer International Publishing, Cham. Available from: http://link.springer.com/10.1007/978-3-319-31973-5

Plath, K., J. Fang, S. K. Mlynarczyk-Evans, R. Cao, K. A. Worringer, H. Wang, C. C. de la Cruz, A. P. Otte, B. Panning, and Y. Zhang. 2003. Role of Histone H3 Lysine 27 Methylation in X Inactivation. Science. 300:131–135. doi:10.1126/science.1084274.

Quinn, J. J., and H. Y. Chang. 2016. Unique features of long non-coding RNA biogenesis and function. Nat. Rev. Genet. 17:47–62. doi:10.1038/nrg.2015.10.

Ramakrishna, N. B., K. Murison, E. A. Miska, and H. G. Leitch. 2021. Epigenetic Regulation during Primordial Germ Cell Development and Differentiation. Sex. Dev. 15:411–431. doi:10.1159/000520412.

Rao, M. R. S. 2017. Long Non Coding RNA Biology. In: Advances in Experimental Medicine and Biology. Vol. 1008. p. 1–46.

Rastetter, R. H., P. Bernard, J. S. Palmer, A.-A. Chassot, H. Chen, P. S. Western, R. G. Ramsay, M.-C. Chaboissier, and D. Wilhelm. 2014. Marker genes identify three somatic cell types in the fetal mouse ovary. Dev. Biol. 394:242–252. doi:10.1016/j.ydbio.2014.08.013.

Reese, S. T., G. A. Franco, R. K. Poole, R. Hood, L. Fernadez Montero, R. V. Oliveira Filho, R. F. Cooke, and K. G. Pohler. 2020. Pregnancy loss in beef cattle: A meta-analysis. Anim. Reprod. Sci. 212:106251. doi:10.1016/j.anireprosci.2019.106251.

Reijo, R. A., D. M. Dorfman, R. Slee, A. A. Renshaw, K. R. Loughlin, H. Cooke, and D. C. Page. 2000. DAZ family proteins exist throughout male germ cell development and transit from nucleus to cytoplasm at meiosis in humans and mice. Biol. Reprod. 63:1490–1496. doi:10.1095/biolreprod63.5.1490.

Richani, D., A. Poljak, B. Wang, S. B. Mahbub, J. Biazik, J. M. Campbell, A. Habibalahi, W. A. Stocker, M. B. Marinova, B. Nixon, S. Bustamante, D. Skerrett-Byrne, C. A. Harrison, E. Goldys, and R. B. Gilchrist. 2022. Oocyte and cumulus cell cooperativity and metabolic plasticity under the direction of oocyte paracrine factors. Developmental Biology. Available from: http://biorxiv.org/lookup/doi/10.1101/2022.09.05.506599

Richards, J. S. 2005. Ovulation: new factors that prepare the oocyte for fertilization. Mol. Cell. Endocrinol. 234:75–79. doi:10.1016/j.mce.2005.01.004.

Rinn, J. L., M. Kertesz, J. K. Wang, S. L. Squazzo, X. Xu, S. A. Brugmann, L. H. Goodnough, J. A. Helms, P. J. Farnham, E. Segal, and H. Y. Chang. 2007. Functional demarcation of active and silent chromatin domains in human HOX loci by noncoding RNAs. Cell. 129:1311–1323. doi:10.1016/j.cell.2007.05.022.

Robert, C. 2021. Nurturing the egg: the essential connection between cumulus cells and the oocyte. Reprod. Fertil. Dev. 34:149–159. doi:10.1071/RD21282.

Ruby, J. R., R. F. Dyer, R. F. Gasser, and R. G. Skalko. 1970. Intercellular connections between germ cells in the developing human ovary. Z. Zellforsch. Mikrosk. Anat. Vienna Austria 1948. 105:252–258. doi:10.1007/BF00335475.

Sasseville, M., L. J. Ritter, T. M. Nguyen, F. Liu, D. G. Mottershead, D. L. Russell, and R. B. Gilchrist. 2010. Growth differentiation factor 9 signaling requires ERK1/2 activity in mouse granulosa and cumulus cells. J. Cell Sci. 123:3166–3176. doi:10.1242/jcs.063834.

Schierding, W., W. Cutfield, and J. O'Sullivan. 2014. The missing story behind Genome Wide Association Studies: single nucleotide polymorphisms in gene deserts have a story to tell. Front. Genet. 5. Available from: https://www.frontiersin.org/articles/10.3389/fgene.2014.00039

S.H. Green and S. Zuckerman. 1951. The number of oocytes in the mature Rhesus monkey (Macaca mulatta). J. Endocrinol. 7:194–202.

Shamsa, A., R. B. Gilchrist, D. M. Robertson, R. J. Rodgers, M. W. Donoghoe, W. L. Ledger, J. A. Abbott, and A. H. Riepsamen. 2022. Oocyte-Secreted Serum Biomarkers GDF9 and BMP15 in Women with Endometriosis. Reprod. Sci. doi:10.1007/s43032-022-01107-6. Available from: https://doi.org/10.1007/s43032-022-01107-6

Shi, M., and M.-A. Sirard. 2022. Metabolism of fatty acids in follicular cells, oocytes, and blastocysts. Reprod. Fertil. 3:R96–R108. doi:10.1530/RAF-21-0123.

Shi, Y., M. Cai, K. Du, X. Bai, L. Tang, X. Jia, S. Chen, J. Wang, and S. Lai. 2021. Dynamics of Known Long Non-Coding RNAs during the Maternal-to-Zygotic Transition in Rabbit. Animals. 11:3592. doi:10.3390/ani11123592.

Sirard, M.-A., F. Richard, P. Blondin, and C. Robert. 2006. Contribution of the oocyte to embryo quality. Theriogenology. 65:126–136. doi:10.1016/j.theriogenology.2005.09.020.

de Souza, G. B., J. Costa, E. V. da Cunha, J. Passos, R. P. Ribeiro, M. Saraiva, R. van den Hurk, and J. Silva. 2017. Bovine ovarian stem cells differentiate into germ cells and oocyte-like structures after culture in vitro. Reprod. Domest. Anim. Zuchthyg. 52:243–250. doi:10.1111/rda.12886.

Sparmann, A., and M. van Lohuizen. 2006. Polycomb silencers control cell fate, development and cancer. Nat. Rev. Cancer. 6:846–856. doi:10.1038/nrc1991.

Spencer, T. E. 2013. Early pregnancy: Concepts, challenges, and potential solutions. Anim. Front. 3:48–55. doi:10.2527/af.2013-0033.

Spicer, L. J., P. Y. Aad, D. Allen, S. Mazerbourg, and A. J. Hsueh. 2006. Growth differentiation factor-9 has divergent effects on proliferation and steroidogenesis of bovine granulosa cells. J. Endocrinol. 189:329–339. doi:10.1677/joe.1.06503.

St. Laurent, G., C. Wahlestedt, and P. Kapranov. 2015. The Landscape of long noncoding RNA classification. Trends Genet. 31:239–251. doi:10.1016/j.tig.2015.03.007.

Su, Y.-Q., K. Sugiura, K. Wigglesworth, M. J. O'Brien, J. P. Affourtit, S. A. Pangas, M. M. Matzuk, and J. J. Eppig. 2008. Oocyte regulation of metabolic cooperativity between mouse cumulus cells and oocytes: BMP15 and GDF9 control cholesterol biosynthesis in cumulus cells. Dev. Camb. Engl. 135:111–121. doi:10.1242/dev.009068.

Sugiura, K., Y.-Q. Su, F. J. Diaz, S. A. Pangas, S. Sharma, K. Wigglesworth, M. J. O'Brien, M. M. Matzuk, S. Shimasaki, and J. J. Eppig. 2007. Oocyte-derived BMP15 and FGFs cooperate to promote glycolysis in cumulus cells. Development. 134:2593–2603. doi:10.1242/dev.006882.

Suzumori, N., K. H. Burns, W. Yan, and M. M. Matzuk. 2003. RFPL4 interacts with oocyte proteins of the ubiquitin-proteasome degradation pathway. Proc. Natl. Acad. Sci. U. S. A. 100:550–555. doi:10.1073/pnas.0234474100.

Svoboda, P., H. Fulka, and R. Malik. 2017. Clearance of Parental Products. In: F. Pelegri, M. Danilchik, and A. Sutherland, editors. Vertebrate Development: Maternal to Zygotic Control. Springer International Publishing, Cham. p. 489–535. Available from: https://doi.org/10.1007/978-3-319-46095-6_10

Tajima, K., M. Orisaka, T. Mori, and F. Kotsuji. 2007. Ovarian theca cells in follicular function. Reprod. Biomed. Online. 15:591–609. doi:10.1016/s1472-6483(10)60392-6.

Tam, P. P., and M. H. Snow. 1981. Proliferation and migration of primordial germ cells during compensatory growth in mouse embryos. J. Embryol. Exp. Morphol. 64:133–147.

Tamaddon, M., M. Azimzadeh, and S. M. Tavangar. 2022. microRNAs and long non-coding RNAs as biomarkers for polycystic ovary syndrome. J. Cell. Mol. Med. 26:654–670. doi:10.1111/jcmm.17139.

Taylor, D. H., E. T.-J. Chu, R. Spektor, and P. D. Soloway. 2015. Long non-coding RNA regulation of reproduction and development. Mol. Reprod. Dev. 82:932–956. doi:10.1002/mrd.22581.

Tejomurtula, J., K.-B. Lee, S. K. Tripurani, G. W. Smith, and J. Yao. 2009. Role of Importin Alpha8, a New Member of the Importin Alpha Family of Nuclear Transport Proteins, in Early Embryonic Development in Cattle. Biol. Reprod. 81:333–342. doi:10.1095/biolreprod.109.077396.

Tong, Z. B., L. Gold, K. E. Pfeifer, H. Dorward, E. Lee, C. A. Bondy, J. Dean, and L. M. Nelson. 2000. Mater, a maternal effect gene required for early embryonic development in mice. Nat. Genet. 26:267–268. doi:10.1038/81547.

Tora, L., and S. D. Vincent. 2021. What defines the maternal transcriptome? Biochem. Soc. Trans. 49:2051–2062. doi:10.1042/BST20201125.

Torroglosa, A., L. Villalba-Benito, R. M. Fernández, B. Luzón-Toro, M. J. Moya-Jiménez, G. Antiñolo, and S. Borrego. 2020. Identification of New Potential LncRNA Biomarkers in Hirschsprung Disease. Int. J. Mol. Sci. 21:5534. doi:10.3390/ijms21155534.

Tripathi, V., J. D. Ellis, Z. Shen, D. Y. Song, Q. Pan, A. T. Watt, S. M. Freier, C. F. Bennett, A. Sharma, P. A. Bubulya, B. J. Blencowe, S. G. Prasanth, and K. V. Prasanth. 2010. The nuclear-retained noncoding RNA MALAT1 regulates alternative splicing by modulating SR splicing factor phosphorylation. Mol. Cell. 39:925–938. doi:10.1016/j.molcel.2010.08.011.

Tripurani, S. K., K.-B. Lee, L. Wang, G. Wee, G. W. Smith, Y. S. Lee, K. E. Latham, and J. Yao. 2011. A Novel Functional Role for the Oocyte-Specific Transcription Factor Newborn Ovary Homeobox (NOBOX) during Early Embryonic Development in Cattle. Endocrinology. 152:1013–1023. doi:10.1210/en.2010-1134.

Uzbekova, S., S. Elis, A.-P. Teixeira-Gomes, A. Desmarchais, V. Maillard, and V. Labas. 2015. MALDI Mass Spectrometry Imaging of Lipids and Gene Expression Reveals Differences in Fatty Acid Metabolism between Follicular Compartments in Porcine Ovaries. Biology. 4:216–236. doi:10.3390/biology4010216.

Vanderhyden, B. C., and E. A. Macdonald. 1998. Mouse Oocytes Regulate Granulosa Cell Steroidogenesis Throughout Follicular Development. Biol. Reprod. 59:1296–1301. doi:10.1095/biolreprod59.6.1296.

Vassena, R., S. Boué, E. González-Roca, B. Aran, H. Auer, A. Veiga, and J. C. I. Belmonte. 2011. Waves of early transcriptional activation and pluripotency program initiation during human preimplantation development. Development. 138:3699–3709. doi:10.1242/dev.064741.

Vitt, U. A., M. Hayashi, C. Klein, and A. J. Hsueh. 2000. Growth differentiation factor-9 stimulates proliferation but suppresses the follicle-stimulating hormone-induced differentiation of cultured granulosa cells from small antral and preovulatory rat follicles. Biol. Reprod. 62:370–377. doi:10.1095/biolreprod62.2.370.

Wang, J., P. P. Koganti, and J. Yao. 2020. Systematic identification of long intergenic non-coding RNAs expressed in bovine oocytes. Reprod. Biol. Endocrinol. RBE. 18:13. doi:10.1186/s12958-020-00573-4.

Wang, J.-J., M.-H. Niu, T. Zhang, W. Shen, and H.-G. Cao. 2020. Genome-Wide Network of lncRNA–mRNA During Ovine Oocyte Development From Germinal Vesicle to Metaphase II in vitro. Front. Physiol. 11. Available from: https://www.frontiersin.org/articles/10.3389/fphys.2020.01019

Weissmann, A. 1893. The germ-plasm: A theory of heredity. Charles Scribner's Sons, New York.

White, Y. A. R., D. C. Woods, Y. Takai, O. Ishihara, H. Seki, and J. L. Tilly. 2012. Oocyte formation by mitotically active germ cells purified from ovaries of reproductive-age women. Nat. Med. 18:413–421. doi:10.1038/nm.2669.

Wu, J., B. Huang, H. Chen, Q. Yin, Y. Liu, Y. Xiang, B. Zhang, B. Liu, Q. Wang, W. Xia, W. Li, Y. Li, J. Ma, X. Peng, H. Zheng, J. Ming, W. Zhang, J. Zhang, G. Tian, F. Xu, Z. Chang, J. Na, X. Yang, and W. Xie. 2016. The landscape of accessible chromatin in mammalian preimplantation embryos. Nature. 534:652–657. doi:10.1038/nature18606.

Wu, J., J. Xu, B. Liu, G. Yao, P. Wang, Z. Lin, B. Huang, X. Wang, T. Li, S. Shi, N. Zhang, F. Duan, J. Ming, X. Zhang, W. Niu, W. Song, H. Jin, Y. Guo, S. Dai, L. Hu, L. Fang, Q. Wang, Y. Li, W. Li, J. Na, W. Xie, and Y. Sun. 2018. Chromatin analysis in human early development reveals epigenetic transition during ZGA. Nature. 557:256–260. doi:10.1038/s41586-018-0080-8.

Wu, Y., H. Xiao, J. Pi, H. Zhang, A. Pan, Y. Pu, Z. Liang, J. Shen, J. Du, and T. Huang. 2021. LncRNA lnc_13814 promotes the cells apoptosis in granulosa cells of duck by acting as apla-miR-145-4 sponge. Cell Cycle. 20:927–942. doi:10.1080/15384101.2021.1911102.

Xing, Z., A. Lin, C. Li, K. Liang, S. Wang, Y. Liu, P. K. Park, L. Qin, Y. Wei, D. H. Hawke, M.-C. Hung, C. Lin, and L. Yang. 2014. lncRNA directs cooperative epigenetic regulation downstream of chemokine signals. Cell. 159:1110–1125. doi:10.1016/j.cell.2014.10.013.

Yamaji, M., Y. Seki, K. Kurimoto, Y. Yabuta, M. Yuasa, M. Shigeta, K. Yamanaka, Y. Ohinata, and M. Saitou. 2008. Critical function of Prdm14 for the establishment of the germ cell lineage in mice. Nat. Genet. 40:1016–1022. doi:10.1038/ng.186.

Yan, L., M. Yang, H. Guo, L. Yang, J. Wu, Rong Li, P. Liu, Y. Lian, X. Zheng, J. Yan, J. Huang, M. Li, X. Wu, L. Wen, K. Lao, Ruiqiang Li, J. Qiao, and F. Tang. 2013. Single-cell RNA-Seq profiling of human preimplantation embryos and embryonic stem cells. Nat. Struct. Mol. Biol. 20:1131–1139. doi:10.1038/nsmb.2660.

Yang, F., X. Deng, W. Ma, J. B. Berletch, N. Rabaia, G. Wei, J. M. Moore, G. N. Filippova, J. Xu, Y. Liu, W. S. Noble, J. Shendure, and C. M. Disteche. 2015. The lncRNA Firre anchors the inactive X chromosome to the nucleolus by binding CTCF and maintains H3K27me3 methylation. Genome Biol. 16:52. doi:10.1186/s13059-015-0618-0.

Yao, X., X. Gao, Y. Bao, M. A. El-Samahy, J. Yang, Z. Wang, X. Li, G. Zhang, Y. Zhang, W. Liu, and F. Wang. 2021. lncRNA FDNCR promotes apoptosis of granulosa cells by targeting the miR-543-3p/DCN/TGF-β signaling pathway in Hu sheep. Mol. Ther. - Nucleic Acids. 24:223–240. doi:10.1016/j.omtn.2021.02.030.

Yap, K., S. Mukhina, G. Zhang, J. S. C. Tan, H. S. Ong, and E. V. Makeyev. 2018. A Short Tandem Repeat-Enriched RNA Assembles a Nuclear Compartment to Control Alternative Splicing and Promote Cell Survival. Mol. Cell. 72:525-540.e13. doi:10.1016/j.molcel.2018.08.041.

Zamboni, L. 1974. Fine morphology of the follicle wall and follicle cell-oocyte association. Biol. Reprod. 10:125–149. doi:10.1095/biolreprod10.2.125.

Zhang, F.-L., N. Li, H. Wang, J.-M. Ma, W. Shen, and L. Li. 2019. Zearalenone Exposure Induces the Apoptosis of Porcine Granulosa Cells and Changes Long Noncoding RNA Expression To Promote Antiapoptosis by Activating the JAK2–STAT3 Pathway. J. Agric. Food Chem. 67:12117–12128. doi:10.1021/acs.jafc.9b05189.

Zhang, P., W. Wu, Q. Chen, and M. Chen. 2019. Non-Coding RNAs and their Integrated Networks. J. Integr. Bioinforma. 16. doi:10.1515/jib-2019-0027. Available from: https://www.ncbi.nlm.nih.gov/pmc/articles/PMC6798851/

Zhang, W., Y. Liu, J. Jiang, Ya-Jie Tang, Ya-ling Tang, and X. Liang. 2020. Extracellular vesicle long non–coding RNA-mediated crosstalk in the tumor microenvironment: Tiny molecules, huge roles. Cancer Sci. 111:2726–2735. doi:10.1111/cas.14494.

Zheng, W., H. Zhang, N. Gorre, S. Risal, Y. Shen, and K. Liu. 2014. Two classes of ovarian primordial follicles exhibit distinct developmental dynamics and physiological functions. Hum. Mol. Genet. 23:920–928. doi:10.1093/hmg/ddt486.

Zhong, L., H. Mu, B. Wen, W. Zhang, Q. Wei, G. Gao, J. Han, and S. Cao. 2018. Long non-coding RNAs involved in the regulatory network during porcine pre-implantation embryonic development and iPSC induction. Sci. Rep. 8:6649. doi:10.1038/s41598-018-24863-5.

Zhou, M., Z. Diao, X. Yue, Y. Chen, H. Zhao, L. Cheng, and J. Sun. 2016. Construction and analysis of dysregulated lncRNA-associated ceRNA network identified novel lncRNA biomarkers for early diagnosis of human pancreatic cancer. Oncotarget. 7:56383–56394. doi:10.18632/oncotarget.10891.

Zlotnik, I. 1948. XIII.—A Comparative Study of the Cytoplasmic Components during the Oogenesis of Dog, Cat, and Rabbit. Proc. R. Soc. Edinb. Sect. B Biol. Sci. 63:200–212. doi:10.1017/S0080455X00000175.

Zuo, Q., J. Jin, K. Jin, J. Zhou, C. Sun, J. Song, G. Chen, Y. Zhang, and B. Li. 2020. P53 and H3K4me2 activate N6-methylated LncPGCAT-1 to regulate primordial germ cell formation via MAPK signaling. J. Cell. Physiol. 235:9895–9909. doi:10.1002/jcp.29805.

Chapter 1

The characterization of three novel oocyte-specific long non-coding RNAs and their functional roles in oocyte maturation and early embryonic development

Jaelyn Z Current[1], Heather L. Chaney[1], Mingxiang Zhang[1], Emily M. Dugan[1], Gianna L. Chimino[1], and Jianbo Yao[1]

[1]Laboratory of Animal Biotechnology and Genomics, Division of Animal and Nutritional Sciences, West Virginia University, Morgantown, WV 26506, United States

KEYWORDS: Non-coding RNA, oocyte maturation, early embryonic development, siRNA-mediated knockdown

ABSTRACT

In mammals, early embryogenesis relies heavily on the regulation of maternal transcripts. Emerging technologies have discovered a vast collection of regulatory non-coding RNAs in the last decade. Long non-coding RNAs (lncRNAs) have recently been identified in bovine oocytes and early embryos. In this study, three novel maternal lncRNAs in bovine oocytes, *OOSNCR1, OOSNCR2,* and *OOSNCR3,* were characterized in somatic tissues, the ovarian follicle, and throughout early embryonic development. Moreover, the functional requirement of each transcript during oocyte maturation and early embryonic development was investigated using siRNA-mediated knockdown. Our data revealed that *OOSNCR1* and *OOSNCR2* are oocyte-specific. Follicular cell expression revealed that all three lncRNAs were expressed highest in the oocyte, with expression detected in the CCs and mGCs. LncRNA expression for all three genes was highest during oocyte maturation, decreased at fertilization, and ceased altogether by the 16-cell stage. LncRNA knockdown in immature oocytes was achieved for all three genes, whereas knockdown in presumptive zygotes was confirmed in *OOSNCR1* and *OOSNCR3.* For all three transcripts, lncRNA knockdown resulted in decreased blastocyst formation. Cumulus expansion was not affected by lncRNA knockdown in immature oocytes. However, the relative abundance of *NPM2, GDF9, BMP15,* and *JY-1* was decreased. The data herein suggest a functional requirement of *OOSNCR1, OOSNCR2,* and *OOSNCR3* during bovine oocyte maturation and early embryogenesis.

INTRODUCTION

Over the past decade, advancements in technology and the advent of deep sequencing have provided genome-wide transcriptional studies that discovered a large portion of the genome is transcribed; much more than the 1-3% that encodes proteins (Djebali et al., 2012). In humans, only 1.2% of the genome represents protein-coding exons, whereas 24% and 75% are attributed to intronic and intergenic non-coding RNA (ncRNAs) (Rao, 2017). Further, ncRNAs have been characterized by specific expression patterns during critical developmental stages localized to certain tissues or prevalent during disease states and play multiple roles in gene expression regulation (Rao, 2017). What once was thought of as "genetic noise" from leaky transcriptional machinery has more recently come to the foreground of modern research in molecular biology due to its broad versatility in regulating gene expression.

Long non-coding RNAs (lncRNAs) are a class of RNAs with lengths greater than 200 nucleotides, no open reading frame, are usually 5' capped, 3' polyadenylated, alternatively spliced, and to date have not been found to encode a protein (ENCODE Project Consortium, 2012). With interest growing in the non-coding transcriptome, more and more lncRNAs are reported to play critical roles in various biological processes, including chromatin modification (Plath et al., 2003; Rinn et al., 2007; Yang et al., 2015), regulation of transcription (Kino et al., 2010; Hung et al., 2011; Xing et al., 2014; Taylor et al., 2015; Jain et al., 2016; Arab et al., 2019), and influence the nuclear architecture and regulation of gene expression at post-transcriptional (Tripathi et al., 2010; Engreitz et al., 2014; Grelet et al., 2017; Yap et al., 2018) and post-translational levels (Karakas and Ozpolat, 2021). With RNA sequencing technology more readily available, many studies have published large data sets identifying lncRNAs present in various reproductive tissues, including the ovary (Peng et al., 2019), oviduct (Sun et al., 2022), pregnant and nonpregnant uteri (Wang et al., 2016), and reproductive tissues inflicted with various gynecological cancers (Zhao et al., 2014).

Multiple studies have identified lncRNAs in ovarian follicular cells, including mural granulosa cells (mGCs) (Hu et al., 2019; Li et al., 2019; Zhang et al., 2019), cumulus cells (CCs) (Caponnetto et al., 2022; Zhao et al., 2022) and oocytes (Wang et al., 2020). According to pathway analyses and bioinformatic predictions, many of these studies predict novel lncRNAs to be associated with various cellular processes, including follicular development, oocyte maturation, cell cycle regulation, ovulation, estrogen production, cell proliferation, and apoptosis. However, functional studies still need to be improved. Despite the minimal number of functional studies during oocyte maturation (Iyyappan et al., 2021), lncRNAs have been identified and functionally characterized as critical regulators of zygotic genome activation (ZGA) in humans (Bouckenheimer et al., 2016), mice (Hamazaki et al., 2015), pigs (Zhong et al., 2018), goats (Deng et al., 2018) and rabbits (Shi et al., 2021).

In mammals, the zygote begins transcriptionally silent, with all initial developmental events controlled by stored maternal RNAs and proteins collectively referred to as maternal-effect genes (Li et al., 2010). Maternal-effect genes are transcribed during oogenesis and enable the activation of the embryonic genome. Maternal transcripts are experimentally differentiated from embryonic transcripts using α-amanitin, an RNA polymerase II inhibitor that induces a developmental block during the maternal-to-zygotic transition (Barnes and First, 1991). These oocyte-specific transcripts produce products that are expressed, stored, and secreted throughout oogenesis that regulates the follicular microenvironment to promote oocyte competence and successful fertilization and drive early embryonic development (De Sousa et al., 1998).

Studies have shown that disrupting maternal transcripts *GDF9* (Dong et al., 1996) and *BMP15* (Yan et al., 2001) during oocyte maturation causes impaired folliculogenesis. In contrast, disruptions of *NPM2* (Burns et al., 2003) and *USF1* (Datta et al., 2015) in the presumptive zygote

directly associates with a decreased number of embryos reaching the blastocyst stage. Moreover, the depletion of maternal transcript *JY-1* at the germinal vesicle stage reduced the proportion of oocytes progressing to metaphase II (MII) and caused partial cumulus expansion (Lee et al., 2014). Further, *JY-1* depletion in presumptive zygote decreased the percentage of embryos developing to the blastocyst stage (Bettegowda et al., 2007: 1; Lee et al., 2014), revealing a functional requirement role for a single oocyte-expressed gene in promoting meiotic maturation and cumulus expansion pre-fertilization, coupled with an additional requirement of the same gene postfertilization.

To date, bovine oocyte-specific lncRNAs and their corresponding mechanisms required for and utilized by the oocyte and early embryo are poorly understood, and our understanding of the contribution of such factors to oocyte maturation and the maternal-to-embryonic transition during early embryogenesis in cattle is limited. Thus, the objectives of this study were to investigate novel oocyte-specific lncRNAs identified previously (Wang et al., 2020) by our laboratory and elucidate their functional roles during oocyte maturation and early embryonic development.

MATERIALS AND METHODS

Bovine Sample Procurement

Bovine tissue samples, including liver, kidney, lung, thymus, spleen, adrenal, cortex, rumen, jejunum, vagina, caruncle, skeletal muscle, cardiac muscle, smooth muscle, fetal and adult ovaries, were collected at a local abattoir (Enterprise, WV) and a commercial facility (Souderton, PA). All tissue samples were excised in 1x1x1mm cubes from freshly slaughtered animals (n = 4), immediately snap-frozen, and then stored in liquid nitrogen. When a fetus was present in slaughtered female animals, sex was determined, and fetal age was predicted using the crown-

rump length (Rexroad et al., 1974). Whole fetal ovaries were immediately snap-frozen upon collection. All samples were stored at -80°C until further analysis.

Follicular Cell Collection and *In Vitro* Embryo Production

Adult ovaries were harvested and stored at room temperature in 0.9% NaCl solution until aspiration. Theca (TC) and mGCs were isolated from visible follicles using a previously established method (Murdoch et al., 1981). The cumulus-oocyte complexes (COCs) were aspirated from 2-12 mm follicles using an 18-gauge needle. After three washes of Boviplus oocyte washing medium (Minitube International; Tiefenbach, Germany) with BSA, heparin, and pen strep per manufacturer's instructions, visibly healthy COCs were selected for IVM. Healthy COCs were defined as COCs with at least two consecutive layers of symmetrical CCs and a uniform cytoplasm. COCs were either collected at the germinal vesicle (GV) stage or pooled into groups of 50 and cultured in 500 μL of bovine IVM media (IVF Bioscience; United Kingdom) under embryo grade mineral oil for 22h at 38.8°C in 5% CO_2 in humidified air.

For GV oocyte and CC samples, CCs were removed using a 1:1 hyaluronidase solution at 10,000 U/mL and vortexed for 5 minutes. Denuded GV oocytes were collected in pools with minimal volume and stored at -80°C. The remaining CCs were centrifuged into a pellet with the excess liquid removed, snap-frozen, and stored, as previously mentioned. Following IVM, the presence of metaphase II (MII) oocytes were confirmed based on the visual criteria of CC expansion and first polar body extrusion. Fully matured COCs were either collected, denuded, and stored in the same manner previously mentioned as MII oocytes and expanded CCs or selected to generate embryos.

Embryos were generated using IVF. The COCs were washed and transferred to the bovine IVF medium (IVF Bioscience). Donated optixcell-extended bovine semen (Select Sires; Plain

City, Ohio) was washed twice with bovine semen preparation medium (IVF Bioscience) per manufacturer's instructions. The sperm were co-cultured with the COCs at a concentration of 2.0 x 10^6 sperm/ mL for 12 h at 38.8°C in 5% CO_2 in humidified air. The presumptive zygotes were denuded and moved into 500 uL of bovine IVC (IVF Bioscience) with an oil overlay and incubated at 38.8°C in 5% CO_2 and 5% O_2 until day 8 post-insemination. Embryos at two-cell, four-cell, eight-cell, and 16-cell stage were collected at 33-, 44-, 52-, and 72-hours post-insemination (hpi), and morula and blastocysts were collected at 5- and 8-days post-insemination.

Quantification of Novel LncRNAs using Real-Time PCR (RT-qPCR)

Total RNA was isolated from tissues using TRIzol reagent (Ambion, Inc.; Austin, TX) according to the manufacturer's instructions following homogenization with a MiniBeadBeater-16 (BioSpec Products; Bartlesville, OK). The RNA was treated with Turbo DNase I (Ambion), and RNA concentration and quality were measured using a Nanodrop Spectrophotometer, examining the absorbances at 260 nm and 280 nm. Total RNA concentrations were normalized before cDNA synthesis. Total RNA from oocytes and embryos was isolated using the RNAqueous™ MicroKit (Invitrogen; Waltham, MA), and cDNA was synthesized using the High-Capacity cDNA Reverse Transcription Kit (Applied Biosystems; Waltham, MA) per the manufacturer's instructions. Gene expression was quantified using Power-Up SYBR Green Master Mix (Applied Biosystems) and a CFX96 Real-Time System machine (Bio-Rad Laboratories, Hercules, CA). The qPCR conditions were as follows: denaturing at 95°C for 2 minutes, 39 PCR cycles (95°C for 15 seconds (denature), 60°C for 1 minute (annealing), and a final extension at 65°C for 5 seconds. A single, sharp peak on a dissociation curve confirmed the homogeneity of the PCR products for each primer set. Relative lncRNA abundance was calculated via the standard

curve method using *RPL19* as an endogenous control or *GFP* as an exogenous control for normalization. The RT-qPCR primers are listed in Table 1.

Prediction of Secondary Structure

Secondary structures were predicted using The Vienna RNA Website (Gruber et al., 2008). Then, for each lncRNA, the optimal minimum free energy (MFE) and centroid structures were generated using the transcript sequence by estimating the lowest free energy value for each base pairing.

Generation of cDNA template for fluorescent *in situ* hybridization

Nested PCR was performed using two sets of primers for *OOSNCR1*. The first primer isolated the lncRNA from fetal ovary cDNA. The second primer incorporated the T7 and SP6 promoters into the cDNA template. Primers are listed in Table 2. Nested PCR was conducted using the Phusion High-Fidelity DNA Polymerase kit (ThermoFisher; Waltham, MA) following the 3-step protocol: initial denaturation 98°C for 30 seconds, 35 cycles (98°C for 10 seconds, 72°C for 30 seconds, and 72°C for 52 seconds) and a final extension for 72°C for 10 minutes. The product of the second reaction was gel purified using the QIAquick Gel Extraction kit (Qiagen; Germantown, MD) and verified by Sanger Sequencing (WVU Genomics Core Facility, Morgantown, WV).

The custom probe was generated using the FISH Tag RNA Kit (Invitrogen) per the manufacturer's instructions. Then, following *in vitro* transcription using the custom cDNA template, the green fluorophore (Alexa Fluor 488: Ex/Em 492/520) was attached, and the probe was stored at -80°C until hybridization.

Fluorescent *in situ* Hybridization of Immature Oocytes

The zona pellucida of denuded oocytes was digestion using 0.05% pronase diluted in Boviplus oocyte washing medium (Minitube International) for 1 minute. Following digestion, oocytes were washed and fixed in 4% paraformaldehyde during a 2.5 h incubation at room temperature with an oil overlay. After fixation, oocytes were washed and permeabilized using triton X-100 for 6 hours. Finally, oocytes were washed and stored in 4% paraformaldehyde at 4°C until hybridization.

Hybridization was performed following the FISH Tag RNA Kit (Invitrogen) with modifications per the manufacturer's instructions. Briefly, oocytes were incubated in probe/hybridization buffer (50% formamide, 5X SSC, 100 μg/mL fragmented salmon testes DNA, 50 μg/mL heparin, 0.1% Tween 20) for 16-20 hrs at 55°C in a PCR machine. Following incubation, oocytes were placed in fresh hybridization buffer and incubated at 55°C for 30 minutes with gentle rocking. After a second incubation under these conditions, oocytes were washed in droplets of 50% PBT (PBS/0.1% Tween 20)/50% hybridization buffer with repeat pipetting, followed by washing in droplets of PBT. Finally, oocytes were transferred to a droplet of 70% glycerol/30% PBT for 10 minutes, then whole-mounted on pre-cleaned slides in minimal volume. DAPI was used for nuclear visualization, and cells were imaged at 20x using the Nikon A1R Confocal microscope (WVU Microscope Imaging Facility, Morgantown, WV).

Inhibition of RNA Polymerase II using α-Amanitin

To determine if *OOSNCR1, OOSNCR2,* and *OOSNCR3* transcripts are maternal or zygotic in origin, presumptive zygotes were cultured in bovine IVC (IVF Bioscience) in the presence and absence of a transcription inhibitor, α-amanitin at 25 μg/mL. Embryos were collected in pools of 10 from each treatment at the two-cell (33 hpi; n = 3), four-cell (44 hpi; n = 6), and eight-cell (52

hpi; n = 6) stages. Samples were collected in a minimal volume and subjected to real-time quantification as previously described for each lncRNA transcript.

siRNA-mediated Knockdown of Three Novel LncRNAs at the Germinal Vesicle Stage

Microinjection of *OOSNCR1*, *OOSNCR2,* and *OOSNCR3* siRNA into GV oocytes was conducted using previously described methodologies with modifications (Datta et al., 2015: 1). Briefly, cumulus-enclosed GV-stage oocytes were microinjected with a cocktail of two siRNA species for each lncRNA. The siRNA species (siRNA-1, siRNA-2) were designed using the custom dicer-substrate siRNA (DsiRNA) design tool (Integrated DNA Technologies, Coralville, IA) targeting *OOSNCR1* at positions 665-690 and 991-1016, *OOSNCR2* at positions 80-105 and 186-211, and *OOSNCR3* at positions 82-107 and 114-139, respectively. Immature COCs were collected and randomly assigned to receive either each lncRNAs' siRNA cocktail (50 μM), the negative control siRNA (50 μM, universal control species 1; Ambion Inc.) or remain as noninjected controls. All COCs injections were performed in M2 medium (Medium 199 containing HEPES supplemented with 2% FBS) with approximately 15 pl injected into each COC. After injection, the effects of treatments on cumulus expansion (n = 5; pools of at least 20 COCs), the relative abundance of select genes linked to bovine oocyte competency (*NPM2, GDF9, BMP15 JY-1,* and *USF-1),* and the percent survival of injected COCs reaching 12 hpi was determined (n = 3; pools of at least 20 COCs). To validate lncRNA knockdown, denuded MII oocytes injected with the siRNA cocktail for *OOSNCR1*, *OOSNCR2*, or *OOSNCR3* were collected in pools of 5 denuded MII oocytes (n =7), and each lncRNA's expression was quantified via RT-qPCR. Moreover, injected COCs were subjected to IVF, and the percent development reaching the blastocysts stage was determined on day 8 (n = 3).

siRNA-mediated Knockdown of Three Novel LncRNAs in Presumptive Zygotes

Microinjection of *OOSNCR1, OOSNCR2,* and *OOSNCR3* siRNA into presumptive zygotes was conducted using previously described methodologies (Lee et al., 2014: 1). Presumptive zygotes were collected 12-16 hpi and injected in the same manner as mentioned above. To validate lncRNA knockdown, presumptive zygotes injected with a siRNA cocktail for each lncRNA (n = 7) were collected at the four-cell stage in pools of 5, and each lncRNA's expression was quantified via RT-qPCR. The percent development reaching the blastocysts stage for each treatment was determined on day 8 (n = 3-5).

Statistical Analysis

All analyses were conducted in JMP Pro version 15.1.0 (JMP 1998-2023). All RT-qPCR data were log-transformed, and embryo data presented as percentages were arcsine transformed. Differences in gene expression and embryonic development were determined using a Student's *t*-test or One-way ANOVA. Following ANOVA, individual mean comparisons were performed using either Tukey's HSD or Dunnett's test. For all experiments, differences were considered statistically significant when $P < 0.05$ with a tendency range of $0.1 \geq P > 0.05$.

RESULTS

Predicted LncRNA Secondary Structure for Three Novel LncRNAs

OOSNCR1 is 2,073 bp long, much longer than the average length of oocyte lncRNAs (782 bp). In contrast, *OOSNCR2* and *OOSNCR3* are short, 292 bp and 384 bp, respectively. Consistent with being a non-coding RNA, *OOSNCR1* does not contain open reading frames (ORFs) larger than 250 bp, and neither *OOSNCR2* nor *OOSNCR3* contains any significant ORFs. BLAST search revealed that all three lncRNAs are intergenic and do not match any lncRNAs in

the NONCODE database (v5.0). The *OOSNCR1* gene contains three exons and two introns spanning about 10 kb on bovine chromosome 1 (Figure 1A). *OOSNCR2* is approximately 67 kb on chromosome 4 and includes three exons and two introns, with intron 2 being about 64 kb (Figure 1B). Further, *OOSNCR3* is the smallest transcript, with about 550 bp in length on chromosome 19, and contains two exons and one intron (Figure 1C). Using The Vienna RNA Website (Gruber et al., 2008), the secondary structures for *OOSNCR1*, *OOSNCR2*, and *OOSNCR3* were predicted based on their calculated lowest free energy value (Figure 2).

Tissue Expression Profiles for Three Novel LncRNAs

To determine if *OOSNCR1*, *OOSNCR2*, and *OOSNCR3* expression are confined to the oocyte, a panel of tissues including liver, kidney, lung, thymus, spleen, adrenal, cortex, rumen, jejunum, vagina, caruncle, skeletal muscle, cardiac muscle, smooth muscle, and fetal ovaries was examined via RT-qPCR. Oocyte-specificity was confirmed for *OOSNCR1* and *OOSNCR2*, with expression detected exclusively in the fetal ovaries (Figure 3AB). In contrast, *OOSNCR3* expression was detected in both the spleen and fetal ovaries (Figure 3C).

Characterization of Novel LncRNAs' Expression in the Bovine Antral Follicle and Throughout Early Embryonic Development

To examine *OOSNCR1*, *OOSNCR2*, and *OOSNCR3* expression in the ovary, follicular cells were isolated and analyzed using RT-qPCR (Figure 4). Follicular cell expression revealed that *OOSNCR1*, *OOSNCR2*, and *OOSNCR3* were highest in oocytes with no significant difference between maturation stages. Moving outward from the oocytes, all three lncRNAs were expressed higher in the CCs than the mural GCs. Due to variation among the samples, the maturity stage was also not significantly different when examining CCs from immature or mature COCs. *OOSNCR1*

was expressed higher in mural granulosa cells when compared to theca cells ($P = 0.025$); however, no difference was detected in *OOSNCR2* and *OOSNCR3* expression.

LncRNA expression was quantified throughout oocyte maturation and early embryonic development. Pools of 20 denuded oocytes (GV and MII) and embryos at two-cell, four-cell, eight-cell, 16-cell stage, morula, and blastocysts were collected. All three lncRNAs exhibited similar patterns of expression (Figure 5). *OOSNCR1*, *OOSNCR2*, and *OOSNCR3* expression was highest in immature and mature oocytes compared to the blastocysts stage ($P < 0.001$). Following fertilization, all three lncRNAs' expression significantly decreased and remained steady until the eight-cell stage. Progressing past the eight-cell stage caused all three lncRNAs to cease expression by the blastocyst stage.

Identification of Novel lncRNA Transcript Origins in Early Embryos

An RNA polymerase II inhibitor, α-amanitin, was used to determine the origins of each of the three lncRNAs in early embryos. *OOSNCR1*, *OOSNCR2*, and *OOSNCR3* exhibited identical patterns following α-amanitin treatment (Figure 6). Each lncRNA cultured under standard conditions increased during the first embryonic division and then decreased by the third division. However, when cultured in the presence of α-amanitin, each lncRNA decreased following the first embryonic division ($P < 0.0001$) and remained steady through the third division. By day 8 post insemination, the blastocysts rate for the control was 44% $\pm$ 5.1 and 0% following α-amanitin treatment (Table 3).

Subcellular Localization of *OOSNCR1* Within Immature Oocytes

As the top candidate for examination, *OOSNCR1* localization in immature oocytes was further investigated. Using a custom probe with T7 and SP6 promoters incorporated into the sense

and antisense template strand, *OOSNCR1* was localized exclusively to the cytoplasm in germinal-stage oocytes (Figure 7).

Effects of siRNA-mediated Knockdown of Three Novel LncRNAs at the Germinal Vesicle Stage on Oocyte Maturation and Subsequent Embryonic Development

The functional role of lncRNAs during oocyte maturation remains unknown; therefore, we addressed the effects of *OOSNCR1, OOSNCR2,* and *OOSNCR3* knockdown on cumulus expansion, the relative abundance of select genes linked to bovine oocyte competency and calculating the percent survival of COCs reaching 12 hpi. LncRNA knockdown was achieved for all three lncRNAs ($P < 0.009$; Figure 8). Examination of CC expansion revealed no difference between uninjected and injected COCs ($P > 0.71$; Figure 9). Following the siRNA-mediated knockdown of all three lncRNAs at the GV stage, *NPM2* was downregulated ($P < 0.0179$; Figure 10A). Additionally, *GDF9* was downregulated in MII oocytes following the knockdown of *OOSNCR1* and *OOSNCR3* ($P < 0.0159$; Figure 10B). Lastly, *OOSNCR1* knockdown caused a decrease in four out of the five selected genes (*NPM2, GDF9, BMP15,* and *JY-1)* linked to oocyte competency ($P < 0.0159$; Figure 10ABCD). LncRNA knockdown did not affect *USF1* expression ($P > 0.645$; Figure 10E). When examining COCs' survival post-injection, the uninjected control COCs had a survival rate of 90.55% $\pm$ 0.05, whereas injected COCs had a decreased survival rate ($P < 0.0254$; Table 4). No difference was detected in the survival of injected COCs regardless of the siRNA cocktail.

To assess the effect of lncRNA knockdown during oocyte maturation on early embryonic development, uninjected and injected COCs were subjected to IVF. The percent development reaching the blastocysts stage was determined on day 8 (Table 5). Control and negative injected COCs resulted in a 25% $\pm$ 0.041 and 21% $\pm$ 0.045 blastocysts rate ($P = 0.796$). Knockdown of

OOSNCR1, *OOSNCR2*, and *OOSNCR3* resulted in a decreased blastocyst rate of 3% ± 0.003, 0% ± 0.0046, and 6% ± 0.04, respectively ($P < 0.012$).

Effects of siRNA-Mediated Knockdown of Three Novel LncRNAs in Presumptive Zygotes on Early Embryonic Development

The functional role of lncRNAs during early embryonic development remains unknown. Therefore, we addressed the effects of *OOSNCR1*, *OOSNCR2*, and *OOSNCR3* knockdown by calculating the percentage of embryos reaching the blastocysts stage by day 8 (Table 6). There was a tendency for knockdown of *OOSNCR1* ($P = 0.055$) and *OOSNCR3* ($P = 0.10$) when compared to the control (Figure 10 AC). However, the knockdown of *OOSNCR2* was not validated using RT-qPCR in presumptive zygotes ($P = 0.60$; Figure 10B). Control and negative injected presumptive zygotes resulted in a 31% ± 0.004 and 30% ± 0.012 average blastocysts rate ($P = 0.976$). In contrast, knockdown of *OOSNCR1*, *OOSNCR2*, and *OOSNCR3* resulted in a decreased blastocyst rate of 14% ± 0.025, 14% ± 0.018, and 15% ± 0.033, respectively ($P < 0.0013$).

DISCUSSION

Emerging technologies and transcriptomic analyses have discovered a vast collection of regulatory non-coding RNAs within the mammalian genome (Mattick et al., 2023). However, elucidating the functional roles of lncRNA remains challenging, with only a small subset of transcripts extensively characterized (Plath et al., 2003; Smits et al., 2008; Clemson et al., 2009: 1; Gupta et al., 2010; Tripathi et al., 2010). Results of the present study identified three novel maternal lncRNAs in cattle and characterized their temporal expression in somatic tissues, the ovarian follicle, and throughout early embryonic development. The data suggest a functional requirement of *OOSNCR1*, *OOSNCR2*, and *OOSNCR3* during bovine oocyte maturation and early embryogenesis.

Previously, using RNA sequencing, our laboratory identified 1,535 lncRNAs present in immature and mature oocytes (Wang et al., 2020). After comparisons to lncRNAs in bovine tissues, 970 transcripts were predicted to be unique to bovine oocytes. Three highly abundant candidate genes were selected based on FPKM scores for further investigation. The present studies demonstrate that bovine *OOSNCR1* and *OOSNCR2* are oocyte-specific due to high abundance exclusively in the fetal ovary in contrast to *OOSNCR3,* which is additionally expressed at low levels in the spleen.

Interestingly, the spleen has been hypothesized to function within the hypothalamus-pituitary-ovary (HPO) axis to act as a reservoir of leukocytes that infiltrate the ovary following ovulation (Oakley et al., 2011). Within the ovary, leukocytes are involved in (1) loosening the follicular wall to facilitate follicle growth and ovulation, (2) tissue repair following rupture, and (3) luteal formation and regression. Despite these roles, localization studies identified only natural killer cells within the follicle and corpora lutea (Fainaru et al., 2010), whereas monocytes/macrophages, neutrophils, lymphocytes, mast cells, and eosinophils were predominately localized in the periphery of the follicle, interstitium, and corpora lutea (Gaytan et al., 1991; Gaytán et al., 2003; Oakley et al., 2010). Interaction of *OOSNCR3* and molecular signals produced by or in response to natural killer cells within the follicle may expose different relationships between the ovary and spleen.

OOSNCR1, OOSNCR2, and *OOSNCR3* were identified throughout the ovarian follicle. All three lncRNAs were expressed highest in the oocyte, with expression decreasing in cell types as the distance from the oocyte increased. Although reduced, all three lncRNAs were expressed higher in immature and mature cumulus cells than in mural granulosa and theca cells. Due to the intricate bi-directional communication system within the COC (Macaulay et al., 2014), this raises

an interesting question. Why does expression decrease in cells further from the oocyte? LncRNAs may originate in the oocyte and travel outward via TZPs. Alternatively, more interestingly, lncRNAs expressed in follicular cells may be packaged and secreted to the oocyte, where they are needed to exert their regulatory function in a time-specific manner regardless of transcriptional silencing. Recently, investigations of TZP structure discovered that mGCs possess multiple protruding cytoplasmic projections that search for the oocyte. Upon contact-mediated paracrine interactions with the oocyte, the CCs differentiate (Baena and Terasaki, 2019). Further studies will be necessary to determine lncRNA expression before CC differentiation and the possible trafficking of these regulatory transcripts within the mammalian follicle among different cell types.

LncRNA expression throughout oocyte maturation and early embryonic development suggests that *OOSNCR1*, *OOSNCR2*, and *OOSNCR3* are maternal and have similar roles in activating the embryonic genome. Each lncRNA was expressed highest during oocyte maturation, followed by a significant decreased post-insemination where expression remained constant until expressed ceased altogether by the 16-cell stage. Further investigations of their origins using α-amanitin revealed that all three lncRNAs were maternal. In cattle, a low level of transcriptional activity (minor genome activation) occurs between the 1- and 4-cell stage embryo, with major genome activation happening at the 8-cell stage (Kaňka et al., 2009). Interestingly, each lncRNA displayed a significant decrease in expression at the second embryonic division following α-amanitin treatment suggesting novel transcription by either the maternal or embryonic genome. During genome activation, a shift from maternal to embryonic control is accompanied by widespread changes in chromatin structure and restructuring of the embryonic epigenome (Halstead et al., 2020). With lncRNAs documented to regulate gene expression by modulating

chromatin structure and function (Statello et al., 2021), future studies should aim to investigate changes in the chromatin landscape during EGA in response to lncRNA ablation.

Our results support an essential role for *OOSNCR1, OOSNCR2,* and *OOSNCR3* during oocyte maturation. Effects of siRNA-mediated gene knockdown in immature COCs support the requirement of each of the lncRNAs for oocyte maturation and subsequent development to the blastocyst stage in cattle. Previous studies knocking down maternal transcripts *GDF9* (Dong et al., 1996), *BMP15* (Su et al., 2004), and *JY-1* (Lee et al., 2014: 1) in the cumulus-enclosed germinal vesicle revealed impaired oocyte maturation, partial cumulus expansion, a significant decreased in early embryos reaching the blastocyst stage, or a combination of outcomes above. Knockdown of oocyte-specific lncRNA *Rose* revealed oocytes underwent nuclear envelope breakdown normally. However, oocytes lacking *Rose* failed to extrude a polar body leading to abnormal MI, irregular polar body extrusion, and symmetrical division (Iyyappan et al., 2021). Further, oocytes that successfully extruded a polar body exhibited irregularities in their mitotic spindles and chromosome organization (Iyyappan et al., 2021). Our findings indicate that cumulus expansion was not affected by lncRNA knockdown. However, COCs survival decreased following injection. Collectively, these data suggest an internal mechanism independent of CCs ultimately disrupting cytoplasmic maturation resulting in oocytes of lesser quality.

To evaluate the potential relationship between lncRNAs and oocyte competency, known genes linked to oocyte quality were quantified in the knockdown MII oocytes. Interestingly, *NPM2* was significantly decreased following the knockdown of each lncRNA. Previously, *NPM2* knockout female mice exhibited fertility defects, including impaired nucleolar organization and disrupted chromatin structure in oocytes and early embryos (Burns et al., 2003). Further, *NPM2* is temporally regulated during early embryogenesis (Lingenfelter et al., 2011) and has been identified

as a histone chaperone in the oocyte and embryo (Platonova et al., 2011). Future studies should investigate *NPM2* as a potential target regulated by lncRNAs. Moreover, potential mechanisms of gene regulation targeting chromatin should be explored. Other oocyte-specific genes decreased following lncRNA knockdown include *GDF9, BMP15,* and *JY-1*. The essential role of *GDF9* and *BMP15* in the ovarian follicle to mediate cell growth and differentiation of follicular cells is undisputed (Paulini and Melo, 2011). Recently, *GDF9* and *BMP15* have been implicated in the pathogenesis of primary ovarian insufficiency (Liu et al., 2021). Specifically, mutations in *BMP15* were associated with reduced mature protein production, activity, or synergy with *GDF9* in patients with primary ovarian insufficiency (Patiño et al., 2017). As members of the TGFβ superfamily, *GDF9* and *BMP15* require post-translational phosphorylation to become bioactive (McMahon et al., 2008). Multiple lncRNAs have been reported to regulate gene expression at the post-transcriptional level (Tripathi et al., 2010; Engreitz et al., 2014; Grelet et al., 2017; Yap et al., 2018). Thus, post-translational regulation of *GDF9* and *BMP15* via interactions with lncRNAs warrants further investigation.

Recently, a meta-analysis of RNA-seq expression data detected lncRNAs presence throughout human (Bouckenheimer et al., 2016), mouse (Hamazaki et al., 2015), pig (Zhong et al., 2018), cattle (Wang et al., 2020), and rabbit (Shi et al., 2021) embryonic development detecting rapid changes in expression patterns contributing to the success of the developmental process. Our study further investigated the functional role of novel lncRNAs by examining early embryonic development following siRNA-mediated knockdown in presumptive zygotes. Collectively, *OOSNCR1, OOSNCR2,* and *OOSNCR3* knockdown exhibited impaired early embryonic development with blastocyst rates approximately half the rate measured in the uninjected and negative injected controls. Knockdown of *JY-1* (Bettegowda et al., 2007) and *USF-1* (Datta et al.,

2015: 1) in presumptive zygotes reported similar findings. Although studies investigating lncRNA knockdown in embryos remain understudied, one group reported accelerated developmental kinetics following lncRNA knockdown (Caballero et al., 2014). A second group reported no significant difference in the progression of embryos reaching the 2-cell stage. However, they observed embryonic arrest at the 2-8 cell stage, and their blastocyst rates were significantly lower (44.21%) after lncRNA knockdown (Iyyappan et al., 2021). Further speculation of the functional roles of lncRNAs in early embryonic development remains hypothetical.

The presence of lncRNAs in reproductive systems is undisputed. However, the current focus of lncRNA research remains on detection using bioinformatic analysis and comparative analysis tools to predict functional roles. Understanding lncRNA regulation and their underlying molecular mechanisms during oocyte maturation and early embryonic development offers basic knowledge to the field and provides potential infertility biomarkers for future interventions in assisted reproductive techniques (ART) to increase reproductive success across multiple species.

Conflict of Interest

The authors declare no conflicts of interest.

Author Contributions

JZC planned the study design, collected samples, performed experiments, analyzed data, interpreted data, and drafted the manuscript. HLC collected ovary samples and performed *in vitro* embryo production. MZ performed *in vitro* embryo production. EMD and GLC assisted with *in vitro* embryo production and gene expression data. JY aided in data analysis, interpretation, and manuscript preparation.

Acknowledgments

This project was supported by the National Institute of Food and Agriculture U.S. Department of Agriculture, award number 2020-38640-31520, the Northeast Sustainable Agriculture Research and Education (SARE) graduate student research grant award number GNE19-196, and the USDA National Institute of Food and Agriculture, Multistate Research Project 1014002. In addition, the authors like to thank Dr. Ida Holaskova for her assistance in statistical analysis, Select Sires (Plain City, OH) for semen donations, and the West Virginia Department of Agriculture, Hyde's Meat Packing (Enterprise, WV), and JBS Beef Plant (Souderton, PA) for their generous donation of bovine ovaries for this work.

REFERENCES

Arab, K., E. Karaulanov, M. Musheev, P. Trnka, A. Schäfer, I. Grummt, and C. Niehrs. 2019. GADD45A binds R-loops and recruits TET1 to CpG island promoters. Nat. Genet. 51:217–223. doi:10.1038/s41588-018-0306-6.

Baena, V., and M. Terasaki. 2019. Three-dimensional organization of transzonal projections and other cytoplasmic extensions in the mouse ovarian follicle. Sci. Rep. 9:1262. doi:10.1038/s41598-018-37766-2.

Barnes, F. L., and N. L. First. 1991. Embryonic transcription in in vitro cultured bovine embryos. Mol. Reprod. Dev. 29:117–123. doi:10.1002/mrd.1080290205.

Bettegowda, A., J. Yao, A. Sen, Q. Li, K.-B. Lee, Y. Kobayashi, O. V. Patel, P. M. Coussens, J. J. Ireland, and G. W. Smith. 2007. JY-1, an oocyte-specific gene, regulates granulosa cell function and early embryonic development in cattle. Proc. Natl. Acad. Sci. 104:17602–17607. doi:10.1073/pnas.0706383104.

Bouckenheimer, J., S. Assou, S. Riquier, C. Hou, N. Philippe, C. Sansac, T. Lavabre-Bertrand, T. Commes, J.-M. Lemaître, A. Boureux, and J. De Vos. 2016. Long non-coding RNAs in human early embryonic development and their potential in ART. Hum. Reprod. Update. 23:19–40. doi:10.1093/humupd/dmw035.

Burns, K. H., M. M. Viveiros, Y. Ren, P. Wang, F. J. DeMayo, D. E. Frail, J. J. Eppig, and M. M. Matzuk. 2003. Roles of NPM2 in chromatin and nucleolar organization in oocytes and embryos. Science. 300:633–636. doi:10.1126/science.1081813.

Caballero, J., I. Gilbert, E. Fournier, D. Gagné, S. Scantland, A. Macaulay, and C. Robert. 2014. Exploring the function of long non-coding RNA in the development of bovine early embryos. Reprod. Fertil. Dev. 27:40–52. doi:10.1071/RD14338.

Caponnetto, A., R. Battaglia, C. Ferrara, M. E. Vento, P. Borzì, M. Paradiso, P. Scollo, M. Purrello, S. Longobardi, T. D'Hooghe, D. Valerio, C. Di Pietro, and Italian Society of Embryology, Reproduction, Research (SIERR). 2022. Down-regulation of long non-coding RNAs in reproductive aging and analysis of the lncRNA-miRNA-mRNA networks in human cumulus cells. J. Assist. Reprod. Genet. 39:919–931. doi:10.1007/s10815-022-02446-8.

Clemson, C. M., J. N. Hutchinson, S. A. Sara, A. W. Ensminger, A. H. Fox, A. Chess, and J. B. Lawrence. 2009. An Architectural Role for a Nuclear Noncoding RNA: NEAT1 RNA Is Essential for the Structure of Paraspeckles. Mol. Cell. 33:717–726. doi:10.1016/j.molcel.2009.01.026.

Datta, T. K., S. K. Rajput, G. Wee, K. Lee, J. K. Folger, and G. W. Smith. 2015. Requirement of the transcription factor USF1 in bovine oocyte and early embryonic development. Reproduction. 149:203–212. doi:10.1530/REP-14-0445.

De Sousa, P. A., A. Caveney, M. E. Westhusin, and A. J. Watson. 1998. Temporal patterns of embryonic gene expression and their dependence on oogenetic factors. Theriogenology. 49:115–128. doi:10.1016/S0093-691X(97)00406-8.

Deng, M., Z. Liu, C. Ren, G. Zhang, J. Pang, Y. Zhang, F. Wang, and Y. Wan. 2018. Long noncoding RNAs exchange during zygotic genome activation in goat. Biol. Reprod. 99:707–717. doi:10.1093/biolre/ioy118.

Djebali, S., C. A. Davis, A. Merkel, A. Dobin, T. Lassmann, A. Mortazavi, A. Tanzer, J. Lagarde, W. Lin, F. Schlesinger, C. Xue, G. K. Marinov, J. Khatun, B. A. Williams, C. Zaleski, J. Rozowsky, M. Röder, F. Kokocinski, R. F. Abdelhamid, T. Alioto, I. Antoshechkin, M. T. Baer, N. S. Bar, P. Batut, K. Bell, I. Bell, S. Chakrabortty, X. Chen, J. Chrast, J. Curado, T. Derrien, J. Drenkow, E. Dumais, J. Dumais, R. Duttagupta, E. Falconnet, M. Fastuca, K. Fejes-Toth, P. Ferreira, S. Foissac, M. J. Fullwood, H. Gao, D. Gonzalez, A. Gordon, H. Gunawardena, C. Howald, S. Jha, R. Johnson, P. Kapranov, B. King, C. Kingswood, O. J. Luo, E. Park, K. Persaud, J. B. Preall, P. Ribeca, B. Risk, D. Robyr, M. Sammeth, L. Schaffer, L.-H. See, A. Shahab, J. Skancke, A. M. Suzuki, H. Takahashi, H. Tilgner, D. Trout, N. Walters, H. Wang, J. Wrobel, Y. Yu, X. Ruan, Y. Hayashizaki, J. Harrow, M. Gerstein, T. Hubbard, A. Reymond, S. E. Antonarakis, G. Hannon, M. C. Giddings, Y. Ruan, B. Wold, P. Carninci, R. Guigó, and T. R. Gingeras. 2012. Landscape of transcription in human cells. Nature. 489:101–108. doi:10.1038/nature11233.

Dong, J., D. F. Albertini, K. Nishimori, T. R. Kumar, N. Lu, and M. M. Matzuk. 1996. Growth differentiation factor-9 is required during early ovarian folliculogenesis. Nature. 383:531–535. doi:10.1038/383531a0.

ENCODE Project Consortium. 2012. An integrated encyclopedia of DNA elements in the human genome. Nature. 489:57–74. doi:10.1038/nature11247.

Engreitz, J. M., K. Sirokman, P. McDonel, A. Shishkin, C. Surka, P. Russell, S. R. Grossman, A. Y. Chow, M. Guttman, and E. S. Lander. 2014. RNA-RNA Interactions Enable Specific Targeting of Noncoding RNAs to Nascent Pre-mRNAs and Chromatin Sites. Cell. 159:188–199. doi:10.1016/j.cell.2014.08.018.

Fainaru, O., H. Amsalem, Y. Bentov, N. Esfandiari, and R. F. Casper. 2010. CD56brightCD16- natural killer cells accumulate in the ovarian follicular fluid of patients undergoing in vitro fertilization. Fertil. Steril. 94:1918–1921. doi:10.1016/j.fertnstert.2009.12.067.

Gaytan, F., J. Aceitero, C. Bellido, J. E. Sánchez-Criado, and E. Aguilar. 1991. Estrous cycle-related changes in mast cell numbers in several ovarian compartments in the rat. Biol. Reprod. 45:27–33. doi:10.1095/biolreprod45.1.27.

Gaytán, F., C. Morales, C. Bellido, E. Tarradas, and J. Eugenio Sánchez-Criado. 2003. Effects of indomethacin on ovarian leukocytes during the periovulatory period in the rat. Reprod. Biol. Endocrinol. RBE. 1:26. doi:10.1186/1477-7827-1-26.

Grelet, S., L. A. Link, B. Howley, C. Obellianne, V. Palanisamy, V. K. Gangaraju, J. A. Diehl, and P. H. Howe. 2017. A regulated PNUTS mRNA to lncRNA splice switch mediates EMT and tumour progression. Nat. Cell Biol. 19:1105–1115. doi:10.1038/ncb3595.

Gruber, A. R., R. Lorenz, S. H. Bernhart, R. Neuböck, and I. L. Hofacker. 2008. The Vienna RNA Websuite. Nucleic Acids Res. 36:W70–W74. doi:10.1093/nar/gkn188.

Gupta, R. A., N. Shah, K. C. Wang, J. Kim, H. M. Horlings, D. J. Wong, M.-C. Tsai, T. Hung, P. Argani, J. L. Rinn, Y. Wang, P. Brzoska, B. Kong, R. Li, R. B. West, M. J. van de Vijver, S. Sukumar, and H. Y. Chang. 2010. Long non-coding RNA HOTAIR reprograms chromatin state to promote cancer metastasis. Nature. 464:1071–1076. doi:10.1038/nature08975.

Halstead, M. M., X. Ma, C. Zhou, R. M. Schultz, and P. J. Ross. 2020. Chromatin remodeling in bovine embryos indicates species-specific regulation of genome activation. Nat. Commun. 11:4654. doi:10.1038/s41467-020-18508-3.

Hamazaki, N., M. Uesaka, K. Nakashima, K. Agata, and T. Imamura. 2015. Gene activation-associated long noncoding RNAs function in mouse preimplantation development. Development. 142:910–920. doi:10.1242/dev.116996.

Hu, K., C. He, H. Ren, H. Wang, K. Liu, L. Li, Y. Liao, and M. Liang. 2019. LncRNA Gm2044 promotes 17β-estradiol synthesis in mpGCs by acting as miR-138-5p sponge. Mol. Reprod. Dev. 86:1023–1032. doi:10.1002/mrd.23179.

Hung, T., Yulei Wang, M. F. Lin, A. K. Koegel, Y. Kotake, G. D. Grant, H. M. Horlings, N. Shah, C. Umbricht, P. Wang, Yu Wang, B. Kong, A. Langerød, A.-L. Børresen-Dale, S. K. Kim, M. van de Vijver, S. Sukumar, M. L. Whitfield, M. Kellis, Y. Xiong, D. J. Wong, and H. Y. Chang. 2011. Extensive and coordinated transcription of noncoding RNAs within cell-cycle promoters. Nat. Genet. 43:621–629. doi:10.1038/ng.848.

Iyyappan, R., D. Aleshkina, L. Zhu, Z. Jiang, V. Kinterova, and A. Susor. 2021. Oocyte specific lncRNA variant Rose influences oocyte and embryo development. Non-Coding RNA Res. 6:107–113. doi:10.1016/j.ncrna.2021.06.001.

Jain, A. K., Y. Xi, R. McCarthy, K. Allton, K. C. Akdemir, L. R. Patel, B. Aronow, C. Lin, W. Li, L. Yang, and M. C. Barton. 2016. LncPRESS1 Is a p53-Regulated LncRNA that Safeguards Pluripotency by Disrupting SIRT6-Mediated De-acetylation of Histone H3K56. Mol. Cell. 64:967–981. doi:10.1016/j.molcel.2016.10.039.

Kaňka, J., K. Kepková, and L. Němcová. 2009. Gene expression during minor genome activation in preimplantation bovine development. Theriogenology. 72:572–583. doi:10.1016/j.theriogenology.2009.04.014.

Karakas, D., and B. Ozpolat. 2021. The Role of LncRNAs in Translation. Non-Coding RNA. 7:16. doi:10.3390/ncrna7010016.

Kino, T., D. E. Hurt, T. Ichijo, N. Nader, and G. P. Chrousos. 2010. Noncoding RNA gas5 is a growth arrest- and starvation-associated repressor of the glucocorticoid receptor. Sci. Signal. 3:ra8. doi:10.1126/scisignal.2000568.

Lee, K.-B., G. Wee, K. Zhang, J. K. Folger, J. G. Knott, and G. W. Smith. 2014. Functional role of the bovine oocyte-specific protein JY-1 in meiotic maturation, cumulus expansion, and subsequent embryonic development. Biol. Reprod. 90:69. doi:10.1095/biolreprod.113.115071.

Li, Y., Y. Liu, S. Chen, X. Chen, D. Ye, X. Zhou, J. Zhe, and J. Zhang. 2019. Down-regulation of long non-coding RNA MALAT1 inhibits granulosa cell proliferation in endometriosis by up-regulating P21 via activation of the ERK/MAPK pathway. Mol. Hum. Reprod. 25:17–29. doi:10.1093/molehr/gay045.

Lingenfelter, B. M., S. K. Tripurani, J. Tejomurtula, G. W. Smith, and J. Yao. 2011. Molecular cloning and expression of bovine nucleoplasmin 2 (NPM2): a maternal effect gene regulated by miR-181a. Reprod. Biol. Endocrinol. 9:40. doi:10.1186/1477-7827-9-40.

Liu, M., K. Zhang, and T. Xu. 2021. The role of BMP15 and GDF9 in the pathogenesis of primary ovarian insufficiency. Hum. Fertil. 24:325–332. doi:10.1080/14647273.2019.1672107.

Macaulay, A. D., I. Gilbert, J. Caballero, R. Barreto, E. Fournier, P. Tossou, M.-A. Sirard, H. J. Clarke, É. W. Khandjian, F. J. Richard, P. Hyttel, and C. Robert. 2014. The gametic synapse: RNA transfer to the bovine oocyte. Biol. Reprod. 91:90. doi:10.1095/biolreprod.114.119867.

Mattick, J. S., P. P. Amaral, P. Carninci, S. Carpenter, H. Y. Chang, L.-L. Chen, R. Chen, C. Dean, M. E. Dinger, K. A. Fitzgerald, T. R. Gingeras, M. Guttman, T. Hirose, M. Huarte, R. Johnson, C. Kanduri, P. Kapranov, J. B. Lawrence, J. T. Lee, J. T. Mendell, T. R. Mercer, K. J. Moore, S. Nakagawa, J. L. Rinn, D. L. Spector, I. Ulitsky, Y. Wan, J. E. Wilusz, and M. Wu. 2023. Long non-coding RNAs: definitions, functions, challenges and recommendations. Nat. Rev. Mol. Cell Biol. 1–17. doi:10.1038/s41580-022-00566-8.

McMahon, H. E., S. Sharma, and S. Shimasaki. 2008. Phosphorylation of Bone Morphogenetic Protein-15 and Growth and Differentiation Factor-9 Plays a Critical Role in Determining Agonistic or Antagonistic Functions. Endocrinology. 149:812–817. doi:10.1210/en.2007-1439.

Murdoch, W. J., R. A. Dailey, and E. K. Inskeep. 1981. Preovulatory Changes in Prostaglandins E2 and F2α in Ovine Follicles2. J. Anim. Sci. 53:192–205. doi:10.2527/jas1981.531192x.

Oakley, O. R., M. L. Frazer, and C. Ko. 2011. Pituitary–ovary–spleen axis in ovulation. Trends Endocrinol. Metab. 22:345–352. doi:10.1016/j.tem.2011.04.005.

Oakley, O. R., H. Kim, I. El-Amouri, P.-C. Patrick Lin, J. Cho, M. Bani-Ahmad, and C. Ko. 2010. Periovulatory Leukocyte Infiltration in the Rat Ovary. Endocrinology. 151:4551–4559. doi:10.1210/en.2009-1444.

Patiño, L. C., K. L. Walton, T. D. Mueller, K. E. Johnson, W. Stocker, D. Richani, D. Agapiou, R. B. Gilchrist, P. Laissue, and C. A. Harrison. 2017. BMP15 Mutations Associated With

Primary Ovarian Insufficiency Reduce Expression, Activity, or Synergy With GDF9. J. Clin. Endocrinol. Metab. 102:1009–1019. doi:10.1210/jc.2016-3503.

Paulini, F., and E. O. Melo. 2011. The Role of Oocyte-Secreted Factors GDF9 and BMP15 in Follicular Development and Oogenesis. Reprod. Domest. Anim. 46:354–361. doi:10.1111/j.1439-0531.2010.01739.x.

Peng, Y., L. Chang, Y. Wang, R. Wang, L. Hu, Z. Zhao, L. Geng, Z. Liu, Y. Gong, J. Li, X. Li, and C. Zhang. 2019. Genome-wide differential expression of long noncoding RNAs and mRNAs in ovarian follicles of two different chicken breeds. Genomics. 111:1395–1403. doi:10.1016/j.ygeno.2018.09.012.

Plath, K., J. Fang, S. K. Mlynarczyk-Evans, R. Cao, K. A. Worringer, H. Wang, C. C. de la Cruz, A. P. Otte, B. Panning, and Y. Zhang. 2003. Role of Histone H3 Lysine 27 Methylation in X Inactivation. Science. 300:131–135. doi:10.1126/science.1084274.

Platonova, O., I. V. Akey, J. F. Head, and C. W. Akey. 2011. Crystal Structure and Function of Human Nucleoplasmin (Npm2): A Histone Chaperone in Oocytes and Embryos. Biochemistry. 50:8078–8089. doi:10.1021/bi2006652.

Rao, M. R. S. 2017. Long Non Coding RNA Biology. In: Advances in Experimental Medicine and Biology. Vol. 1008. p. 1–46.

Rexroad, C. E., L. E. Casida, and W. J. Tyler. 1974. Crown-Rump Length of Fetuses in Purebred Holstein-Friesian Cows1,2. J. Dairy Sci. 57:346–347. doi:10.3168/jds.S0022-0302(74)84891-5.

Rinn, J. L., M. Kertesz, J. K. Wang, S. L. Squazzo, X. Xu, S. A. Brugmann, L. H. Goodnough, J. A. Helms, P. J. Farnham, E. Segal, and H. Y. Chang. 2007. Functional demarcation of active and silent chromatin domains in human HOX loci by noncoding RNAs. Cell. 129:1311–1323. doi:10.1016/j.cell.2007.05.022.

Shi, Y., M. Cai, K. Du, X. Bai, L. Tang, X. Jia, S. Chen, J. Wang, and S. Lai. 2021. Dynamics of Known Long Non-Coding RNAs during the Maternal-to-Zygotic Transition in Rabbit. Animals. 11:3592. doi:10.3390/ani11123592.

Smits, G., A. J. Mungall, S. Griffiths-Jones, P. Smith, D. Beury, L. Matthews, J. Rogers, A. J. Pask, G. Shaw, J. L. VandeBerg, J. R. McCarrey, M. B. Renfree, W. Reik, and I. Dunham. 2008. Conservation of the H19 noncoding RNA and H19-IGF2 imprinting mechanism in therians. Nat. Genet. 40:971–976. doi:10.1038/ng.168.

Statello, L., C.-J. Guo, L.-L. Chen, and M. Huarte. 2021. Gene regulation by long non-coding RNAs and its biological functions. Nat. Rev. Mol. Cell Biol. 22:96–118. doi:10.1038/s41580-020-00315-9.

Su, Y.-Q., X. Wu, M. J. O'Brien, F. L. Pendola, J. N. Denegre, M. M. Matzuk, and J. J. Eppig. 2004. Synergistic roles of BMP15 and GDF9 in the development and function of the oocyte-cumulus cell complex in mice: genetic evidence for an oocyte-granulosa cell regulatory loop. Dev. Biol. 276:64–73. doi:10.1016/j.ydbio.2004.08.020.

Sun, Z., Z. Zhang, Y. Liu, C. Ren, X. He, Y. Jiang, Y. Ouyang, Q. Hong, and M. Chu. 2022. Integrated Analysis of mRNAs and Long Non-Coding RNAs Expression of Oviduct That Provides Novel Insights into the Prolificacy Mechanism of Goat (Capra hircus). Genes. 13:1031. doi:10.3390/genes13061031.

Taylor, D. H., E. T.-J. Chu, R. Spektor, and P. D. Soloway. 2015. Long non-coding RNA regulation of reproduction and development. Mol. Reprod. Dev. 82:932–956. doi:10.1002/mrd.22581.

Tripathi, V., J. D. Ellis, Z. Shen, D. Y. Song, Q. Pan, A. T. Watt, S. M. Freier, C. F. Bennett, A. Sharma, P. A. Bubulya, B. J. Blencowe, S. G. Prasanth, and K. V. Prasanth. 2010. The nuclear-retained noncoding RNA MALAT1 regulates alternative splicing by modulating SR splicing factor phosphorylation. Mol. Cell. 39:925–938. doi:10.1016/j.molcel.2010.08.011.

Wang, J., P. P. Koganti, and J. Yao. 2020. Systematic identification of long intergenic non-coding RNAs expressed in bovine oocytes. Reprod. Biol. Endocrinol. RBE. 18:13. doi:10.1186/s12958-020-00573-4.

Wang, Y., S. Xue, X. Liu, H. Liu, T. Hu, X. Qiu, J. Zhang, and M. Lei. 2016. Analyses of Long Non-Coding RNA and mRNA profiling using RNA sequencing during the pre-implantation phases in pig endometrium. Sci. Rep. 6:20238. doi:10.1038/srep20238.

Xing, Z., A. Lin, C. Li, K. Liang, S. Wang, Y. Liu, P. K. Park, L. Qin, Y. Wei, D. H. Hawke, M.-C. Hung, C. Lin, and L. Yang. 2014. lncRNA directs cooperative epigenetic regulation downstream of chemokine signals. Cell. 159:1110–1125. doi:10.1016/j.cell.2014.10.013.

Yan, C., P. Wang, J. DeMayo, F. J. DeMayo, J. A. Elvin, C. Carino, S. V. Prasad, S. S. Skinner, B. S. Dunbar, J. L. Dube, A. J. Celeste, and M. M. Matzuk. 2001. Synergistic Roles of Bone Morphogenetic Protein 15 and Growth Differentiation Factor 9 in Ovarian Function. Mol. Endocrinol. 15:854–866. doi:10.1210/mend.15.6.0662.

Yang, F., X. Deng, W. Ma, J. B. Berletch, N. Rabaia, G. Wei, J. M. Moore, G. N. Filippova, J. Xu, Y. Liu, W. S. Noble, J. Shendure, and C. M. Disteche. 2015. The lncRNA Firre anchors the inactive X chromosome to the nucleolus by binding CTCF and maintains H3K27me3 methylation. Genome Biol. 16:52. doi:10.1186/s13059-015-0618-0.

Yap, K., S. Mukhina, G. Zhang, J. S. C. Tan, H. S. Ong, and E. V. Makeyev. 2018. A Short Tandem Repeat-Enriched RNA Assembles a Nuclear Compartment to Control Alternative Splicing and Promote Cell Survival. Mol. Cell. 72:525-540.e13. doi:10.1016/j.molcel.2018.08.041.

Zhang, F.-L., N. Li, H. Wang, J.-M. Ma, W. Shen, and L. Li. 2019. Zearalenone Exposure Induces the Apoptosis of Porcine Granulosa Cells and Changes Long Noncoding RNA Expression To Promote Antiapoptosis by Activating the JAK2–STAT3 Pathway. J. Agric. Food Chem. 67:12117–12128. doi:10.1021/acs.jafc.9b05189.

Zhao, L., Y. Pan, M. Wang, Junqian Wang, Y. Wang, X. Han, Jinglei Wang, T. Zhang, T. Zhao, H. He, Y. Cui, and S. Yu. 2022. Integrated analysis of the expression profiles of the lncRNA-

miRNA-mRNA ceRNA network in granulosa and cumulus cells from yak ovaries. BMC Genomics. 23:633. doi:10.1186/s12864-022-08848-3.

Zhao, M., Y. Qiu, B. Yang, L. Sun, K. Hei, X. Du, and Y. Li. 2014. Long Non-Coding RNAs Involved in Gynecological Cancer. Int. J. Gynecol. Cancer. 24. doi:10.1097/IGC.0000000000000212. Available from: https://ijgc.bmj.com/content/24/7/1140

Zhong, L., H. Mu, B. Wen, W. Zhang, Q. Wei, G. Gao, J. Han, and S. Cao. 2018. Long non-coding RNAs involved in the regulatory network during porcine pre-implantation embryonic development and iPSC induction. Sci. Rep. 8:6649. doi:10.1038/s41598-018-24863-5.

Figure 1. The schematic diagram for three novel lncRNAs. (A) *OOSNCR1* is 2,073 bps in length and contains 3 exons and 2 introns spanning about 10 kb on bovine chromosome 1. (B) *OOSNCR2* is 292 bps on chromosome 4 and contains 3 exons and 2 introns spanning approximately 67kb with intron 2 being about 64 kb. (C) *OOSNCR3* is 384 bps and is the smallest transcript with about 550 bp in length on chromosome 19 and contains 2 exons and 1 intron.

Figure 2. The predicted secondary structures for three novel lncRNAs. Secondary structures were predicted using The Vienna RNA Website (Gruber et al., 2008). The optimal minimum free energy (MFE) and centroid secondary structures were predicted based on the lowest free energy value denoting a more stable structure. (A) *OOSNCR1,* (B) *OOSNCR2,* and (C) *OOSNCR3* had a minimum free energy of -595.54 kcal/mol, -71.80 kcal/mol, and -88.00 kcal/mol, respectively.

Figure 3. Tissue expression profiles for three novel lncRNAs. Relative abundance levels of (A) *OOSNCR1,* (B) *OOSNCR2,* and (C) *OOSNCR3* in the liver, kidney, lung, thymus, spleen, adrenal, cortex, rumen, jejunum, vagina, caruncle, skeletal muscle, cardiac muscle, smooth muscle, and fetal ovaries. All data are quantified using RT-qPCR and normalized to *RPL19* as an endogenous control. *OOSNCR1* and *OOSNCR2* were detected exclusively in early fetal ovaries (gestation day 90-105) and late fetal ovaries (gestation day 160-280), suggesting oocyte-specificity. In contrast, *OOSNCR3* was detected at low levels in the spleen and the fetal ovaries. All tissue samples were collected from the same animal (n = 4) and examined for each lncRNA.

Figure 4. Characterization of novel lncRNAs' expression in the bovine antral follicle. Relative abundance of novel lncRNAs (A) *OOSNCR1,* (B) *OOSNCR2,* and (C) *OOSNCR3* in bovine follicular cells. Theca and mural granulosa cells were isolated from individual follicles (n = 7), whereas cumulus cells were denuded from immature and mature oocytes in pools of 20 (n = 7).

All data were quantified via RT-qPCR and normalized to *RPL19* as an endogenous control. *OOSNCR1, OOSNCR2,* and *OOSNCR3* were all detected at the highest level in the oocytes regardless of maturation status ($P > 0.32$). Moving outward from the oocyte, all three lncRNAs were more abundant in the CCs than the mGCs and TCs. Moreover, the maturation stage was not significant due to variation among the CC samples ($P = 0.24$). At the furthest reaches of the follicle, *OOSNCR1* was expressed higher ($P = 0.025$) in the mGCs than in the TCs. In contrast, no difference was detected in the expression of *OOSNCR2* and *OOSNCR3* ($P = 0.48$) in these outer cell types.

Figure 5. Characterization of novel lncRNAs' expression throughout oocyte maturation and early embryonic development. Relative abundance of novel lncRNAs (A) *OOSNCR1,* (B) *OOSNCR2,* and (C) *OOSNCR3* in pools of 20 denuded oocytes (GV and MII) and early embryos at the two-cell, four-cell, eight-cell, 16-cell, morula, and blastocysts stage was examined using RT-qPCR. All three lncRNAs exhibited similar patterns of expression. *OOSNCR1, OOSNCR2,* and *OOSNCR3* were highest in immature and mature oocytes ($P < 0.001$) compared to the blastocysts stage. All three lncRNAs' expression decreased following fertilization ($P < 0.06$) and remained steady until the eight-cell stage ($P = 0.99$). Following the eight-cell stage, all three lncRNAs ceased expression by the blastocyst stage ($P < 0.02$).

Figure 6. Identifying the origins of *OOSNCR1, OOSNCR2,* and *OOSNCR3* in early embryos. The origin of novel lncRNAs (A) *OOSNCR1,* (B) *OOSNCR2,* and (C) *OOSNCR3* was examined in early embryos following α-amanitin treatment. All data were quantified via RT-qPCR and normalized to *GFP* as an exogenous control. Treated and control embryos were collected in pools of 10 at the first (33 hpi; n = 3), second (44 hpi; n = 6), and third embryonic division (52 hpi; n = 6). All three lncRNAs exhibited an identical pattern following treatment. When cultured under

standard conditions, each lncRNA increased during the first embryonic division and then decreased by the third division. However, when cultured in the presence of α-amanitin, each lncRNA decreased following the first embryonic division ($P < 0.0001$) and remained steady through the third division ($P < 0.27$).

Figure 7. Subcellular localization of *OOSNCR1* within immature oocytes. A representative image of *OOSCNR1* detection in germinal vesicle stage oocytes. Fluorescent *in situ* hybridization with a custom probe detected the candidate lncRNA solely in the cytoplasm of immature oocytes.

Figure 8. Validation of siRNA-mediated knockdown of three novel lncRNAs in mature oocytes quantified using RT-qPCR. Relative abundance of novel lncRNAs (A) *OOSNCR1*, (B) *OOSNCR2*, and (C) *OOSNCR3* in pools of 5 denuded mature oocytes (n = 7) was analyzed to validate gene knockdown. COCs were injected with a universal control, a cocktail of 2 siRNA species targeting each lncRNA, or remained as uninjected controls. LncRNA knockdown during oocyte maturation was achieved in all three lncRNAs ($P < 0.009$).

Figure 9. Cumulus cell expansion during oocyte maturation following siRNA-mediated knockdown of *OOSNCR1, OOSNCR2,* and *OOSNCR3.* (A) Representative image of COC expansion following treatment. (B) Effects of lncRNA knockdown on cumulus expansion for each candidate gene, *OOSNCR1*, *OOSNCR2*, and *OOSNCR3*, compared to the injected and uninjected control. The area was measured for individual COCs, with each replicate (n = 5) having at least 20 COCs present. The average area was determined for each replicate. No difference in cumulus expansion following knockdown was detected in any treatment group ($P > 0.71$).

Figure 10. **Relative abundance of select genes linked to bovine oocyte competency.** Select genes (*NPM2, GDF9, BMP15, JY-1* and *USF1)* were quantified using RT-qPCR in denuded MII

oocytes (n = 7; pools of 5) following siRNA-mediated knockdown of *OOSNCR1, OOSNCR2,* and *OOSNCR3*. (A) *NPM2* expression was downregulated following the knockdown of all three lncRNAs ($P < 0.0179$). (B) *GDF9* was downregulated following the knockdown of *OOSNCR1* and *OOSNCR3* ($P < 0.0159$). (C) *BMP15* and (D) *JY-1* were downregulated following *OOSNCR1* knockdown ($P < 0.012$). (E) *USF1* expression was not affected by lncRNA knockdown ($P > 0.645$).

Figure 11. Validation of siRNA-mediated knockdown of three novel lncRNAs in presumptive zygotes quantified using RT-qPCR. Relative abundance of novel lncRNAs (A) *OOSNCR1,* (B) *OOSNCR2,* and (C) *OOSNCR3* in pools of 5 four-cell embryos (n = 7) was analyzed to validate gene knockdown. Presumptive zygotes were injected with a universal control, a cocktail of 2 siRNA species targeting each lncRNA, or remained as uninjected controls. There was a tendency for knockdown of *OOSNR1* ($P = 0.055$) and *OOSNCR3* ($P = 0.10$), but ablation was not achieved with *OOSNCR2* ($P = 0.6$).

Figure 1

A

B

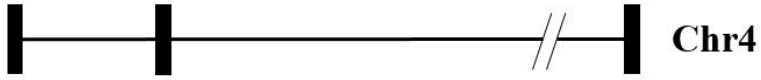

C

Figure 2

A

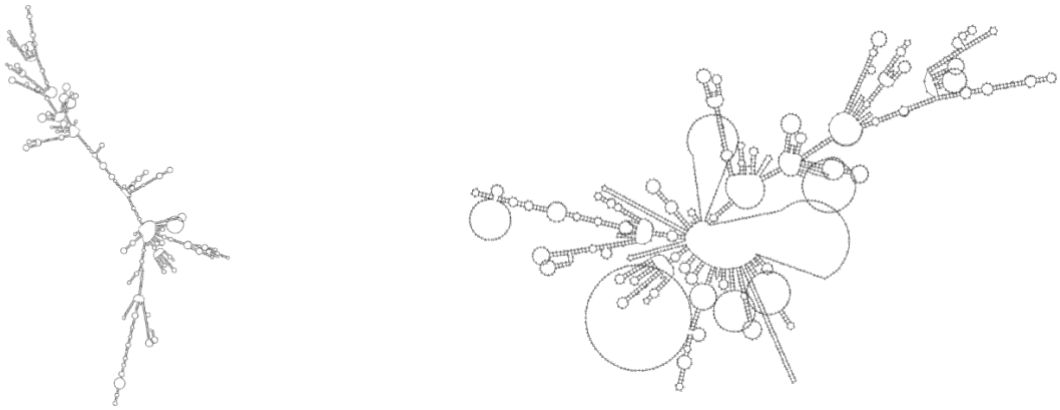

B

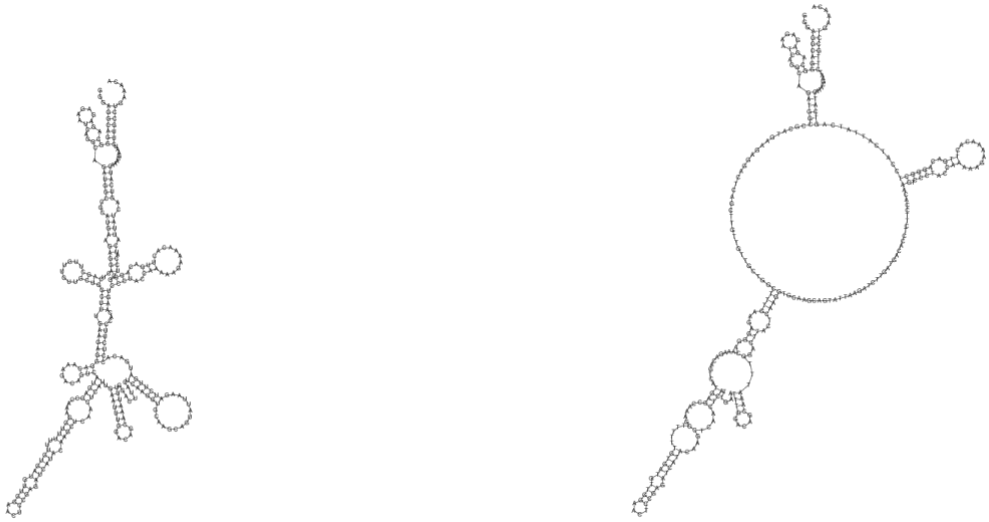

C

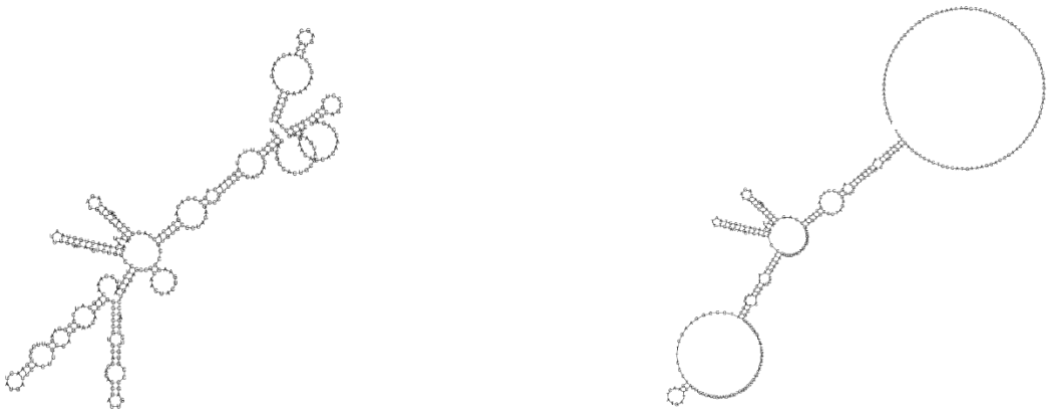

Figure 3

A.

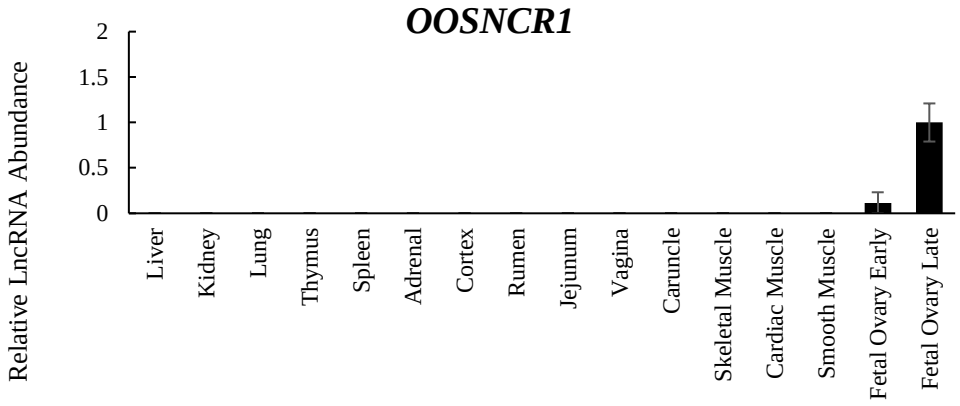
OOSNCR1
Relative LncRNA Abundance
2
1.5
1
0.5
0
Liver
Kidney
Lung
Thymus
Spleen
Adrenal
Cortex
Rumen
Jejunum
Vagina
Caruncle
Skeletal Muscle
Cardiac Muscle
Smooth Muscle
Fetal Ovary Early
Fetal Ovary Late

B.

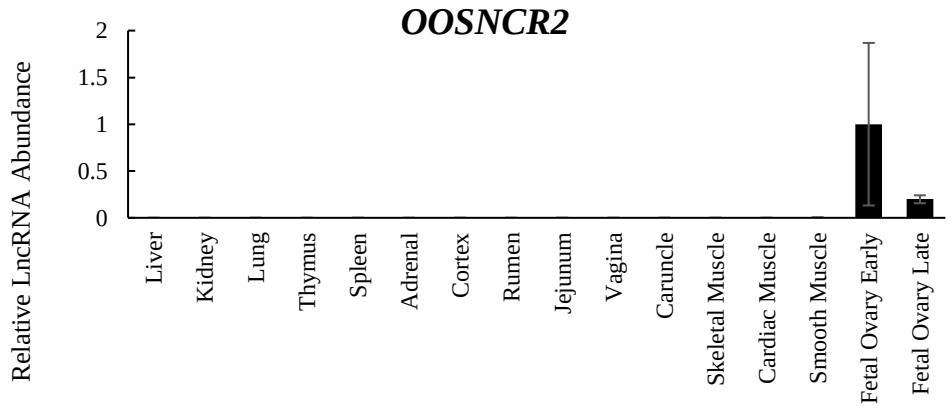
OOSNCR2
Relative LncRNA Abundance
2
1.5
1
0.5
0
Liver
Kidney
Lung
Thymus
Spleen
Adrenal
Cortex
Rumen
Jejunum
Vagina
Caruncle
Skeletal Muscle
Cardiac Muscle
Smooth Muscle
Fetal Ovary Early
Fetal Ovary Late

C.

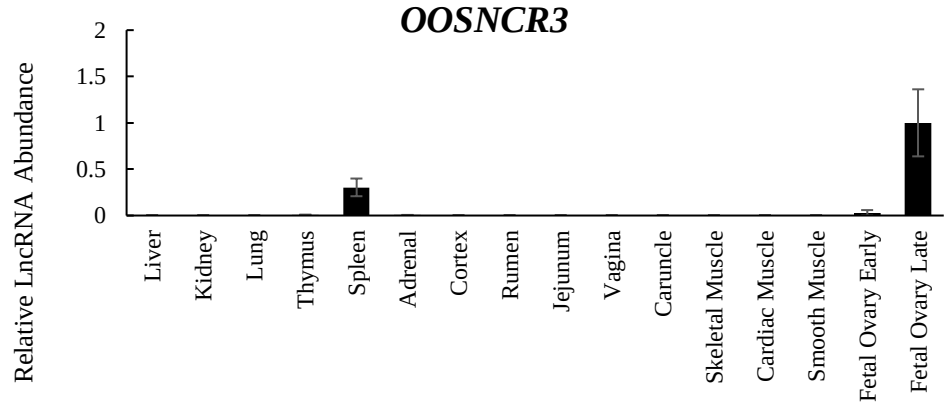
OOSNCR3
Relative LncRNA Abundance
2
1.5
1
0.5
0
Liver
Kidney
Lung
Thymus
Spleen
Adrenal
Cortex
Rumen
Jejunum
Vagina
Caruncle
Skeletal Muscle
Cardiac Muscle
Smooth Muscle
Fetal Ovary Early
Fetal Ovary Late

Figure 4

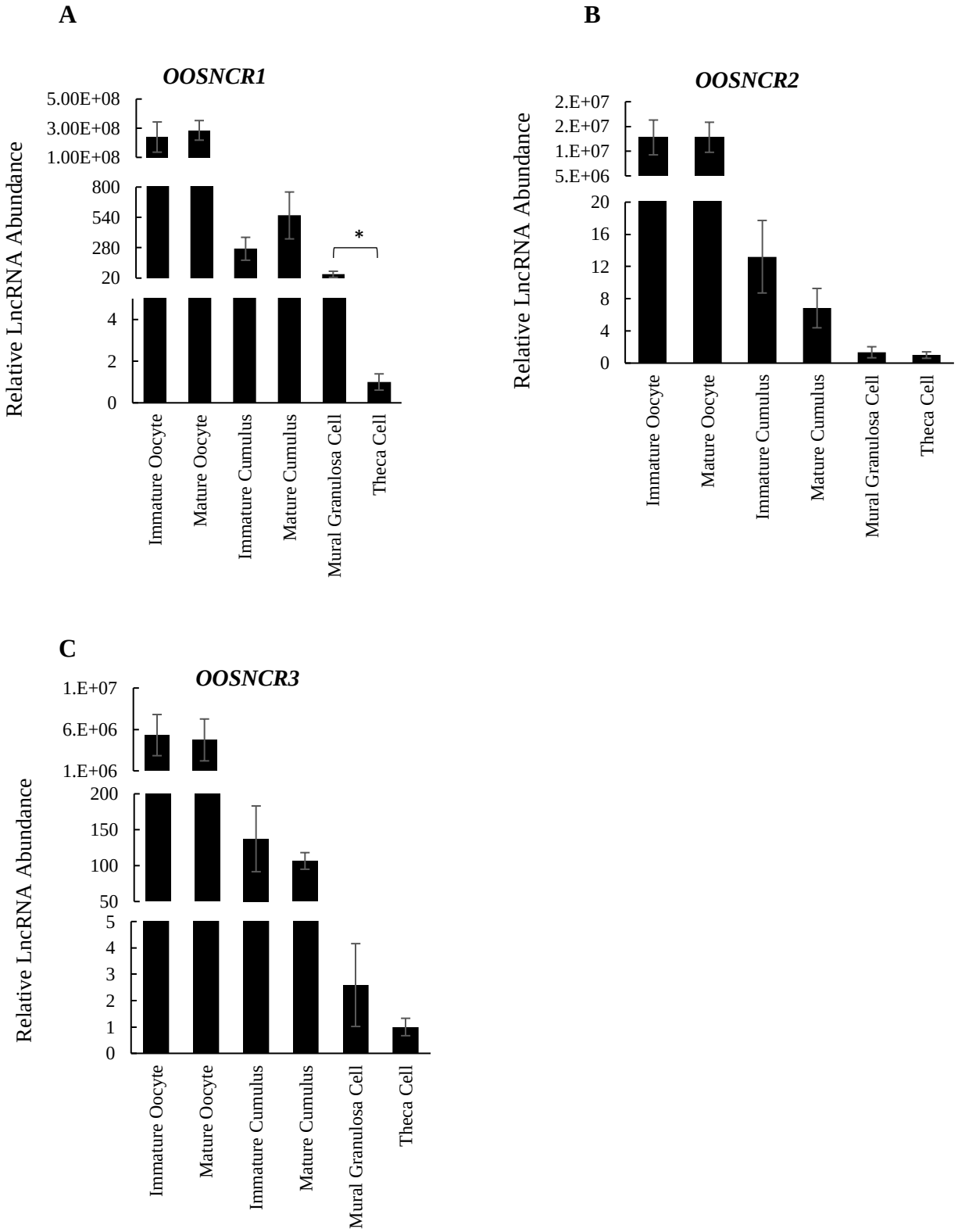
A
OOSNCR1
Relative LncRNA Abundance
5.00E+08
3.00E+08
1.00E+08
800
540
280
20
4
2
0
*
Immature Oocyte
Mature Oocyte
Immature Cumulus
Mature Cumulus
Mural Granulosa Cell
Theca Cell
B
OOSNCR2
Relative LncRNA Abundance
2.E+07
2.E+07
1.E+07
5.E+06
20
16
12
8
4
0
Immature Oocyte
Mature Oocyte
Immature Cumulus
Mature Cumulus
Mural Granulosa Cell
Theca Cell
C
OOSNCR3
Relative LncRNA Abundance
1.E+07
6.E+06
1.E+06
200
150
100
50
5
4
3
2
1
0
Immature Oocyte
Mature Oocyte
Immature Cumulus
Mature Cumulus
Mural Granulosa Cell
Theca Cell

Figure 5

A.

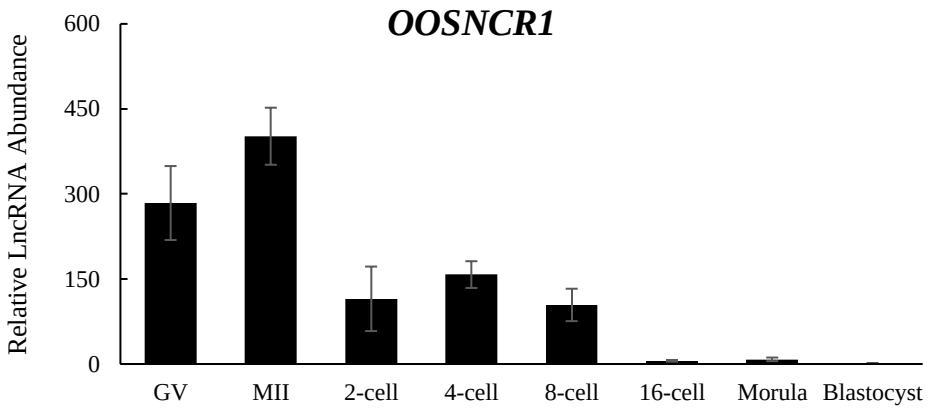
OOSNCR1
Relative LncRNA Abundance
600
450
300
150
0
GV
MII
2-cell
4-cell
8-cell
16-cell
Morula
Blastocyst

B.

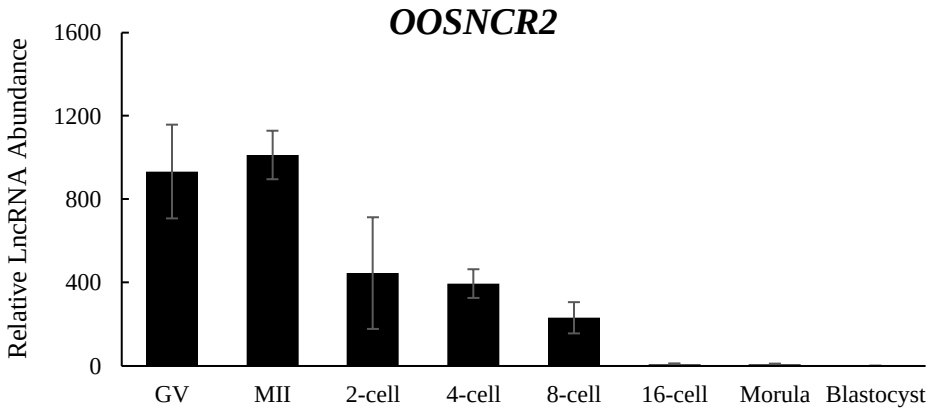
OOSNCR2
Relative LncRNA Abundance
1600
1200
800
400
0
GV
MII
2-cell
4-cell
8-cell
16-cell
Morula
Blastocyst

C.

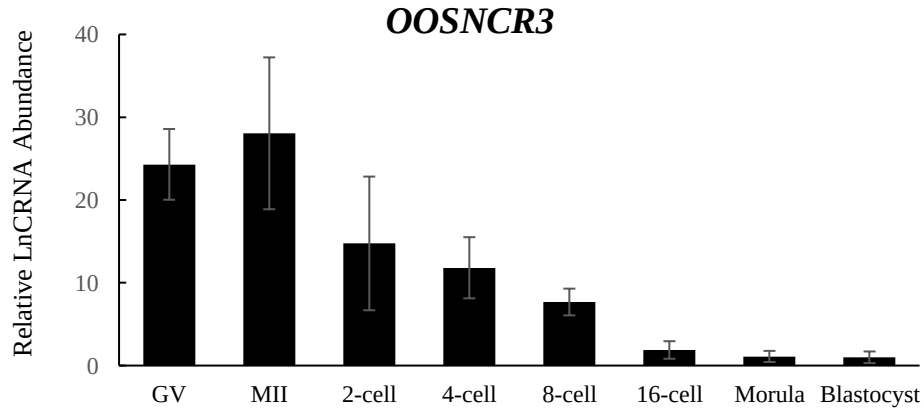
OOSNCR3
Relative LnCRNA Abundance
40
30
20
10
0
GV
MII
2-cell
4-cell
8-cell
16-cell
Morula
Blastocyst

Figure 6.

A

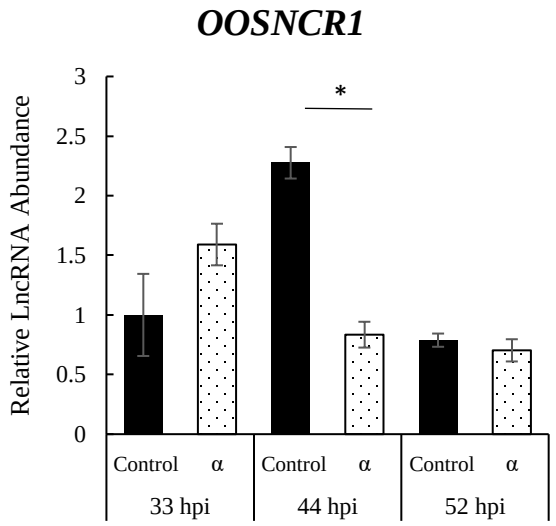
OOSNCR1
Relative LncRNA Abundance
3
2.5
2
1.5
1
0.5
0
*
Control
α
Control
α
Control
α
33 hpi
44 hpi
52 hpi

B

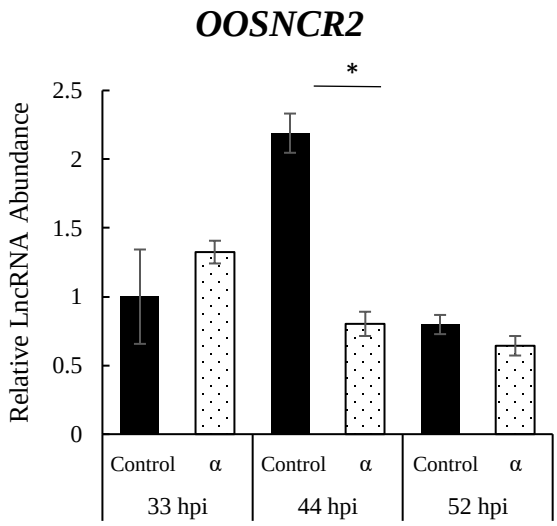
OOSNCR2
Relative LncRNA Abundance
2.5
2
1.5
1
0.5
0
*
Control
α
Control
α
Control
α
33 hpi
44 hpi
52 hpi

C

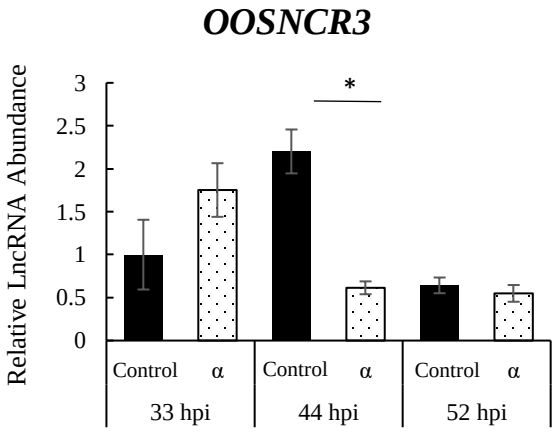
OOSNCR3
Relative LncRNA Abundance
3
2.5
2
1.5
1
0.5
0
*
Control
α
Control
α
Control
α
33 hpi
44 hpi
52 hpi

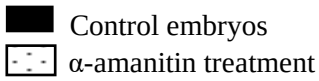
Control embryos
α-amanitin treatment

Figure 7

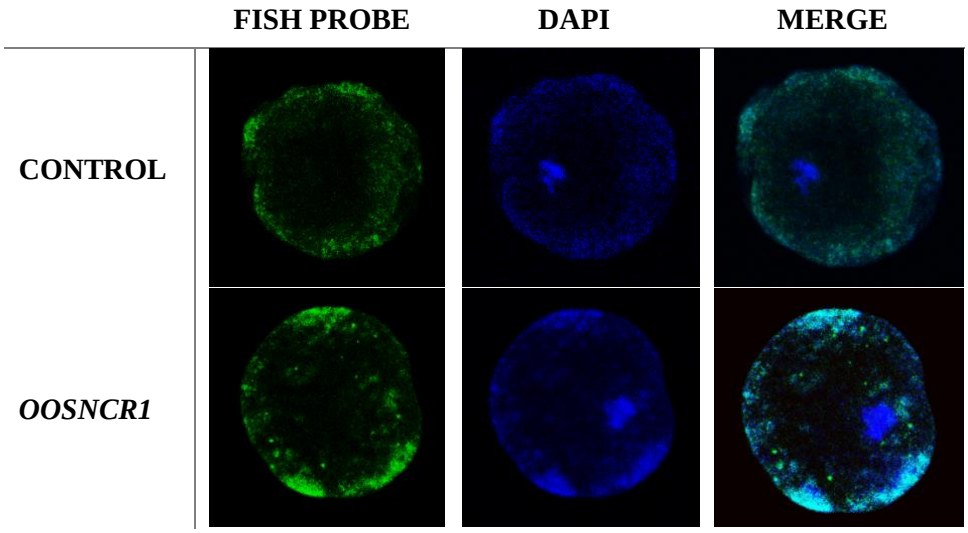

Figure 8

A

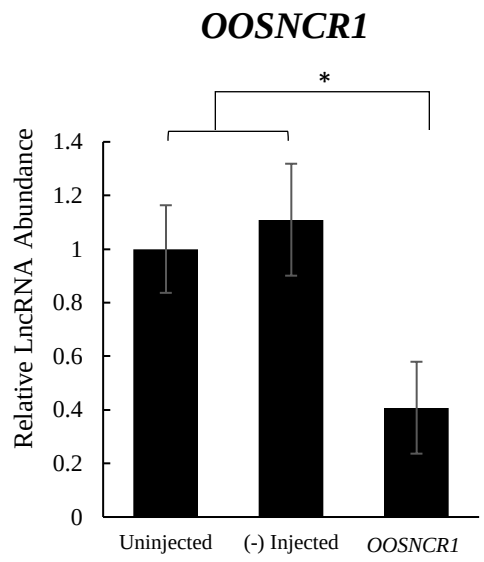
OOSNCR1
*
Relative LncRNA Abundance
1.4
1.2
1
0.8
0.6
0.4
0.2
0
Uninjected
(-) Injected
OOSNCR1

B

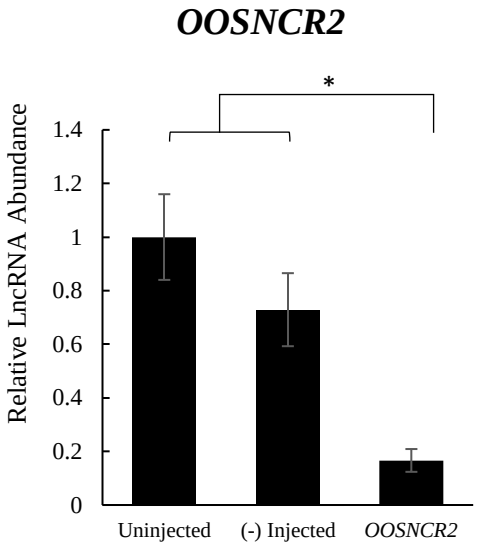
OOSNCR2
*
Relative LncRNA Abundance
1.4
1.2
1
0.8
0.6
0.4
0.2
0
Uninjected
(-) Injected
OOSNCR2

C

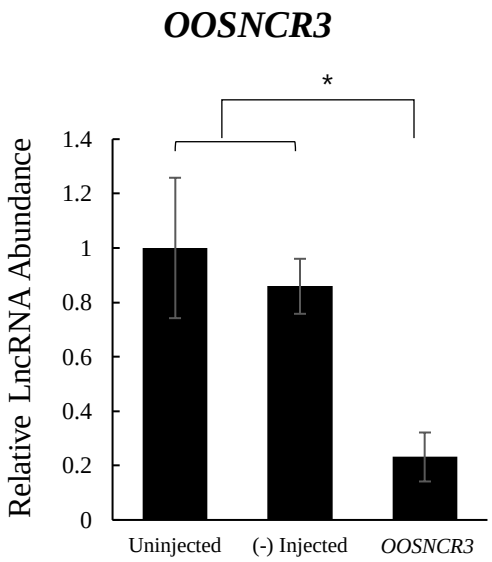
OOSNCR3
*
Relative LncRNA Abundance
1.4
1.2
1
0.8
0.6
0.4
0.2
0
Uninjected
(-) Injected
OOSNCR3

Figure 9

A

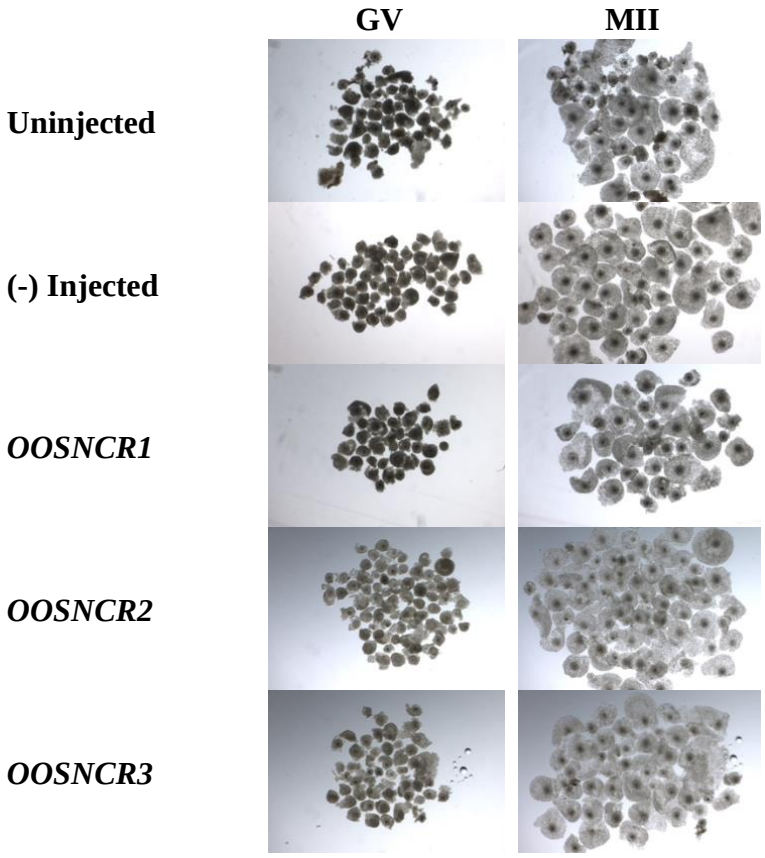
GV
MII
Uninjected
(-) Injected
OOSNCR1
OOSNCR2
OOSNCR3

B

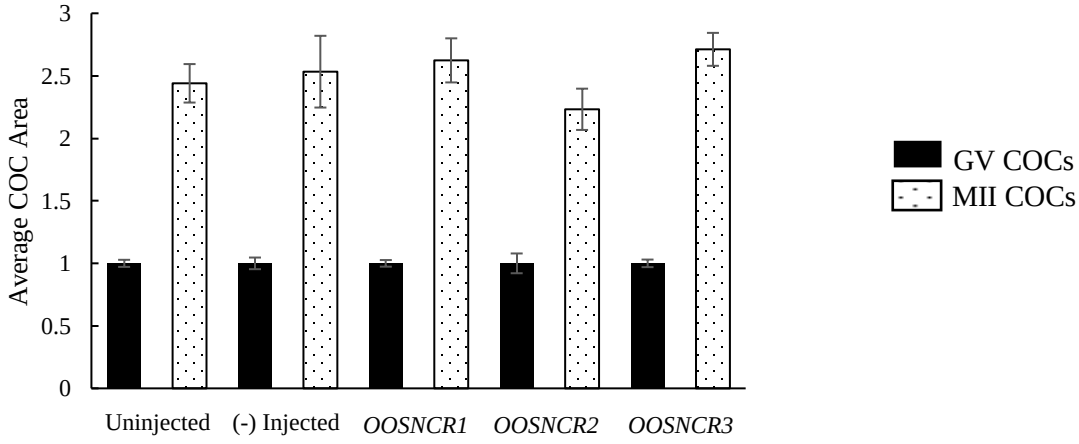
Average COC Area
3
2.5
2
1.5
1
0.5
0
Uninjected
(-) Injected
OOSNCR1
OOSNCR2
OOSNCR3
GV COCs
MII COCs

Figure 10

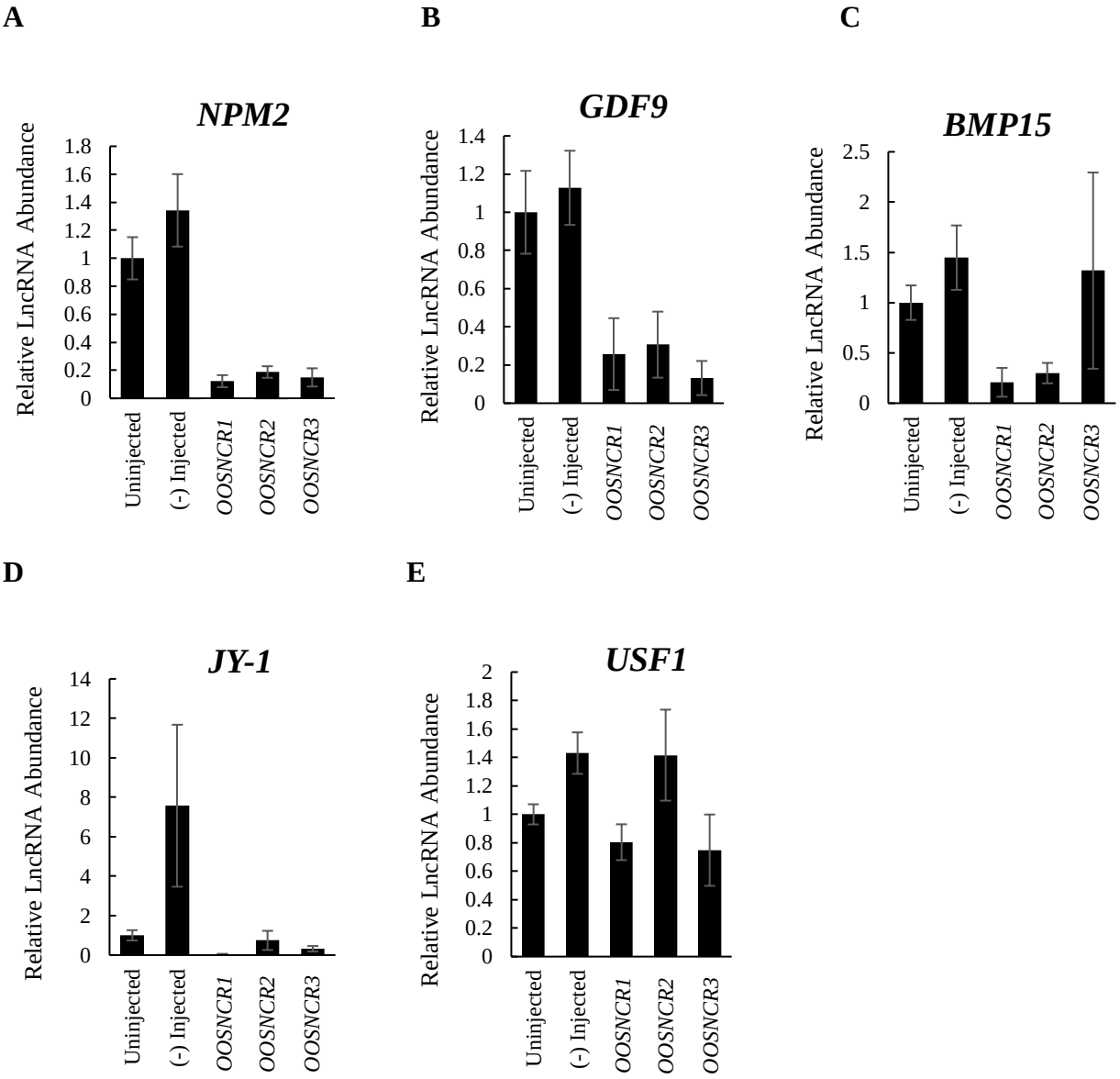
A
NPM2
Relative LncRNA Abundance
1.8
1.6
1.4
1.2
1
0.8
0.6
0.4
0.2
0
Uninjected
(-) Injected
OOSNCR1
OOSNCR2
OOSNCR3
B
GDF9
Relative LncRNA Abundance
1.4
1.2
1
0.8
0.6
0.4
0.2
0
Uninjected
(-) Injected
OOSNCR1
OOSNCR2
OOSNCR3
C
BMP15
Relative LncRNA Abundance
2.5
2
1.5
1
0.5
0
Uninjected
(-) Injected
OOSNCR1
OOSNCR2
OOSNCR3
D
JY-1
Relative LncRNA Abundance
14
12
10
8
6
4
2
0
Uninjected
(-) Injected
OOSNCR1
OOSNCR2
OOSNCR3
E
USF1
Relative LncRNA Abundance
2
1.8
1.6
1.4
1.2
1
0.8
0.6
0.4
0.2
0
Uninjected
(-) Injected
OOSNCR1
OOSNCR2
OOSNCR3

Figure 11

A

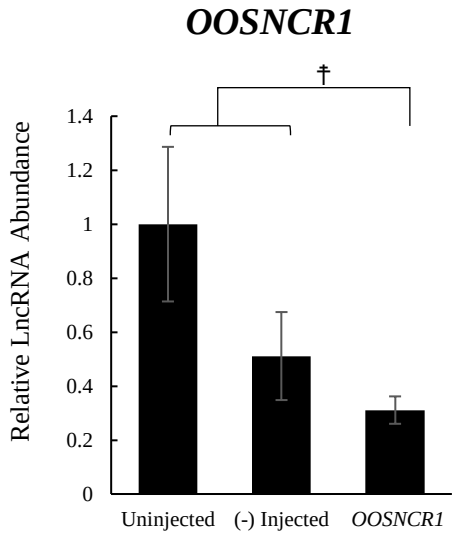

B

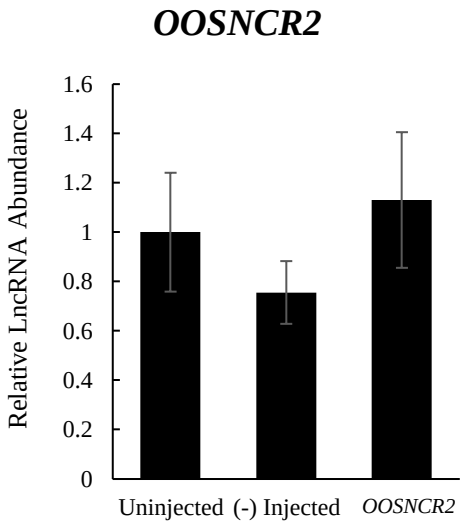

C

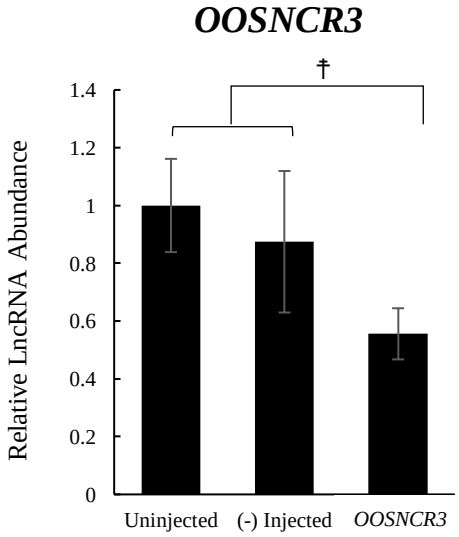

Table 1. Primers used for RT-qPCR

Gene	Primer	Primer Sequence (5'-3')	Application
RPL19	Forward	GAAATCGCCAATGCCAACTC	RT-qPCR
	Reverse	GAGCCTTGTCTGCCTTCA	
GFP	Forward	CAACAGCCACAACGTCTATATCATG	RT-qPCR
	Reverse	ATGTTGTGGCGGATCTTGAAG	
OOSNCR1	Forward	CCAACAGCTCATCTGTCAATT	RT-qPCR
	Reverse	GTTTCCTTGTGGCCATCTTTG	
OOSNCR2	Forward	GCAGAGAGAATCAGGCAGATG	RT-qPCR
	Reverse	GTATGATCTCGGAGTTCCAAC	
OOSNCR3	Forward	CTCTCATTCCAAACAGCATCC	RT-qPCR
	Reverse	CACACGGGCTTCAGTAGTTGC	

Table 2. Custom primers used for FISH

Probe	Primers	Primer Sequence (5'-3')	Nested PCR
OOSNCR1	Forward	TTTCAAGCAATCAGTAGCCAC	1st RXN
	Reverse	CCTACTGGTGCCTAAGCATTG	
	Forward – T7	GAAATTAATACGACTCACTATAGATTAACACGACCCCTCCAATC	2nd RXN
	Reverse – SP6	GAAATATTTAGGTGACACTATAGGCTCAGCAGTGCTTGTCTTCT	

Table 3. Blastocyst rates following α-Amanitin treatment in presumptive zygotes

	Blastocyst Rate (%) ± SEM
Control	44 ± 5.1
α-Amanitin	0

Table 4. The percent survival of uninjected and injected COCs at 12 hpi

Treatment	Alive at 12 hpi	Dead at 12 hpi	Survival at 12 hpi (%)	Average Survival (%) ± SEM
Uninjected	31	6	83.78	90.55 ± 4.87[a]
	29	4	87.88	
	17	0	100.00	
(-) Injected	8	2	80.00	59.49 ± 10.44[b]
	11	13	45.83	
	10	9	52.63	
OOSNCR1	10	30	25.00	21.42 ± 2.48[b]
	7	24	22.58	
	4	20	16.67	
OOSNCR2	10	16	38.46	35.68 ± 3.58[b]
	8	20	28.57	
	18	27	40.00	
OOSNCR3	9	7	56.25	48.33 ± 4.14[b]
	11	15	42.31	
	13	15	46.43	

[b] Different from the uninjected control; $P < 0.05$

Table 5. Blastocyst rates following siRNA-mediated knockdown in immature oocytes

	Blastocyst Rate (%) ± SEM
Uninjected	25 ± 0.04[a]
(-) Injected	21 ± 0.05[a]
OOSNCR1	3 ± 0.003[b]
OOSNCR2	2 ± 0.0046[b]
OOSNCR3	6 ± 0.04[b]

[b] Different from the uninjected control; $P < 0.05$

Table 6. Blastocyst rates following siRNA-mediated knockdown in presumptive zygotes

	Blastocyst Rate (% ± SEM)
Uninjected	31 ± 0.004[a]
(-) Injected	30 ± 0.012[a]
OOSNCR1	14 ± 0.025[b]
OOSNCR2	14 ± 0.018[b]
OOSNCR3	15 ± 0.033[b]

[b] Different from the uninjected; $P < 0.05$

Chapter 2

Novel long non-coding RNA expression and its relationship with oocyte quality

Jaelyn Z. Current[1], Heather L. Chaney[1], Mingxiang Zhang[1], Emily M. Dugan[1], Gianna L. Chimino[1], and Jianbo Yao[1]

[1]Laboratory of Animal Biotechnology and Genomics, Division of Animal and Nutritional Sciences, West Virginia University, Morgantown, WV 26506, United States

KEYWORDS: Non-coding RNA, oocyte quality, follicle size, heat stress

ABSTRACT

It is well documented that the constitution of the early embryo depends upon the oocyte's composition. However, defining oocyte quality remains enigmatic. With the advent of deep sequencing techniques, an ever-growing collection of regulatory non-coding RNAs within the mammalian genome has appeared. This study quantified novel long non-coding RNAs (lncRNAs) in bovine oocytes of varying quality. Specifically, lncRNA expression was examined in COCs (1) collected from small and large follicles before and after maturation, (2) differentially stained using BCB, and (3) exposed to heat stress (41°C) during oocyte maturation. In single oocytes, novel lncRNAs, *OOSNCR1* and *OOSNCR3,* were accumulated during maturation, whereas *OOSNCR2* and *OOSNCR4* degraded. *OOSNCR1*, *OOSNCR2*, and *OOSNCR4* were more abundant in oocytes collected from small follicles; specifically, *OOSNCR2* and *OOSNCR4* were expressed highest in immature oocytes. Conversely, *OOSNCR3* was more abundant in mature oocytes collected from large follicles. Following BCB staining, *OOSNCR3* was expressed lower in BCB+ oocytes. Maturating in a heat-stressed environment caused *OOSNCR1* to decrease expression, whereas *OOSNCR3, OOSNCR4,* and *OOSNCR5* increased. In conclusion, five novel lncRNAs were identified in bovine oocytes and revealed dynamic expression profiles in immature oocytes of varying quality before and after maturation.

INTRODUCTION

In cattle, the fertilization rate is ~90%, with an average calving rate of about 55%, indicating an embryonic-fetal mortality rate of roughly 35% (Diskin et al., 2006). Further, 70-80% of total embryonic loss in cattle occurs during the first three weeks after insemination, particularly between days 7-16 (Spencer, 2013). Growing evidence indicates that the oocyte plays an active role in regulating critical aspects of the reproductive process required for successful fertilization, embryo development, and pregnancy. The influence of oocyte quality on the embryo's developmental potential has been recognized in cattle (Lonergan et al., 2001; Merton et al., 2003; Lonergan, 2011).

It is well-documented that the constitution of the early embryo depends upon the composition of the oocyte (Gilbert et al., 2015). However, defining oocyte quality remains challenging because developmental competence remains "a convenient but biologically fuzzy concept" (Duranthon and Renard, 2001). Currently, the accepted methods to define oocyte quality include focusing on the morphology of the cloud of somatic cells surrounding the oocyte and the visual aspect of the gamete's cytoplasm (Blondin and Sirard, 1995). As a result, oocytes are subjectively selected based on visual inspection of their cumulus-oocyte complexes (COCs). However, these results rarely go beyond 50% blastulation rates, and even more confounding, oocytes below the selection criteria have been documented to produce viable embryos. With more bovine embryos being produced *in vitro* than *in vivo* (Viana, 2020), it has become imperative to understand the underlying molecular mechanisms dictating oocyte quality.

Within the ovary, folliculogenesis, and oogenesis are regulated by endocrine, paracrine, and autocrine factors that work concurrently to result in the ovulation of a developmentally competent oocyte. To achieve developmental competence, oocytes must undergo oocyte maturation, a process consisting of three phases: (1) meiotic maturation – the spontaneous cascade

of nuclear events induced by the luteinizing hormone (LH) surge or by the removal of the oocyte from its follicular environment (2) cytoplasmic maturation – a series of spontaneous changes marked by modifying the transcription and translation machinery in addition to a re-distribution of organelles and (3) molecular maturation – maternal mRNAs and proteins are produced intrinsically and "stockpiled" until after ovulation and are hypothesized to determine the fate of the early embryo (Sirard et al., 2006). However, despite years of research, identifying the driving force underlying oocyte quality remains elusive. Many speculate it is the summation of numerous small modulations in gene expression rather than one transcript or gene network driving oocyte maturation.

The relationship between oocyte quality and follicle size has been studied extensively (Wittmaack et al., 1994; Arnot et al., 1995; Blondin and Sirard, 1995; Dubey et al., 1995; Bergh et al., 1998). Early investigations revealed that significantly more oocytes were collected from 2-6 mm follicles than from those greater than 6 mm (Lonergan et al., 1994). Despite the increased yield, oocytes collected from larger follicles produced significantly higher blastocysts rates than those from small follicles (Lonergan et al., 1994; Blondin and Sirard, 1995; Hagemann et al., 1999; Machatkova et al., 2004; Lequarre et al., 2005; Blondin et al., 2012). Research has speculated that oocytes from small follicles are lower in quality due to an inadequate accumulation and storage of essential RNAs and proteins, resulting in partial cytoplasmic maturation. More recently, the RNA composition in GV oocytes was investigated when transcriptome analysis using microarrays detected a gradual modulation of mRNA abundance in bovine oocytes in response to increasing follicle size (Labrecque et al., 2016). Although genome-wide approaches may not be sensitive enough to detect the small modulations driving oocyte competence, transcriptomic datasets have become widely available, identifying individual genes of interest.

Brilliant cresyl blue (BCB) staining selects developmentally competent COCs for *in vitro* maturation. The efficacy of BCB staining to differentiate oocytes has been validated in various species, including pigs, mice, goats, cattle, and buffalo (Opiela and Kątska-Książkiewicz, 2013). The enzyme glucose-6-phosphate dehydrogenase (G6PDH) is a highly active enzyme in growing oocytes, whereas enzymatic activity ceases in fully grown oocytes (Mangia and Epstein, 1975). Due to G6PDH's ability to convert BCB stain from blue to colorless (Ericsson et al., 1993), it has been used to differentially stain actively growing and fully grown oocytes. Various studies have demonstrated that oocytes stained with BCB displayed higher developmental competence following oocyte maturation and yielded increased blastocyst rates (Roca et al., 1998; Rodríguez-González et al., 2002; Pujol et al., 2004; Lee et al., 2020; Walker et al., 2022).

Increased ambient temperature during the summer months is the leading cause of stress for cattle (Roth et al., 2000; Takahashi, 2012). Cattle experiencing heat stress have inhibited follicular development (Wolfenson et al., 1995; Roth et al., 2000). In addition, high ambient temperatures have been documented to significantly decrease the number of oocytes and their developmental competence following *in vitro* fertilization (Hansen et al., 2001). Specifically, heat stress during oocyte maturation disrupts nuclear maturation by causing malformations in the cytoskeleton causing disorganized microtubules and unaligned chromosomes (Roth and Hansen, 2005). Moreover, alternations in the cytoskeleton are speculated to promote the apoptotic response mediated by group II caspases previously reported in heat-stressed oocytes (Roth and Hansen, 2004).

Previous studies have identified various scenarios in which oocyte quality is directly affected. With technological advancements, researchers can revisit previous experiments to understand better the dynamic molecular mechanisms dictating the intricate relationship between

the oocyte, its nurse cells, and the surrounding environment. Therefore, this study aimed to identify and quantify novel lncRNA transcripts in bovine oocytes exhibiting various degrees of quality.

MATERIALS AND METHODS

Oocyte Collection and *in vitro* Embryo Production

Unless otherwise stated, all chemicals were purchased through Sigma-Aldrich (Milwaukee, WI). Bovine ovaries were harvested from a commercial abattoir (Souderton, PA) and stored at room temperature in 0.9% NaCl solution until aspiration. The COCs were aspirated from 2-12 mm visible follicles using an 18-gauge needle. After three washes of Boviplus oocyte washing medium (Minitube International; Tiefenbach, Germany) with BSA, heparin, and pen strep per manufacturer's instructions, visibly healthy COCs were selected for IVM. Healthy COCs were defined as COCs with at least two consecutive layers of symmetrical cumulus cells (CCs) and a uniform cytoplasm. COCs were either collected at the germinal vesicle (GV) stage or pooled into groups of 50 and cultured in 500 μL of bovine IVM media (IVF Bioscience; United Kingdom) under oil for 22 h at 38.8°C in 5% CO_2 in humidified air. For GV oocyte samples, CCs were removed using a 1:1 hyaluronidase solution at 10,000 U/mL and vortexed for 5 minutes. Denuded GV oocytes were collected either individually or in pools with minimal volume and stored at -80°C. Following IVM, the presence of metaphase II (MII) oocytes were confirmed based on the visual criteria of cumulus cell expansion and first polar body extrusion. Fully matured COCs were either collected, denuded, and stored in the same manner previously mentioned as MII oocytes or selected to generate embryos.

Embryos were generated using IVF. The COCs were washed and transferred to the bovine IVF medium (IVF Bioscience). Donated optixcell-extended bovine semen (Select Sires; Plain City, Ohio) was washed twice with bovine semen preparation medium (IVF Bioscience) per

manufacturer's instructions. The sperm were co-cultured with the COCs at a concentration of 2.0 x 10^6 sperm/ mL for 12 h at 38.8°C in 5% CO_2 in humidified air. The presumptive zygotes were denuded and moved into 500 uL of bovine IVC (IVF Bioscience) with an oil overlay and incubated at 38.8°C in 5% CO_2 and 5% O_2 until day 8 post-insemination.

Quantitative Real-Time PCR (RT-qPCR)

Total RNA from oocytes was isolated using the RNAqueous™ MicroKit (Invitrogen; Waltham, MA), and cDNA was synthesized using the High Capacity cDNA Reverse Transcription Kit (Applied Biosystems; Waltham, MA) per the manufacturer's instructions. Gene expression was quantified using Power-Up SYBR Green Master Mix (Applied Biosystems) and a CFX96 Real-Time System machine (Bio-Rad Laboratories, Hercules, CA). The qPCR conditions were denaturing at 95°C for 2 minutes, 39 PCR cycles (95°C for 15 seconds, 60°C for 1 minute), and a final extension at 65°C for 5 seconds. A single, sharp peak on a dissociation curve confirmed the homogeneity of the PCR products for each primer set. In addition, relative lncRNA abundance was calculated via the standard curve method using *RPL19* as an endogenous control for normalization. The RT-qPCR primers are listed in Table 1.

Experiment 1: Follicle Size and Maturity Stage

To examine the relationship between follicle size and maturity stage with lncRNA abundance, oocytes were aspirated from small (< 4mm; SF) and large (> 6 mm; LF) antral follicles using a syringe and needle. Follicle size was determined using calipers to measure the average diameter of two perpendicular measurements of each antral follicle. Once aspirated, CCs were removed, and GV oocytes (n = 10) were stored individually at -80°C or cultured to MII using the previously mentioned procedure. Following maturation, COCs were denuded, and individual MII oocytes (n = 10) were stored in minimal volume at -80°C until further analysis.

Experiment 2: Brilliant Cresyl Blue Staining

LncRNA abundance was assessed in oocytes of differing developmental competencies using BCB staining. Intact COCs at the GV stage were washed three times in modified DPBS (mDPBS) with 0.4% BSA and then incubated in 26 μM BCB for 90 minutes at 38.8°C. Following incubation, the COCs were washed twice in mDPBS and separated according to their cytoplasmic coloration. COCs exhibiting a blue cytoplasm were classified as BCB+ or fully grown, whereas COCs with no coloration post-incubation were classified as BCB-; or actively growing. Differentially stained COCs were either collected at the GV stage or subjected to IVF and cultured to day 8 post-insemination to obtain the number of embryos reaching the blastocysts stage. For oocytes collected at the GV stage, CCs were removed, and differentially stained oocytes were collected in pools of 5 (n = 7) with minimal volume. All samples were stored at -80°C.

Experiment 3: Maturation in a Heat-Stressed Environment

To determine a potential relationship between lncRNAs and cellular stress, COCs were matured in a heat-stressed environment. Briefly, morphologically healthy COCs were either denuded at the GV stage and collected in pools of 20 (n = 5) or cultured under oil for 22h at 38.8°C (standard temperature; ST) or 41°C (heat-stressed; HS) in 5% CO_2 in humidified air. Following maturation, mature COCs cultured in either the ST or HS environment were denuded and stored in pools of 20 (n = 5) or subjected to IVF and cultured to day 8 post-insemination.

Statistical Analysis

All analyses were conducted in JMP Pro version 15.1.0 (JMP 1998-2023). All RT-qPCR data were log-transformed, and embryo data presented as percentages were arcsine transformed. Experiment one assessed the differences in lncRNA abundance using a two-way ANOVA that included the main effect of follicle size and maturity stage and their interaction. After determining

model interaction significance, individual mean comparisons were performed using Tukey's HSD. Experiments two and three calculated the differences in lncRNA abundance and blastocyst formation using Dunnett's or Student *t*-test. For all experiments, differences were considered statistically significant when $P < 0.05$ with a tendency range of $0.1 \geq P \geq 0.05$.

RESULTS

Experiment 1: Follicle Size and Maturity Stage

Relative abundance was determined for five novel lncRNAs to examine their expression during oocyte maturation in small and large follicles. Based on single-cell data, *OOSNCR1* and *OOSNCR3* accumulated during maturation, whereas *OOSNCR2* and *OOSNCR4* degraded with maturation ($P < 0.021$; Figure 1). *OOSNCR5* tended to degrade during maturation ($P = 0.10$). In addition to its accumulation, immature and mature oocytes expressed *OOSNCR1* higher when collected from small follicles ($P = 0.03$; Figure 1A) than large ones. Moreover, immature oocytes collected from small follicles expressed *OOSNCR2* and *OOSNCR4* higher than mature oocytes collected from either small or large follicles ($P < 0.03$; Figure 1BD). In contrast, *OOSNCR3* was expressed highest in mature oocytes collected from large follicles ($P = 0.007$; Figure 1C).

Experiment 2: Brilliant Cresyl Blue Staining

Fully grown (BCB+) GV oocytes exhibited less *OOSNCR3* expression than actively growing (BCB-) oocytes when using BCB stain as a visual selection criterion to differentiate between oocytes of different developmental capacities ($P = 0.03$; Figure 2C). Moreover, no significant difference was detected among the four other lncRNAs analyzed ($P > 0.05$; Figure 2). COCs differentially stained using BCB as actively growing (BCB-) exhibited a decreased blastocyst rate compared to the control ($P = 0.058$; Table 2).

Experiment 3: Maturation in a Heat-Stressed Environment

Heat stress during maturation caused a decrease in cumulus cell expansion (P = 0.046; Figure 3E). Further, oocytes cultured in a heat-stressed environment revealed a tendency to decrease *OOSNCR1* expression (P = 0.091; Figure 3A). In contrast, maturation in the stressed environment increased *OOSNCR3, OOSNCR4,* and *OOSNCR5* expression ($P < 0.05$; Figure 3CDE). No statistical difference was detected in *OOSNCR2*. However, it exhibited a similar pattern as the previously mentioned three lncRNAs (P = 0.12; Figure 2B).

DISCUSSION

Despite years of research, defining oocyte quality remains enigmatic. Recently, many have abandoned the notion that one single transcript or gene network modulates oocyte competence. Instead, it is speculated that a vast network of transcripts modulates gene expression. Furthermore, the advent of deep sequencing techniques paired with emerging technologies reveals an ever-growing collection of regulatory non-coding RNAs within the mammalian genome (Mattick et al., 2023). As such, researchers must revisit previous studies to examine the findings with an updated perspective. The data published herein supports that novel lncRNAs may be regulating oocyte quality.

Previously, using RNA sequencing, our laboratory identified 1,535 lncRNAs present in immature and mature oocytes (Wang et al., 2020). After comparisons to lncRNAs in bovine tissues, 970 transcripts were predicted to be unique to bovine oocytes. Five highly abundant candidate genes were selected based on FPKM scores for further investigation. Results of the present study demonstrate that bovine *OOSNCR1, OOSNCR2, OOSNCR3, OOSNCR4,* and *OOSNCR5* exhibit dynamic expression profiles in immature oocytes of varying quality before and after maturation.

Experiment one utilizing single oocytes revealed that lncRNAs are accumulated and degraded during oocyte maturation. Our data discovered that three out of five lncRNAs were degraded during maturation, supporting the notion of transcriptional silencing in fully grown GV oocytes in response to the LH surge. Interestingly, two lncRNAs, *OOSNCR1* and *OOSNCR3,* were accumulated during this period of transcriptional quiescence. Although transcriptionally quiet, the oocyte maintains an active, specialized, multi-layered RNA processing system (Christou-Kent et al., 2020). Specifically, oocyte RNA binding proteins (RBPs) bind and repress mRNA transcripts until their requirement during meiotic maturation or fertilization (Piqué et al., 2008). With known functions as a protein scaffold (Plath et al., 2003), lncRNAs may accumulate during maturation to interact with RBPs facilitating the release of specific mRNA transcripts from their repressed states, enabling translation.

Additionally, small non-coding RNAs, microRNAs (miRNAs), and endogenous small interfering RNAs (endo-siRNAs) are critical mediators of post-transcriptional regulation, and they are highly abundant in mammalian oocytes (Salilew-Wondim et al., 2020). Recently, lncRNAs have been investigated as miRNA sponges in a variety of cancers (Liang et al., 2018; Zhang et al., 2018; D'Angelo et al., 2019; Joo et al., 2019; Han et al., 2020), degenerative musculoskeletal diseases (Zheng et al., 2021), brain development (Ang et al., 2020), angiogenesis (Zhao et al., 2020), and early embryos (Caballero et al., 2014). More recently, lncRNA-miRNA interactions have gained interest in reproductive fields using miRNAs as biomarkers for infertility in men (Zhao et al., 2021) and women (Tamaddon et al., 2022). Consequently, the possibility of lncRNAs interacting with miRNAs during oocyte maturation as a mechanism of gene regulation should be investigated further.

Experiment one also revealed that three out of five lncRNAs were more abundant in oocytes collected from small rather than large follicles. Specifically, two lncRNAs, *OOSNCR2* and *OOSNCR4,* were highest in immature oocytes collected from small follicles. The literature agrees that oocytes collected from small follicles display lower developmental competence and consistently produce significantly fewer blastocysts than oocytes collected from large follicles (Lonergan et al., 1994; Blondin and Sirard, 1995; Hagemann et al., 1999; Machatkova et al., 2004; Lequarre et al., 2005; Blondin et al., 2012). As such, oocytes from immature follicles are speculated to lack unknown factors required for improved developmental competence within their cytoplasm. A recently published study characterized the lipid composition and follicular metabolic and stress markers in oocytes from small and large follicles. Their data revealed that large follicles had an increased lipid content in conjunction with increased glucose levels, reactive oxygen species, glutathione, and superoxide dismutase activity in their follicular fluid (Annes et al., 2019). These data suggest a more optimal microenvironment in large follicles paired with oocytes rich in energy stores.

Admittingly, lipid metabolism in the oocyte is an intricate balancing act (Liu et al., 2022). From one perspective, lipids act as a protective factor (Khalil et al., 2013; Dunning et al., 2014; Chen et al., 2020; Current et al., 2022) during folliculogenesis, providing fatty acids that meet the energy demands associated with meiotic resumption and fertilization. However, on the other, long-term exposure to a high-fat environment increases lipid content in oocytes inducing oxidative stress and inflammation levels and disruption of spindles and chromosome structure, substantially interfering with oocyte meiosis as seen in patients with maternal obesity and polycystic ovary syndrome (Hou et al., 2016; Yun et al., 2019; Rao et al., 2020). Furthermore, lncRNAs enter the equation following numerous clinical studies demonstrating that lncRNAs impair cholesterol

homeostasis and have an essential role in the progression of lipid-related diseases (Huang et al., 2021). Specifically, lncRNAs have been identified as indirect participants in lipid metabolism by regulating essential genes, networks, and pathways involved in lipid biosynthesis, cholesterol transport, lipid uptake, and cholesterol efflux (Huang et al., 2021). Therefore, with high levels of lipids reported in oocytes and lncRNAs, regulating lipid metabolism interactions of the two seems likely.

Experiment two utilized BCB staining as a non-invasive analysis of the bioactivity of immature oocytes. As such, the staining can differentially select immature oocytes that are actively growing from those that are fully grown and yield higher blastocyst rates in the BCB+ oocytes. The results of the present study corroborated previous findings in that following BCB staining, our BCB- oocytes exhibited a decrease in blastocyst formation. Furthermore, overlaying lncRNA expression, our data found that *OOSNCR3* was upregulated in BCB- oocytes.

Similarly, Lee et al. investigated the molecular signaling of COCs following BCB staining. Their results demonstrated that BCB- oocytes had a significantly decreased percentage of cleavage and blastocyst formation during subsequent embryonic development, paired with cumulus cells with reduced expression of sonic hedgehog signaling (SHH) proteins and increased rates of apoptosis (Lee et al., 2020). The data suggest a critical role for the surrounding cumulus cells and the follicular environment. Future studies should investigate lncRNA expression within the cumulus cells and possibly the tracking of transcripts to the oocyte via TZPs. Interestingly, when co-culturing BCB-stained COCs (-/+), non-competent (BCB-) oocytes reduced the capacity of competent (BCB+) oocytes to undergo embryo development and achieve blastocyst development (Salviano et al., 2016)—further indicating a more significant role in the communication system within the COC.

Finally, experiment three quantified novel lncRNA expression in oocytes matured at standard conditions or in a heat-stressed environment. As previously noted, heat stress during oocyte maturation disrupts nuclear development through the rearrangement of the cytoskeletal elements (Roth and Hansen, 2005) and promotes apoptosis (Roth and Hansen, 2004) within the COC. Additionally, impaired cumulus expansion has been reported (Ahmed et al., 2017). Our data revealed a decrease in average cumulus cell expansion and increased lncRNA expression in four of the five candidate genes, suggesting an association with gene dysregulation among oocytes of poorer quality. Fascinatingly, lncRNAs have been characterized as modulators of cytoskeleton architecture with implications in cellular homeostasis and tumorigenesis (García-Padilla et al., 2022). Further investigation of lncRNA regulation at both the transcriptional and post-transcriptional levels mediating cytoskeleton remodeling and turnover in the oocyte is necessary.

Interestingly, *OOSNCR1* tended to decrease following heat stress. Alongside the malformations mentioned above, Camargo et al. reported alterations of the embryo's chromatin, influencing the accumulation of histone H3 lysine 9 trimethylation (H3K9me3) and heterochromatin protein 1 (HPI) in early bovine embryos (Camargo et al., 2019). Further, lncRNA regulation of chromatin architecture and gene expression has been reported (Isoda et al., 2017; Mumbach et al., 2019). Thus, as new advanced techniques become more readily available, interactions among specific lncRNAs and chromatin architecture will be of great interest. Specifically, lncRNAs' ability to act as scaffolds to bring distant regions of a linear genome into a spatial proximity (Li et al., 2017).

Technological advancements make it easy to chase the next big idea. However, revising previous experiments with updated technology and increased knowledge allows researchers to investigate deeper and further characterize the molecular mechanisms dictating cell physiology.

The data presented herein represents a starting point for future investigations in identifying novel regulators of oocyte maturation and early embryonic development.

Conflict of Interest

The authors declare no conflicts of interest.

Author Contributions

JZC planned the study design, collected samples, performed experiments, analyzed data, interpreted data, and drafted the manuscript. HLC collected ovary samples and performed *in vitro* embryo production. MZ performed *in vitro* embryo production. EMD and GLC assisted with *in vitro* embryo production and gene expression data. JY aided in data analysis, interpretation, and manuscript preparation.

Acknowledgments

This project was supported by the National Institute of Food and Agriculture U.S. Department of Agriculture, award number 2020-38640-31520, the Northeast Sustainable Agriculture Research and Education (SARE) graduate student research grant award number GNE19-196, and the USDA National Institute of Food and Agriculture, Multistate Research Project 1014002. In addition, the authors like to thank Dr. Ida Holaskova for her assistance in statistical analysis, Select Sires (Plain City, OH) for semen donations, and the West Virginia Department of Agriculture, Hyde's Meat Packing (Enterprise, WV), and JBS Beef Plant (Souderton, PA) for their generous donation of bovine ovaries for this work.

REFERENCES

Ahmed, J. A., N. Nashiruddullah, D. Dutta, R. K. Biswas, and P. Borah. 2017. Cumulus cell expansion and ultrastructural changes in in vitro matured bovine oocytes under heat stress. Iran. J. Vet. Res. 18:203–207.

Ang, C. E., A. E. Trevino, and H. Y. Chang. 2020. Diverse lncRNA mechanisms in brain development and disease. Curr. Opin. Genet. Dev. 65:42–46. doi:10.1016/j.gde.2020.05.006.

Annes, K., D. B. Müller, J. A. P. Vilela, R. S. Valente, D. P. Caetano, F. W. S. Cibin, M. P. Milazzotto, F. S. Mesquita, K. R. A. Belaz, M. N. Eberlin, and M. J. Sudano. 2019. Influence of follicle size on bovine oocyte lipid composition, follicular metabolic and stress markers, embryo development and blastocyst lipid content. Reprod. Fertil. Dev. 31:462–472. doi:10.1071/RD18109.

Arnot, A. M., P. Vandekerckhove, M. A. DeBono, and A. J. Rutherford. 1995. Physiology: Follicular volume and number during in-vitro fertilization: association with oocyte developmental capacity and pregnancy rate. Hum. Reprod. 10:256–261. doi:10.1093/oxfordjournals.humrep.a135925.

Bergh, C., H. Broden, K. Lundin, and L. Hamberger. 1998. Comparison of fertilization, cleavage and pregnancy rates of oocytes from large and small follicles. Hum. Reprod. 13:1912–1915. doi:10.1093/humrep/13.7.1912.

Blondin, P., and M.-A. Sirard. 1995. Oocyte and follicular morphology as determining characteristics for developmental competence in bovine oocytes. Mol. Reprod. Dev. 41:54–62. doi:10.1002/mrd.1080410109.

Blondin, P., C. Vigneault, A. L. Nivet, and M. A. Sirard. 2012. Improving oocyte quality in cows and heifers - What have we learned so far? Anim. Reprod. 9:281–289.

Caballero, J., I. Gilbert, E. Fournier, D. Gagné, S. Scantland, A. Macaulay, and C. Robert. 2014. Exploring the function of long non-coding RNA in the development of bovine early embryos. Reprod. Fertil. Dev. 27:40–52. doi:10.1071/RD14338.

Camargo, L. S. A., T. Aguirre-Lavin, P. Adenot, T. D. Araujo, V. R. A. Mendes, I. D. Louro, N. Beaujean, and E. D. Souza. 2019. Heat shock during in vitro maturation induces chromatin modifications in the bovine embryo. Reproduction. 158:313. doi:10.1530/REP-19-0245.

Chen, L., J.-J. Zhang, X. Zhang, X. Liu, S. Zhao, L.-J. Huo, J. Zhou, and Y.-L. Miao. 2020. Melatonin protects against defects induced by malathion during porcine oocyte maturation. J. Cell. Physiol. 235:2836–2846. doi:10.1002/jcp.29189.

Christou-Kent, M., M. Dhellemmes, E. Lambert, P. F. Ray, and C. Arnoult. 2020. Diversity of RNA-Binding Proteins Modulating Post-Transcriptional Regulation of Protein Expression in the Maturing Mammalian Oocyte. Cells. 9:662. doi:10.3390/cells9030662.

Current, J. Z., M. Mentler, and B. D. Whitaker. 2022. Linoleic and linolenic acids reduce the effects of heat stress–induced damage in pig oocytes during maturation in vitro. Vitro Cell. Dev. Biol. - Anim. doi:10.1007/s11626-022-00708-4. Available from: https://doi.org/10.1007/s11626-022-00708-4

D'Angelo, D., P. Mussnich, R. Sepe, M. Raia, L. del Vecchio, P. Cappabianca, S. Pellecchia, S. Petrosino, S. Saggio, D. Solari, F. Fraggetta, and A. Fusco. 2019. RPSAP52 lncRNA is overexpressed in pituitary tumors and promotes cell proliferation by acting as miRNA sponge for HMGA proteins. J. Mol. Med. 97:1019–1032. doi:10.1007/s00109-019-01789-7.

Diskin, M. G., J. J. Murphy, and J. M. Sreenan. 2006. Embryo survival in dairy cows managed under pastoral conditions. Anim. Reprod. Sci. 96:297–311. doi:10.1016/j.anireprosci.2006.08.008.

Dubey, A. K., H. An Wang, P. Duffy, and A. S. Penzias. 1995. The correlation between follicular measurements, oocyte morphology, and fertilization rates in an in vitro fertilization program*. Fertil. Steril. 64:787–790. doi:10.1016/S0015-0282(16)57855-8.

Dunning, K. R., D. L. Russell, and R. L. Robker. 2014. Lipids and oocyte developmental competence: the role of fatty acids and β-oxidation. Reprod. Camb. Engl. 148:R15-27. doi:10.1530/REP-13-0251.

Duranthon, V., and J. P. Renard. 2001. The developmental competence of mammalian oocytes: a convenient but biologically fuzzy concept. Theriogenology. 55:1277–1289. doi:10.1016/S0093-691X(01)00482-4.

Ericsson, S. A., M. L. Boice, H. Funahashi, and B. N. Day. 1993. Assessment of porcine oocytes using brilliant cresyl blue. Theriogenology. 39:214. doi:10.1016/0093-691X(93)90069-H.

García-Padilla, C., M. del M. Muñoz-Gallardo, E. Lozano-Velasco, J. M. Castillo-Casas, S. Caño-Carrillo, V. García-López, A. Aránega, D. Franco, V. García-Martínez, and C. López-Sánchez. 2022. New Insights into the Roles of lncRNAs as Modulators of Cytoskeleton Architecture and Their Implications in Cellular Homeostasis and in Tumorigenesis. Non-Coding RNA. 8:28. doi:10.3390/ncrna8020028.

Gilbert, I., A. Macaulay, and C. Robert. 2015. Oocyte developmental competence and embryo quality: distinction and new perspectives.

Hagemann, L. J., S. E. Beaumont, M. Berg, M. J. Donnison, A. Ledgard, A. J. Peterson, A. Schurmann, and H. R. Tervit. 1999. Development during single IVP of bovine oocytes from dissected follicles: Interactive effects of estrous cycle stage, follicle size and atresia. Mol. Reprod. Dev. 53:451–458. doi:10.1002/(SICI)1098-2795(199908)53:4<451::AID-MRD11>3.0.CO;2-3.

Han, T.-S., K. Hur, H.-S. Cho, and H. S. Ban. 2020. Epigenetic Associations between lncRNA/circRNA and miRNA in Hepatocellular Carcinoma. Cancers. 12:2622. doi:10.3390/cancers12092622.

Hansen, P., M. Drost, R. Rivera, F. F. Paula-Lopes, Y. M. Al-Katanani, C. E. Krininger III, and C. C. Chase Jr. 2001. Adverse impact of heat stress on embryo production: causes and strategies for mitigation - ScienceDirect. Theriogenology. 55:91–103.

Hou, Y.-J., C.-C. Zhu, X. Duan, H.-L. Liu, Q. Wang, and S.-C. Sun. 2016. Both diet and gene mutation induced obesity affect oocyte quality in mice. Sci. Rep. 6:18858. doi:10.1038/srep18858.

Huang, S.-F., X.-F. Peng, L. Jiang, C. Y. Hu, and W.-C. Ye. 2021. LncRNAs as Therapeutic Targets and Potential Biomarkers for Lipid-Related Diseases. Front. Pharmacol. 12. Available from: https://www.frontiersin.org/articles/10.3389/fphar.2021.729745

Isoda, T., A. J. Moore, Z. He, V. Chandra, M. Aida, M. Denholtz, J. P. van Hamburg, K. M. Fisch, A. N. Chang, S. Fahl, D. L. Wiest, and C. Murre. 2017. Non-Coding Transcription Instructs Cohesin-Dependent Chromatin Folding and Compartmentalization to Dictate Enhancer-Promoter Communication and T Cell Fate. Cell. 171:103-119.e18. doi:10.1016/j.cell.2017.09.001.

Joo, M. S., S.-B. Shin, E. J. Kim, H. J. Koo, H. Yim, and S. G. Kim. 2019. Nrf2-lncRNA controls cell fate by modulating p53-dependent Nrf2 activation as an miRNA sponge for Plk2 and p21cip1. FASEB J. 33:7953–7969. doi:10.1096/fj.201802744R.

Khalil, W. A., W. F. A. Marei, and M. Khalid. 2013. Protective effects of antioxidants on linoleic acid-treated bovine oocytes during maturation and subsequent embryo development. Theriogenology. 80:161–168. doi:10.1016/j.theriogenology.2013.04.008.

Labrecque, R., E. Fournier, and M.-A. Sirard. 2016. Transcriptome analysis of bovine oocytes from distinct follicle sizes: Insights from correlation network analysis. Mol. Reprod. Dev. 83:558–569. doi:10.1002/mrd.22651.

Lee, S., H.-G. Kang, P.-S. Jeong, T. Nanjidsuren, B.-S. Song, Y. B. Jin, S.-R. Lee, S.-U. Kim, and B.-W. Sim. 2020. Effect of Oocyte Quality Assessed by Brilliant Cresyl Blue (BCB) Staining on Cumulus Cell Expansion and Sonic Hedgehog Signaling in Porcine during In Vitro Maturation. Int. J. Mol. Sci. 21:4423. doi:10.3390/ijms21124423.

Lequarre, A.-S., C. Vigneron, F. Ribaucour, P. Holm, I. Donnay, R. Dalbiès-Tran, H. Callesen, and P. Mermillod. 2005. Influence of antral follicle size on oocyte characteristics and embryo development in the bovine. Theriogenology. 63:841–859. doi:10.1016/j.theriogenology.2004.05.015.

Li, X., B. Zhou, L. Chen, L.-T. Gou, H. Li, and X.-D. Fu. 2017. GRID-seq reveals the global RNA-chromatin interactome. Nat. Biotechnol. 35:940–950. doi:10.1038/nbt.3968.

Liang, L., J. Xu, M. Wang, G. Xu, N. Zhang, G. Wang, and Y. Zhao. 2018. LncRNA HCP5 promotes follicular thyroid carcinoma progression via miRNAs sponge. Cell Death Dis. 9:1–13. doi:10.1038/s41419-018-0382-7.

Liu, T., J. Qu, M. Tian, R. Yang, X. Song, R. Li, J. Yan, and J. Qiao. 2022. Lipid Metabolic Process Involved in Oocyte Maturation During Folliculogenesis. Front. Cell Dev. Biol. 10. Available from: https://www.frontiersin.org/articles/10.3389/fcell.2022.806890

Lonergan, P. 2011. Influence of progesterone on oocyte quality and embryo development in cows. Theriogenology. 76:1594–1601. doi:10.1016/j.theriogenology.2011.06.012.

Lonergan, P., P. Monaghan, D. Rizos, M. P. Boland, and I. Gordon. 1994. Effect of follicle size on bovine oocyte quality and developmental competence following maturation, fertilization, and culture in vitro. Mol. Reprod. Dev. 37:48–53. doi:10.1002/mrd.1080370107.

Lonergan, P., D. Rizos, F. Ward, and M. P. Boland. 2001. Factors influencing oocyte and embryo quality in cattle. Reprod. Nutr. Dev. 41:427–437. doi:10.1051/rnd:2001142.

Machatkova, M., K. Krausova, E. Jokesova, and M. Tomanek. 2004. Developmental competence of bovine oocytes: effects of follicle size and the phase of follicular wave on in vitro embryo production. Theriogenology. 61:329–335. doi:10.1016/S0093-691X(03)00216-4.

Mangia, F., and C. J. Epstein. 1975. Biochemical studies of growing mouse oocytes: Preparation of oocytes and analysis of glucose-6-phosphate dehydrogenase and lactate dehydrogenase activities. Dev. Biol. 45:211–220. doi:10.1016/0012-1606(75)90061-5.

Mattick, J. S., P. P. Amaral, P. Carninci, S. Carpenter, H. Y. Chang, L.-L. Chen, R. Chen, C. Dean, M. E. Dinger, K. A. Fitzgerald, T. R. Gingeras, M. Guttman, T. Hirose, M. Huarte, R. Johnson, C. Kanduri, P. Kapranov, J. B. Lawrence, J. T. Lee, J. T. Mendell, T. R. Mercer, K. J. Moore, S. Nakagawa, J. L. Rinn, D. L. Spector, I. Ulitsky, Y. Wan, J. E. Wilusz, and M. Wu. 2023. Long non-coding RNAs: definitions, functions, challenges and recommendations. Nat. Rev. Mol. Cell Biol. 1–17. doi:10.1038/s41580-022-00566-8.

Merton, J. S., A. P. W. de Roos, E. Mullaart, L. de Ruigh, L. Kaal, P. L. A. M. Vos, and S. J. Dieleman. 2003. Factors affecting oocyte quality and quantity in commercial application of embryo technologies in the cattle breeding industry. Theriogenology. 59:651–674. doi:10.1016/S0093-691X(02)01246-3.

Mumbach, M. R., J. M. Granja, R. A. Flynn, C. M. Roake, A. T. Satpathy, A. J. Rubin, Y. Qi, Z. Jiang, S. Shams, B. H. Louie, J. K. Guo, D. G. Gennert, M. R. Corces, P. A. Khavari, M. K. Atianand, S. E. Artandi, K. A. Fitzgerald, W. J. Greenleaf, and H. Y. Chang. 2019. HiChIRP reveals RNA-associated chromosome conformation. Nat. Methods. 16:489–492. doi:10.1038/s41592-019-0407-x.

Opiela, J., and L. Kątska-Książkiewicz. 2013. The utility of Brilliant Cresyl Blue (BCB) staining of mammalian oocytes used for in vitro embryo production (IVP). Reprod. Biol. 13:177–183. doi:10.1016/j.repbio.2013.07.004.

Piqué, M., J. M. López, S. Foissac, R. Guigó, and R. Méndez. 2008. A combinatorial code for CPE-mediated translational control. Cell. 132:434–448. doi:10.1016/j.cell.2007.12.038.

Plath, K., J. Fang, S. K. Mlynarczyk-Evans, R. Cao, K. A. Worringer, H. Wang, C. C. de la Cruz, A. P. Otte, B. Panning, and Y. Zhang. 2003. Role of Histone H3 Lysine 27 Methylation in X Inactivation. Science. 300:131–135. doi:10.1126/science.1084274.

Pujol, M., M. López-Béjar, and M.-T. Paramio. 2004. Developmental competence of heifer oocytes selected using the brilliant cresyl blue (BCB) test. Theriogenology. 61:735–744. doi:10.1016/S0093-691X(03)00250-4.

Rao, A., A. Satheesh, G. Nayak, P. S. Poojary, S. Kumari, S. G. Kalthur, S. Mutalik, S. K. Adiga, and G. Kalthur. 2020. High-fat diet leads to elevated lipid accumulation and endoplasmic reticulum stress in oocytes, causing poor embryo development. Reprod. Fertil. Dev. 32:1169–1179. doi:10.1071/RD20112.

Roca, J., E. Martinez, J. M. Vazquez, and X. Lucas. 1998. Selection of immature pig oocytes for homologous in vitro penetration assays with the brilliant cresyl blue test. Reprod. Fertil. Dev. 10:479–486. doi:10.1071/rd98060.

Rodríguez-González, E., M. López-Béjar, E. Velilla, and M. T. Paramio. 2002. Selection of prepubertal goat oocytes using the brilliant cresyl blue test. Theriogenology. 57:1397–1409. doi:10.1016/S0093-691X(02)00645-3.

Roth, Z., and P. J. Hansen. 2004. Involvement of Apoptosis in Disruption of Developmental Competence of Bovine Oocytes by Heat Shock During Maturation1. Biol. Reprod. 71:1898–1906. doi:10.1095/biolreprod.104.031690.

Roth, Z., and P. J. Hansen. 2005. Disruption of nuclear maturation and rearrangement of cytoskeletal elements in bovine oocytes exposed to heat shock during maturation. Reproduction. 129:235–244. doi:10.1530/rep.1.00394.

Roth, Z., R. Meidan, R. Braw-Tal, and D. Wolfenson. 2000. Immediate and delayed effects of heat stress on follicular development and its association with plasma FSH and inhibin concentration in cows. J. Reprod. Fertil. 120:83–90. doi:10.1016/S0378-4320(00)00102-0.

Salilew-Wondim, D., S. Gebremedhn, M. Hoelker, E. Tholen, T. Hailay, and D. Tesfaye. 2020. The Role of MicroRNAs in Mammalian Fertility: From Gametogenesis to Embryo Implantation. Int. J. Mol. Sci. 21:585. doi:10.3390/ijms21020585.

Salviano, M. B., F. J. F. Collares, B. S. Becker, B. A. Rodrigues, and J. L. Rodrigues. 2016. Bovine non-competent oocytes (BCB–) negatively impact the capacity of competent (BCB+) oocytes to undergo in vitro maturation, fertilisation and embryonic development. Zygote. 24:245–251. doi:10.1017/S0967199415000118.

Sirard, M.-A., F. Richard, P. Blondin, and C. Robert. 2006. Contribution of the oocyte to embryo quality. Theriogenology. 65:126–136. doi:10.1016/j.theriogenology.2005.09.020.

Spencer, T. E. 2013. Early pregnancy: Concepts, challenges, and potential solutions. Anim. Front. 3:48–55. doi:10.2527/af.2013-0033.

Takahashi, M. 2012. Heat stress on reproductive function and fertility in mammals. Reprod. Med. Biol. 11:37–47. doi:10.1007/s12522-011-0105-6.

Tamaddon, M., M. Azimzadeh, and S. M. Tavangar. 2022. microRNAs and long non-coding RNAs as biomarkers for polycystic ovary syndrome. J. Cell. Mol. Med. 26:654–670. doi:10.1111/jcmm.17139.

Viana, J. 2020. 2019 Statistics of embryo production and transfer in domestic farm animals: Divergent trends for IVD and IVP embryos. Embryo Technol. Newsl. 38.

Walker, B. N., J. Nix, C. Wilson, M. A. Marrella, S. L. Speckhart, L. Wooldridge, C.-N. Yen, J. S. Bodmer, L. T. Kirkpatrick, S. E. Moorey, D. E. Gerrard, A. D. Ealy, and F. H. Biase. 2022. Tight gene co-expression in BCB positive cattle oocytes and their surrounding cumulus cells. Reprod. Biol. Endocrinol. 20:119. doi:10.1186/s12958-022-00994-3.

Wang, J., P. P. Koganti, and J. Yao. 2020. Systematic identification of long intergenic non-coding RNAs expressed in bovine oocytes. Reprod. Biol. Endocrinol. RBE. 18:13. doi:10.1186/s12958-020-00573-4.

Wittmaack, F. M., D. O. Kreger, L. Blasco, R. W. Tureck, L. Mastroianni, and B. A. Lessey. 1994. Effect of follicular size on oocyte retrieval, fertilization, cleavage, and embryo quality in in vitro fertilization cycles: a 6-year data collection. Fertil. Steril. 62:1205–1210. doi:10.1016/S0015-0282(16)57186-6.

Wolfenson, D., W. W. Thatcher, L. Badinga, J. D. Savi0, R. Meidan, B. J. Lew, R. Braw-tal, and A. Berman. 1995. Effect of Heat Stress on Follicular Development during the Estrous Cycle in Lactating Dairy Cattle1. Biol. Reprod. 52:1106–1113. doi:10.1095/biolreprod52.5.1106.

Yun, Y., Z. Wei, and N. Hunter. 2019. Maternal obesity enhances oocyte chromosome abnormalities associated with aging. Chromosoma. 128:413–421. doi:10.1007/s00412-019-00716-6.

Zhang, J., L. Liu, J. Li, and T. D. Le. 2018. LncmiRSRN: identification and analysis of long non-coding RNA related miRNA sponge regulatory network in human cancer. Bioinformatics. 34:4232–4240. doi:10.1093/bioinformatics/bty525.

Zhao, S., N. Heng, B. Weldegebriall Sahlu, H. Wang, and H. Zhu. 2021. Long Noncoding RNAs: Recent Insights into Their Role in Male Infertility and Their Potential as Biomarkers and Therapeutic Targets. Int. J. Mol. Sci. 22:13579. doi:10.3390/ijms222413579.

Zhao, Z., W. Sun, Z. Guo, J. Zhang, H. Yu, and B. Liu. 2020. Mechanisms of lncRNA/microRNA interactions in angiogenesis. Life Sci. 254:116900. doi:10.1016/j.lfs.2019.116900.

Zheng, Y.-L., G. Song, J.-B. Guo, X. Su, Y.-M. Chen, Z. Yang, P.-J. Chen, and X.-Q. Wang. 2021. Interactions Among lncRNA/circRNA, miRNA, and mRNA in Musculoskeletal Degenerative Diseases. Front. Cell Dev. Biol. 9. Available from: https://www.frontiersin.org/articles/10.3389/fcell.2021.753931

Figure 1. The effect of follicle size and maturation status on five novel lncRNAs expressed in bovine oocytes. Relative abundance levels of novel lncRNAs (A) *OOSNCR1* (B) *OOSNCR2* (C) *OOSNCR3* (D) *OOSNCR4* and (E) *OOSNCR5* in denuded immature (GV) and mature (MII) oocytes collected from small (spotted bars) and large (solid bars) follicles. All data are quantified using RT-qPCR and normalized to *RPL19* as an endogenous control. The main effect of the maturity stage was significant for the relative abundance of *OOSNCR1, OOSNCR2, OOSNCR3,* and *OOSNCR4,* with a tendency for significance in *OOSNCR5.* The main effect of follicle size was significant in *OOSNCR1, OOSNCR2, OOSNCR3,* and *OOSNCR4.* The interaction of follicle size and maturity stage was significant for *OOSNCR2, OOSNCR3,* and *OOSNCR4.* For experiment one, n = 5 individual denuded oocytes per follicle size per maturation status.

Figure 2. Five novel lncRNAs' relative abundance in fully grown and actively growing GV oocytes using BCB stain as a separation criterion. Relative abundance levels of novel lncRNAs (A) *OOSNCR1* (B) *OOSNCR2* (C) *OOSNCR3* (D) *OOSNCR4* and (E) *OOSNCR5* in immature (GV) oocytes selected by BCB staining. *OOSNCR3* expression was decreased in fully grown oocytes ($P = 0.026$). Values with a * indicate a significant difference ($P < 0.05$); n = 7 pools of 5 denuded oocytes per group.

Figure 3. Cumulus cell expansion during oocyte maturation in a heat-stressed environment. (AB) Representative image of immature bovine COCs cultured for 22h at (C) standard temperature or under (D) heat stress. The area was measured for individual COCs, with each replicate (n = 3) having at least 20 COCs present. The average area was determined for each replicate. (E) Maturation at 41°C caused a decrease in cumulus cell expansion ($P = 0.046$).

Figure 4. Five novel lncRNAs' relative abundance in mature oocytes following maturation in a heat-stressed environment. Relative abundance levels of novel lncRNAs (A) *OOSNCR1* (B) *OOSNCR2* (C) *OOSNCR3* (D) *OOSNCR4* and (E) *OOSNCR5* in mature (MII) oocytes following maturation at standard temperate (38.8°C) and heat-stressed (41°C). Values with a * indicate a significant difference ($P < 0.05$) whereas † indicates a tendency for significance ($0.05 \leq P \leq 0.1$); n = 5 pools of 20 denuded oocytes per group.

Figure 1.

A.

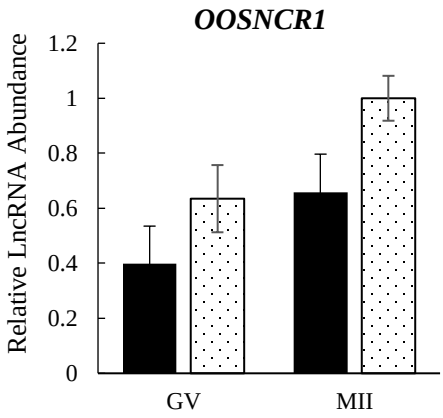

B.

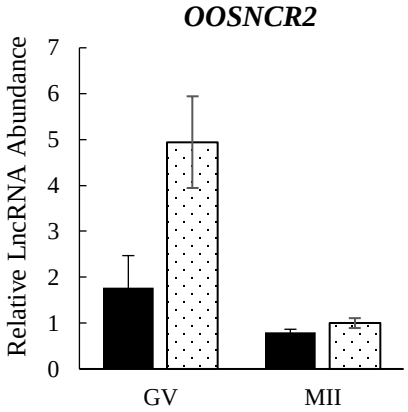

C.

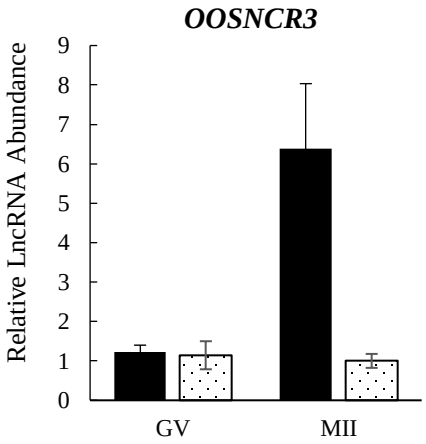

D.

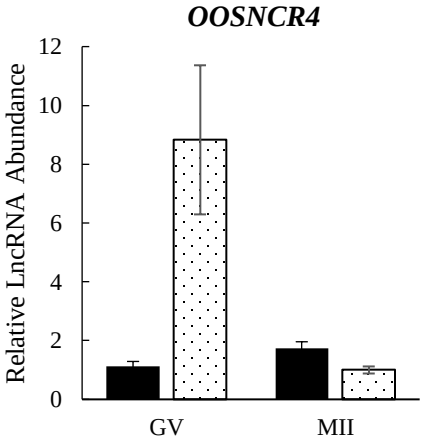

E.

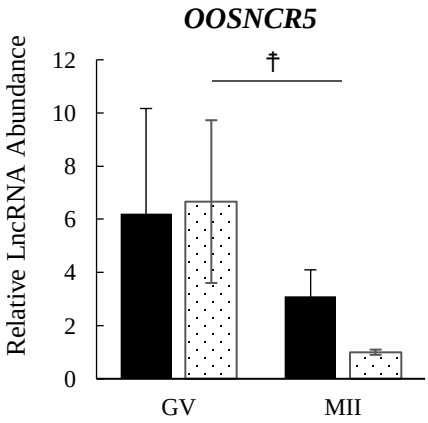

Oocytes collected from large follicles

Oocytes collected from small follicles

Figure 2

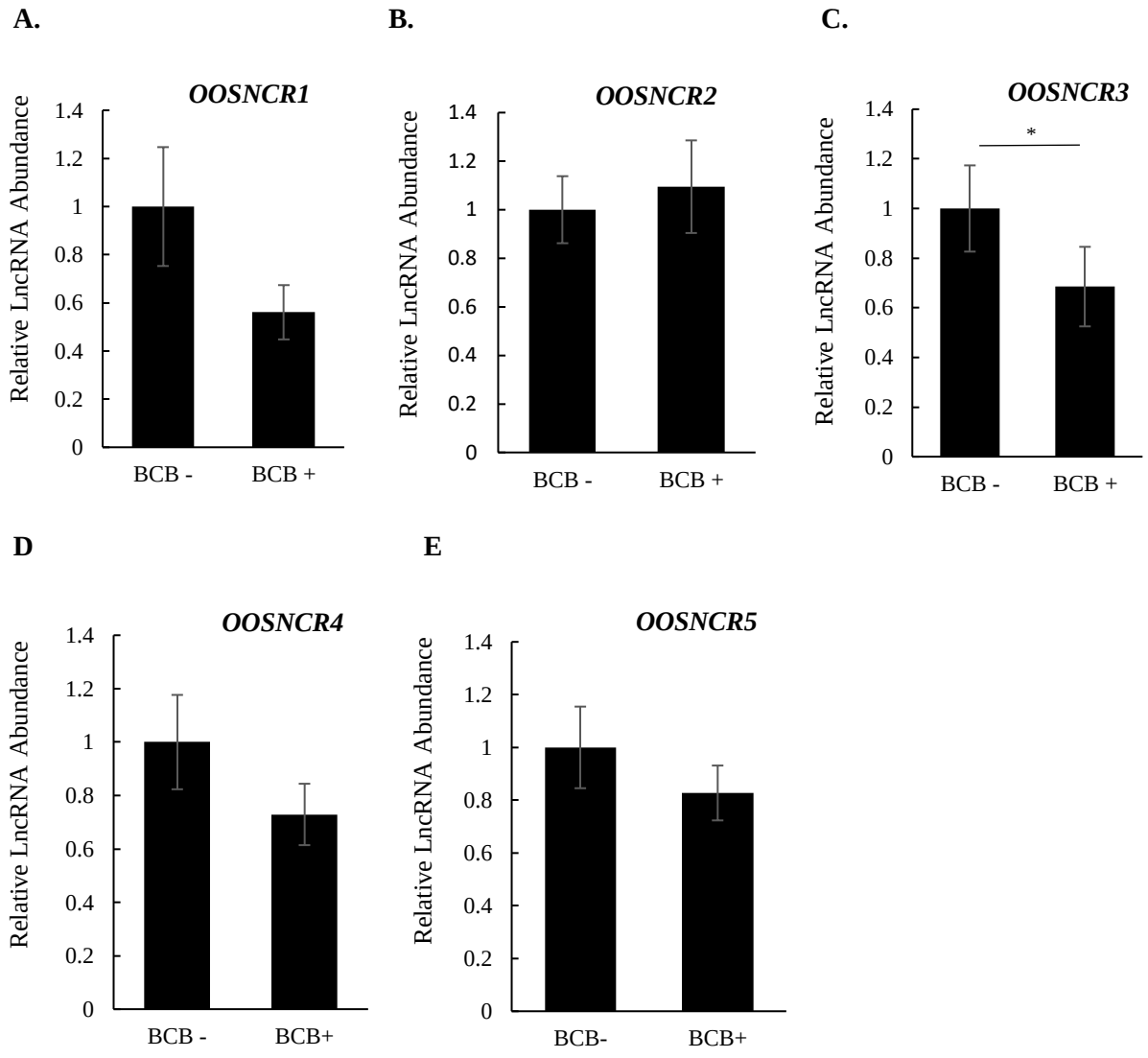
A.
OOSNCR1
Relative LncRNA Abundance
1.4
1.2
1
0.8
0.6
0.4
0.2
0
BCB -
BCB +
B.
OOSNCR2
Relative LncRNA Abundance
BCB -
BCB +
C.
OOSNCR3
*
Relative LncRNA Abundance
BCB -
BCB +
D
OOSNCR4
Relative LncRNA Abundance
BCB -
BCB+
E
OOSNCR5
Relative LncRNA Abundance
BCB-
BCB+

Figure 3

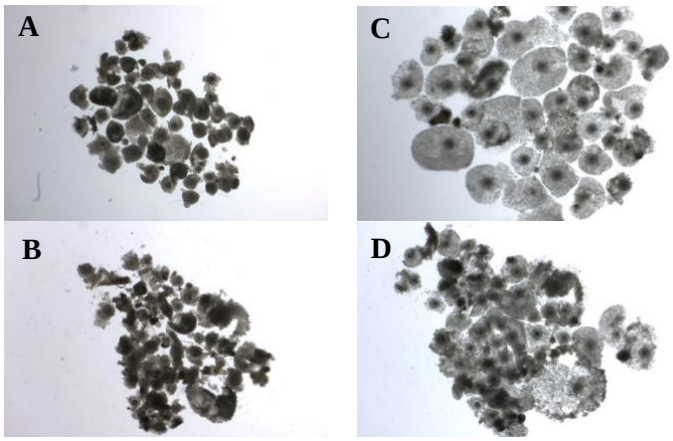
A
C
B
D

E

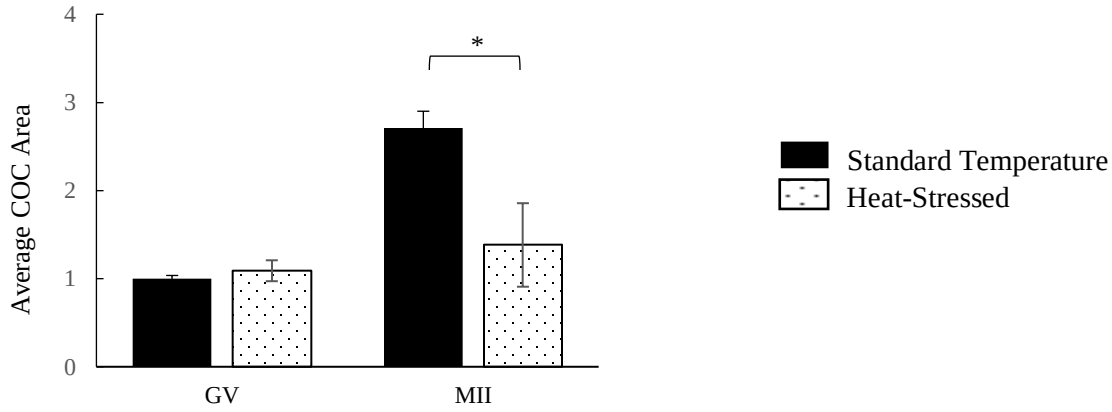
Average COC Area
4
3
2
1
0
*
GV
MII
Standard Temperature
Heat-Stressed

Figure 4

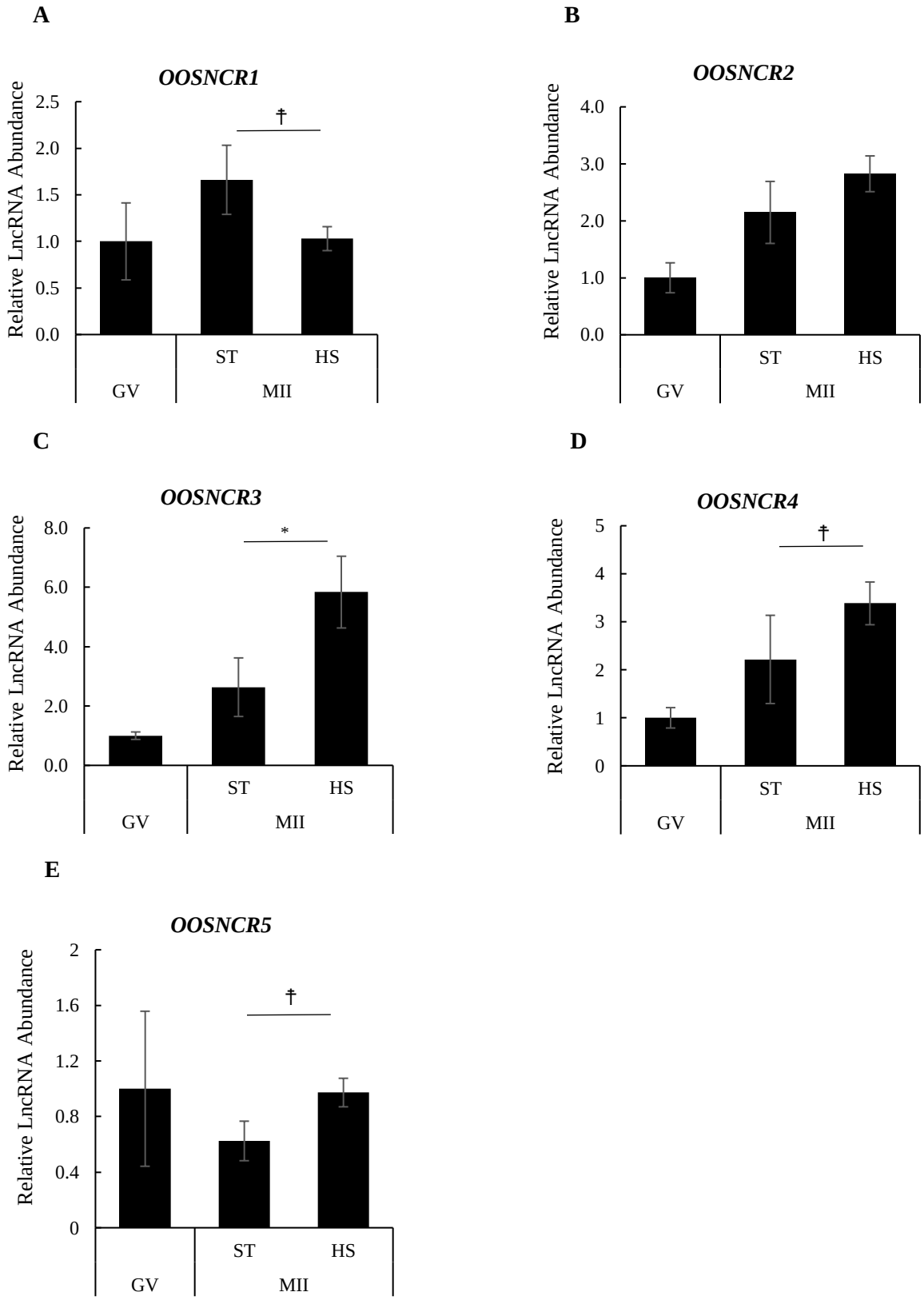
A
OOSNCR1
Relative LncRNA Abundance
2.5
2.0
1.5
1.0
0.5
0.0
†
ST
HS
GV
MII
B
OOSNCR2
Relative LncRNA Abundance
4.0
3.0
2.0
1.0
0.0
ST
HS
GV
MII
C
OOSNCR3
Relative LncRNA Abundance
8.0
6.0
4.0
2.0
0.0
*
ST
HS
GV
MII
D
OOSNCR4
Relative LncRNA Abundance
5
4
3
2
1
0
†
ST
HS
GV
MII
E
OOSNCR5
Relative LncRNA Abundance
2
1.6
1.2
0.8
0.4
0
†
ST
HS
GV
MII

Table 1. Primers used for RT-qPCR

Gene	Primer	Primer Sequence (5'-3')	Application
RPL19	Forward	GAAATCGCCAATGCCAACTC	RT-qPCR
	Reverse	GAGCCTTGTCTGCCTTCA	
OOSNCR1	Forward	CCAACAGCTCATCTGTCAATT	RT-qPCR
	Reverse	GTTTCCTTGTGGCCATCTTTG	
OOSNCR2	Forward	GCAGAGAGAATCAGGCAGATG	RT-qPCR
	Reverse	GTATGATCTCGGAGTTCCAAC	
OOSNCR3	Forward	CTCTCATTCCAAACAGCATCC	RT-qPCR
	Reverse	CACACGGGCTTCAGTAGTTGC	
OOSNCR4	Forward	AGCAAGTGGTTAAAGGGCAGG	RT-qPCR
	Reverse	AGAAGCTTCCGGTCAGCTGTG	
OOSNCR5	Forward	AGATTGCTGCAAACTCTGCAG	RT-qPCR
	Reverse	CCTGTTTATTAGCTGTGTGAC	

Table 2. Blastocyst rates of differentially stained immature oocytes using BCB.

COC BCB Status	Blastocyst Rate (% $\pm$ SEM)
Control	31.69 ± 0.0031^{a}
BCB+	25.5 ± 7.84^{a}
BCB-	6.08 ± 0.0082^{b}

[b] Different from the control and BCB+ stained oocytes; $P < 0.05$

Table 3. Blastocyst rates following oocyte maturation in a heat-stressed environment

COC Maturation Temperature	Blastocyst Rate (% $\pm$ SEM)
Standard Temperature	17.16 ± 0.0049^{a}
Heat Stressed	6.88 ± 0.0063^{b}

[b] Different among groups; $P < 0.05$

SUMMARY

With the advent of deep sequencing, researchers have discovered a vast collection of non-coding RNAs, many of whose function remains to be investigated. Long non-coding RNAs represent a portion of these transcripts and have been documented to regulate gene expression through various complex mechanisms. Further, many lncRNAs have been predicted using emerging technologies and transcriptome analyses. However, investigations often fail to go beyond identification. Despite the limited studies, few have reported that lncRNAs have essential roles in oocyte maturation and early embryonic development.

The present studies focused on three lncRNAs that were predicted to be highly abundant and oocyte-specific according to RNA sequencing results. Thus, the objectives were to characterize *OOSNCR1, OOSNCR2,* and *OOSNCR3* expression throughout bovine somatic tissues, follicular cells, and early embryonic development. Further, the functional role of each lncRNA during oocyte maturation and early embryonic development was examined using siRNA-mediated knockdown. Moreover, five novel lncRNAs were further characterized in bovine oocytes of varying quality to begin investigations on a potential relationship between oocyte developmental competence and lncRNAs.

The data presented herein validated RNA sequencing results such that *OOSNCR1* and *OOSNCR2* were highly abundant solely in fetal ovaries, denoting oocyte-specificity. *OOSNCR3* was highly abundant in the oocyte; however, low expression was detected in the spleen. Investigations of lncRNA expression throughout follicular cells revealed that all three lncRNAs were detected in all cell types within the bovine follicle. As suspected, all three lncRNAs were highest in the oocyte. Still, interestingly, expression decreased as distance from the oocyte increased, suggesting possible trafficking of the transcript among cell types within the follicle.

Expression panels for each lncRNAs' expression before and after oocyte maturation and throughout early embryonic development revealed identical patterns suggesting a maternal origin. Moreover, the origin of each transcript was further assessed using an RNA polymerase II inhibitor, α-amanitin. Expression patterns were similar for all three genes indicating a maternal origin. Additionally, a wave of maternal transcripts being transcribed during the minor genome activation at the 2-cell stage was observed for each gene. As the top candidate gene, *OOSNCR1* was further investigated to determine its subcellular localization. Using FISH and confocal microscopy, *OOSNCR1* was localized to the cytoplasm of immature oocytes.

The functional role of each lncRNA during oocyte maturation was examined using siRNA-mediated knockdown. *OOSNCR1, OOSNCR2,* and *OOSNCR3* knockdown during oocyte maturation was validated using RT-qPCR. Further, cumulus cell expansion, percent survival at 12 hpi, the relative abundance of genes linked to oocyte competency, and the percentage of embryos reaching the blastocyst stage was assessed following lncRNA knockdown. Cumulus cell expansion was unaffected by lncRNA knockdown despite the microinjection process exerting a degree of lethality on the injected oocytes. In addition, four of five oocyte-specific genes (*NPM2, GDF9, BMP15,* and *JY-1*) were decreased in response to lncRNA knockdown, with no effect observed in *USF1* expression. Lastly, the knockdown of each lncRNA resulted in a significant decrease in blastocyst rate implicating essential roles for each lncRNA during oocyte maturation.

Further, the functional role of each lncRNA during early embryonic was examined using siRNA-mediated knockdown in the presumptive zygote. *OOSNCR1* and *OOSNCR3* tended to knock down in the 4-cell embryo. However, the knockdown of *OOSNCR2* was not validated. Interestingly, blastocyst development was decreased roughly by half following each lncRNA's knockdown.

The second major area of interest was to examine a potential relationship between oocyte quality and lncRNA expression during oocyte maturation. As such, the relative abundance of five novel lncRNAs was quantified in bovine oocytes of varying quality. Specifically, lncRNA expression was examined in COCs (1) collected from small and large follicles before and after maturation, (2) differentially stained using BCB, and (3) exposed to heat stress (41^0C) during oocyte maturation. In single oocytes, novel lncRNAs, *OOSNCR1* and *OOSNCR3,* were accumulated during maturation, whereas *OOSNCR2* and *OOSNCR4* degraded. Further, *OOSNCR1, OOSNCR2,* and *OOSNCR4* were more abundant in oocytes collected from small follicles; specifically, *OOSNCR2* and *OOSNCR4* were expressed highest in immature oocytes.

Conversely, *OOSNCR3* was more abundant in mature oocytes collected from large follicles. Further, following BCB staining, *OOSNCR3* was expressed lower in BCB+ oocytes. Lastly, maturation in a heat-stressed environment decreased CC expansion while causing *OOSNCR1* to decrease expression. Conversely, the relative abundance of *OOSNCR3, OOSNCR4,* and *OOSNCR5* increased. Altogether, the data presented herein represents a starting point for future investigations in identifying novel regulators of oocyte maturation and early embryonic development.

FUTURE DIRECTIONS

Whole genome sequencing has undoubtedly changed the direction of molecular biology. The discovery of the non-coding transcriptome as a vast regulatory network and not "genetic noise" from leaky transcriptional machinery has completely changed how we view gene regulation. Specifically, gene regulation in a variety of disease states. Interestingly, lncRNAs are being investigated as potential biomarkers in a variety of diseases, including coronary artery disease (Li et al., 2018), pancreatic cancer (Zhou et al., 2016), lung squamous cell carcinoma (Li et al., 2019), tumor initiation, progression, and metastasis (Gao et al., 2020), Hirschsprung disease (Torroglosa et al., 2020), Alzheimer's disease (Khodayi et al., 2022), and many more.

With lncRNA gaining popularity, researchers within reproduction are attempting to characterize the molecular mechanisms utilized by lncRNAs within mGCs, CCs, oocytes, and early embryos for clinical applications in the form of biomarkers, ultimately striving for non-invasively tests identifying oocytes and embryos with high developmental potential. For example, various miRNAs and lncRNAs present in CCs are being investigated as potential biomarkers for polycystic ovary syndrome (Tamaddon et al., 2022). Moreover, GCs extracted from women with diminished ovarian reserve differentially expressed lncRNAs *NEAT1*, *GNG12*, and *ZEB2-AS1* with enrichment in pathways involving cell adhesion and apoptosis, steroid biosynthesis, and the immune system (Dong et al., 2022). Most recently, trophectoderm samples collected from women of various maternal ages (young, intermediate, and advanced) revealed young maternal age samples exhibited higher lncRNAs expression predicted to upregulate steroidogenesis and genes encoding inflammatory molecules promoting successful implantation (Ntostis et al., 2022). As studies continue to emerge, lncRNA presence, functional roles regulating reproductive processes, and potential as disease biomarkers in various species appear inevitable.

REFERENCES

Dong, L., X. Xin, H.-M. Chang, P. C. K. Leung, C. Yu, F. Lian, and H. Wu. 2022. Expression of long noncoding RNAs in the ovarian granulosa cells of women with diminished ovarian reserve using high-throughput sequencing. J. Ovarian Res. 15:119. doi:10.1186/s13048-022-01053-6.

Gao, N., Yueheng Li, J. Li, Z. Gao, Z. Yang, Yong Li, H. Liu, and T. Fan. 2020. Long Non-Coding RNAs: The Regulatory Mechanisms, Research Strategies, and Future Directions in Cancers. Front. Oncol. 10. Available from: https://www.frontiersin.org/articles/10.3389/fonc.2020.598817

Khodayi, M., M. Khalaj-Kondori, M. A. Hoseinpour Feizi, M. Jabarpour Bonyadi, and M. Talebi. 2022. Plasma lncRNA profiling identified BC200 and NEAT1 lncRNAs as potential blood-based biomarkers for late-onset Alzheimer's disease. EXCLI J. 21:772–785. doi:10.17179/excli2022-4764.

Li, L., L. Wang, H. Li, X. Han, S. Chen, B. Yang, Z. Hu, H. Zhu, C. Cai, J. Chen, X. Li, J. Huang, and D. Gu. 2018. Characterization of LncRNA expression profile and identification of novel LncRNA biomarkers to diagnose coronary artery disease. Atherosclerosis. 275:359–367. doi:10.1016/j.atherosclerosis.2018.06.866.

Li, R., Y.-E. Yang, J. Jin, M.-Y. Zhang, X. Liu, X.-X. Liu, Y.-H. Yin, and Y.-Q. Qu. 2019. Identification of lncRNA biomarkers in lung squamous cell carcinoma using comprehensive analysis of lncRNA mediated ceRNA network. Artif. Cells Nanomedicine Biotechnol. 47:3246–3258. doi:10.1080/21691401.2019.1647225.

Ntostis, P., G. Swanson, G. Kokkali, D. Iles, J. Huntriss, A. Pantou, M. Tzetis, K. Pantos, H. M. Picton, S. A. Krawetz, and D. Miller. 2022. Trophectoderm non-coding RNAs reflect the higher metabolic and more invasive properties of young maternal age blastocysts. Syst. Biol. Reprod. Med. 0:1–17. doi:10.1080/19396368.2022.2153636.

Tamaddon, M., M. Azimzadeh, and S. M. Tavangar. 2022. microRNAs and long non-coding RNAs as biomarkers for polycystic ovary syndrome. J. Cell. Mol. Med. 26:654–670. doi:10.1111/jcmm.17139.

Torroglosa, A., L. Villalba-Benito, R. M. Fernández, B. Luzón-Toro, M. J. Moya-Jiménez, G. Antiñolo, and S. Borrego. 2020. Identification of New Potential LncRNA Biomarkers in Hirschsprung Disease. Int. J. Mol. Sci. 21:5534. doi:10.3390/ijms21155534.

Zhou, M., Z. Diao, X. Yue, Y. Chen, H. Zhao, L. Cheng, and J. Sun. 2016. Construction and analysis of dysregulated lncRNA-associated ceRNA network identified novel lncRNA biomarkers for early diagnosis of human pancreatic cancer. Oncotarget. 7:56383–56394. doi:10.18632/oncotarget.10891.